MOMENT-ROTATION BEHAVIOUR OF DOUBLE WEB ANGLE CONNECTIONS

by

© Charles C. Onuah

A Thesis
Presented to the University of Manitoba
in Partial Fulfillment of the
Requirements for the Degree of

Master of Science

in the Department of Civil Engineering

Winnipeg, Manitoba

October, 1988

ISBN 0-315-48024-6

MOMENT - ROTATION BEHAVIOUR OF DOUBLE WEB ANGLE CONNECTIONS

BY

CHARLES C. ONUAH

A thesis submitted to the Faculty of Graduate Studies of
the University of Manitoba in partial fulfillment of the requirements
of the degree of

MASTER OF SCIENCE

ABSTRACT

The moment-rotation behaviour of bolted beam-to-column double web angle connections are evaluated. Also, the effect on that behaviour of connection geometric parameters are determined both experimentally and analytically.

The experimental testing program is designed to isolate the effect of each connection size parameter on the moment-rotation behaviour. Twenty specimens with bolted connections are tested, each involving two similar double-web-angle beam-to-column connections. Three sizes of beam section and three sizes of angle thickness are tested to determine the moment-rotation behaviour. The test specimen arrangement consists of two beam segments attached to the flanges of a heavy column stub by pairs of bolted web angles.

A multiple regression analysis procedure is used in the development of a standardized moment-rotation function for double web angle connections. The standardized function is expressed in terms of the significant geometric parameters for double web angle connections. Five different standardized functions are presented, based upon moment-rotation data for the connections tested in this study, then for those data plus data from similar connections tested by others, and finally for all usable data for double web angle connections.

Test results show that the angle thickness, the gauge on the column, the length of the angle, the beam depth and the number of bolts per angle leg on the column flange

exhibit significant influence on the moment-rotation behaviour of the double web angle connections. The angle thickness and the number of bolts per angle leg have greater influence on the connection behaviour than the other connection size parameters considered.

The standardized moment-rotation curves match closely the corresponding experimentally-measured moment-rotation data. The standardized function based upon the usable test data for double web angle connections compares well with that based upon data from bolted-bolted double web angle connections. A standardized moment-rotation function is proposed for double web angle connections.

ACKNOWLEDGEMENTS

The author wishes to express his sincere thanks to Dr. Glenn Morris for proposing the topic of this thesis. Sincere thanks are extended to Dr. Glenn Morris and Dr. Emmanuel Attiogbe for providing excellent guidance and assistance in the preparation of this thesis.

The assistance given by Messrs Moray McVey, Ed Lemke, Marty Green and Dr. Bruce Pinkney during the experimental and analytical work is greatly appreciated.

The research project was financially assisted by the Natural Sciences and Engineering Research Council of Canada.

Finally, the author is indebted to his wife, Chinelo, and family, for their support and encouragement throughout his studies. To them he affectionately dedicates this thesis.

TABLE OF CONTENTS

PAGE

PAGE

LIST OF TABLES

LIST OF FIGURES

PAGE

PAGE

PAGE

PAGE

NOTATION

a_j, b_j, c_j, d_j exponents which indicate the effect of the j^{th} size parameters

b number of bolts per angle leg on column flange

C_1, C_2, C_3 constants in standardized M-Ø equation

d beam depth

E modulus of elasticity

EI flexural ridity of beam

g gauge on column

g_1 gauge on beam

H height of column stub

I second moment of area of the beam about its bending axis

K standardization factor

l angle length

L span length of the beam segment

m number of connection size parameters

M connection moment

M_1 moment at support

M_2 moment at connection

M_i experimental moment

M_l moment coordinate of final data point

M_o reference moment

M_r moment range

M_{ci} moment computed from approximating function

n shape factor for M-Ø curve

N number of data points

p bolt pitch

P	applied load
P_j, q_j	j^{th} connection size parameter
r_m	moment residuals
r_r	rotation residuals
S	initial slope or stiffness
S_p	plastic modulus
t	angle thickness
Δ	column drift or vertical deflection
θ	chord rotation
ϕ	connection rotation
ϕ_1	beam rotation at support
ϕ_2	beam rotation at connection
ϕ_i	experimental rotation
ϕ_l	rotation coordinate of final data point
ϕ_o	reference rotation
ϕ_r	rotation range
ϕ_{ci}	rotation computed from approximating function

CHAPTER 1
INTRODUCTION

1.1 GENERAL

Beam-to-column connections constitute a small percentage of the weight of a structure, yet they are expensive to fabricate and they play an important role in determining the internal force distribution and the structural displacements under load. Bergquist (1977) pointed out that connection deformations sometimes contribute substantially to the overall displacements of a structure. Using Bergquist's test results, Jones, Kirby and Nethercot (1982) and Lui and Chen (1983) demonstrated that the lateral stiffness and strength of a column restrained at its ends by flexible connections are greater than those for a similar pin-ended column. Connection deformation in a moment-resistant, unbraced frame can contribute significantly to the horizontal drift of the structure under lateral load. In addition, the connection moments and lateral displacements can amplify the P-Δ effect. The results of a study by Ang and Morris (1984) revealed that the maximum drift in a rigidly connected frame was increased by 11 percent when P-Δ effects were accounted for. When top and seat angle connections were used in the frame, the P-Δ effect accounted for a 100 percent increase in drift.

The results of an investigation carried out by Lewitt, Chesson and Munse (1969) revealed that double web angle connections developed as much as 20 percent of the beam

fixed-end moment at the specified load level. Such connections are usually designed as pinned. A study by Batho and Rowan (1934) concluded that about 20 percent of the overall beam weight could be saved if the end restraint provided by flexible connections were taken into account in the design procedures.

"Pinned" connections may develop unanticipated column moments. These moments may produce column end fixity that reduces the effective length of the column. On the other hand, for checkerboard loading, the end moments may produce severe column loading.

In general, six components of force are transmitted through a beam-to-column connection. These force components are associated with six corresponding components of deformation in the connection. The dominant force and deformation components in a connection are the flexural moment, M, about a horizontal axis normal to the beam web, and the corresponding rotational deformation, Ø. These components are usually referred to simply as the connection moment and rotation.

The contribution of beam-to-column connections to the overall structural behaviour of steel frames, has not been addressed well by the steel design specifications. Lack of sufficient experimental moment-rotation data and an efficient procedure for incorporating moment-rotation data into a structural analysis computer program are the main reasons. As a result, designers who wish to incorporate

connection behaviour into their design procedures have to resort to experimental data to define the moment-rotation relationships for the connections.

The Canadian Standards Association Specification CAN3-S16.1-M84 (CSA 1984) mandates that all connections of beams, girders and trusses be designed as either "rigid" or "simple". Real connections are neither " rigid " nor " simple ", but rather are semi-rigid. Under certain conditions, the American Institute of Steel Construction Specification (AISC 1983) permits the assumption of partial connection restraint. Such provision is seldom used however (Goverdhan 1984).

To incorporate the end restraint provided by flexible connections into a structural analysis procedure, accurate modelling of the moment-rotation behaviour of the connections is essential. Adequate experimental data are needed in this effort.

1.2 OVERVIEW OF CONNECTION STUDIES

The five most commonly used beam-to-column connection types are the single web angle, the double web angle, the header plate, the end plate, and the top and seat angle. Experimental research into the behaviour of structural connections dates at least as far back as 1917 (Wilson and Moore, 1917). Most investigations have been carried out on riveted connections, which are 10 to 15 percent less stiff than bolted ones, and which are now obsolete. While the

results from the investigations have provided much useful information on connection shear strength, ductility, stiffness and overall behaviour, in most of them moment-rotation relationships have not been recorded. Thus, while more than 800 tests of steel beam-to-column connections have been reported, in only about 330 have moment-rotation data been measured and reported. In most of the experimental test programs reported, the effects of individual parameters have not been isolated.

It is impractical to incorporate into a structural analysis computer program the moment-rotation data for all possible combinations of size parameters for all connection types. Thus, an alternative that has been tried is to develop a standardized moment-rotation function for each connection type. Then, when the connection size parameters are substituted into the standardized function, the moment-rotation behaviour for the specific connection can be computed by the program and incorporated into the structural analysis.

Three different approaches have been used by investigators to standardize the moment-rotation functions. In one of them the functions have been based on elasto-plastic behaviour of the connection. Functions based on this approach are simple in form. However, linear or bilinear functions give poor approximations to the real moment-rotation behaviour, especially as regards the slope of the moment-rotation curve.

A second approach has been to develop empirical or semi-empirical functions based on specific test programs. The resulting functions normally provide a good fit to the test data on which they are based, but they usually yield poor result when applied to other experimental data.

Finally, a generalized function, calibrated to fit all available experimental data, has been proposed. Several attempts have been made to develop such generalized functions (Sommer 1969, Frye and Morris 1975, Altman et al. 1982, Ang and Morris 1984, Lui 1985). Generally, these attempts have not yielded good accuracy. The problem is that they require sets of experimental data for two or more connections that are similar except for one geometric parameter. Unfortunately, not enough of these data are available. To overcome this problem, Attiogbe, Morris and Onuah (1989) recently attempted a curve fitting procedure that enabled all available experimental data to be utilized.

1.3 OBJECTIVE AND SCOPE

The objectives of this study are the following:

i) to identify the connection geometric parameters that influence most significantly the moment-rotation behaviour of double web angle connections;

ii) to evaluate experimentally the effect of the most significant of those parameters on the moment-rotation behaviour;

iii) using the moment-rotation data for all of the specimens tested, and a multiple regression analysis procedure (Attiogbe, Morris and Onuah 1989), to develop a standardized moment-rotation function for double web angle connections.

1.4 ASSUMPTIONS AND LIMITATIONS

The imposed assumptions and limitations are the following:

i) Except for two of the test specimens which were subjected to four cycles of loading and unloading, only static monotonic loading is considered.

ii) Only connections in which the web angles are bolted to the beam and to the column flange are considered. Eighteen of the test specimens employed ASTM A325 bolts, while the remaining two used ASTM A307 bolts.

iii) The connection design and detailing are in accordance with the provisions of Canadian Standards Association Specicification CAN3 S16.1-M84 (CSA 1984).

iv) Only pairs of connections, symmetrically placed on opposite faces of a W-section stub column, are considered. Thus, shearing deformation in the column web, which would occur in a specimen with only a single connection, is ignored.

v) Bare steel framing only, as opposed to composite construction, is considered.

CHAPTER 2
PREVIOUS STUDIES

2.1 GENERAL

Various studies have been performed with the aim of quantifying the moment-rotation behaviour of commonly used steel beam-to-column connections. A summary of these investigations is presented in this chapter. The connections investigated were riveted, bolted and welded-bolted.

2.2 EXPERIMENTAL INVESTIGATIONS

Several summary papers have been published on experimental investigations of the behaviour of the commonly-used steel beam-to-column connection types (Goverdhan 1984, Nethercot 1985, Kishi and Chen 1986 and Morris and Packer 1987). The summary presented here deals with double web angle connections only.

Tests have been conducted on double web angle connections using both rivets and bolts as fasteners. Tests on riveted connections, conducted by Wilson and Moore (1917) and Rathbun (1936), showed that the behaviour of riveted connections is similar to that of bolted connections.

Munse, Bell and Chesson (1959) performed four tests on double web angle connections to study the effect on connection behaviour of high strength bolts used in conjunction with rivets. They found that the moment-to-shear ratio did not influence the connection behaviour. Flexure of the angles was the primary cause of failure, since none of

the fasteners failed.

Lewitt, Chesson and Munse (1969) carried out investigations on double web angle connections using both rivets and high strength bolts. The results of their tests confirmed that the assumptions made in the derivation of their predictive equation for the moment-rotation curve were in good agreement with the actual behaviour of the connections. They also found that due to the clamping action of high strength bolts, bolted connections were stiffer than riveted ones. The stiffness of the bolted connection was increased if hardened steel washers were used.

Sommer (1969) conducted a comprehensive test program on shear connections, including four double web angle specimens and twenty header plate specimens. He reported that the double web angle connections, which had their angles welded to the beam web, behaved like header plate connections. He further pointed out that the only difference between the two types of connection was the moment value at which contact was made between the flanges of the beam and the column.

Thompson, Mckee and Visintainer (1970) carried out tests on double web angle connections to determine the effect on connection performance of the size of the connecting angles, the gauge distances on the column, and the material yield strength. The main conclusions from this test program were that the connections were flexible enough to sustain the anticipated rotations, and that the design

method recommended by the American Institute of Steel Construction (AISC) was satisfactory.

Most of the tests described above were not designed to determine the effects of individual connection size parameters on the moment-rotation behaviour. The determination of such effects requires a group of tests in which only one size parameter at a time is varied.

2.3 MODELLING FUNCTIONS

The behaviour of all steel connections is nonlinear. Researchers have modelled the nonlinear behaviour of steel connections using a variety of functions. Early investigators (Lothers 1951, Lewitt, Chesson and Munse 1969) employed linear or bilinear functions to model the behaviour. Obviously, the linear or bilinear functions do not approximate the nonlinear moment-rotation behaviour very closely.

Sommer (1969), Frye and Morris (1975) and Altman et al. (1982) modelled the moment-rotation behaviour with a polynomial function. The polynomial function provides a better approximation than the linear or bilinear ones. However, due to its inherent oscillatory nature (Jones, Kirby and Nethercot 1980), it may yield erratic approximations to the connection stiffness at various values of rotation.

The cubic B - spline procedure proposed by Jones, Kirby and Nethercot (1981) provides a good approximation to the

nonlinear moment-rotation curve. However, it requires a large number of parameters for its evaluation.

Lui (1985) recently proposed an exponential model which provides a good representation of the moment-rotation behaviour. However, the model may not do well when the connection is subjected to strain hardening. Furthermore, it requires at least six parameters for its evaluation.

The Ramberg-Osgood (1943) and Richard (1975) functions have been used to obtain good approximations to experimental moment-rotation curves, using only three and four parameters, respectively. The Richard function has been shown to be more accurate than other functions in modelling the moment-rotation behaviour of five commonly used connection types (Attiogbe, Morris and Pinkney 1988).

2.4 STANDARDIZATION OF MODELLING FUNCTIONS

To standardize the modelling function, that is to develop a moment-rotation function expressed in terms of the geometric parameters for a given connection type, two approaches have been used. The first involves elastic and plastic analyses of the connection, incorporating phenomena observed in tests of the connection. The prediction equations based on this approach are either linear or bilinear and thus are obviously incapable of matching closely the experimental moment-rotation curves.

The second approach requires the availability of experimental moment-rotation data for the connection. The

procedure involves identifying those geometric parameters that most strongly affect the moment-rotation behaviour of a particular connection type. The effect of each of the geometric parameters in turn is isolated using experimental moment-rotation curves for connections that are identical except for one geometric parameter. Unfortunately, since few connection test programs have been designed to isolate the effects of individual geometric parameters, only a small proportion of the available experimental data can be used in this procedure.

Using elastic analysis, Lothers (1951) derived a linear equation to predict the initial rotational stiffness for double web angle connections. He also derived an allowable resisting moment equation in terms of allowable bending stress and geometric parameters of double web angle connections. Since the actual connection behaves inelastically even at low moments, these equations may be inaccurate at moment values in the service load range.

Lewitt, Chesson and Munse (1969) derived a prediction equation for the moment-rotation behaviour of double web angle connections based on three stages of connection behaviour, namely: elastic, elasto - plastic and plastic. The equation is not suited for general application since it contains constants which have to be evaluated empirically. In addition, the application of the equation is restricted to a small number of angle sizes and gauge distances.

Using the second approach for standardizing moment-

rotation curves, Sommer (1969) developed a more general standardized moment-rotation equation, of the form:

$$\emptyset = C_1(KM) + C_2(KM)^3 + C_3(KM)^5 \qquad (2.1)$$

which he applied to a series of header plate connections that he had tested. In Equation (2.1), $\emptyset$ and M are the connection rotation and moment, respectively. C_1, C_2 and C_3 are constants determined by performing a least squares curve fit of the experimental data. K is a standardization factor of the form:

$$K = \prod_{j=1}^{m} P_j^{a_j} \qquad (2.2)$$

where

P_j is the j^{th} connection size parameter.

a_j is an exponent which indicates the effect of the j^{th} size parameter.

m is the number of size parameters.

The exponents a_j are determined by considering a family of experimentally obtained moment-rotation curves for connections that are identical except for parameter p_j.

Frye and Morris (1975) used Sommer's procedure to develop standardized polynomial functions to predict the moment-rotation behaviour of seven types of semi-rigid connections. Altman et al. (1982) used a modified version of Sommer's procedure to develop a different standardized

polynomial expression for modelling the moment-rotation behaviour of top and seat angle connections.

Ang and Morris (1984) used the Ramberg-Osgood function to replace the polynomial function in the development of standardized moment-rotation expressions for five connection types. The difficulty with the above procedure is that it requires variation of one parameter at a time. To overcome this problem, Attiogbe, Morris and Onuah (1989) employed a multiple regression analysis procedure, in conjunction with the Richard function, to develop a standardized moment-rotation function for double web angle connections. The advantage of the latter procedure is that it is able to employ all appropriate available experimental data in its derivation.

CHAPTER 3
MODELLING PROCEDURE

3.1 GENERAL

In this chapter, the results of a recent study (Attiogbe, Morris and Pinkney 1988,1989), which compared the accuracy of several modelling functions are summarized. That study showed that the Richard function provided the most accurate fit to the moment-rotation data for the connections considered. In addition, a summary of the standardization procedure outlined by Attiogbe, Morris and Onuah (1989) is presented. As described in Chapter 6, the latter procedure, using the Richard function, was used to develop a standardized moment-rotation function for the double web angle connections tested in this study.

3.2 MODELLING FUNCTION

In a recent study by Attiogbe, Morris and Pinkney (1988,1989), the accuracy of the Ramberg-Osgood and Richard functions and the cubic B - spline curve fitting procedure was compared. In the study, the method of least squares and a procedure employing selected points were used to fit the three types of function to experimental data. The least squares method was found to yield the more accurate fits. Figure 3.1 shows both Richard and Ramberg-Osgood fits to three sets of moment-rotation data, for double web angle connections, using the least squares method. It can be observed from the figure that the Richard function provided

the better fit for two of the three data sets. The Richard function also did better than the cubic B - spline procedure when the least squares fit was used. Figures 3.2 and 3.3 show cubic B - spline and Richard function fits, respectively, for a set of moment-rotation data that exhibit a long post-yielding region. The error of approximation for the cubic B - spline fit is three times larger than that for the Richard function fit. The error of approximation was defined in terms of the residual of the data points relative to the approximating function. The procedure for computing the error of approximation is illustrated in Figure 3.4.

For a typical experimental data point i, the moment and rotation residuals relative to the approximating function were computed as follows:

$$r_m = M_i - M_{ci} \tag{3.1}$$

$$r_r = \phi_i - \phi_{ci} \tag{3.2}$$

where

M_i = experimental moment,

M_{ci} = moment computed from approximating function,

ϕ_i = experimental rotation, and

ϕ_{ci} = rotation computed from approximating function.

For comparisons on a normalized basis, the error of approximation was computed as follows:

$$\text{Error of Approximation} = \frac{\sum_{i=1}^{N}(M_i - M_{ci})^2 \quad \sum_{i=1}^{N}(\phi_i - \phi_{ci})^2}{M_r^2 \phi_r^2} \tag{3.3}$$

M_r and $\emptyset_r$ are the moment and rotation ranges, respectively, for the given data, and N is the number of data points. When expressed in percent, the approximation error, as defined, can be very large, thus conveying a false impression of gross inaccuracy. Thus, it is emphasized that the approximation error is relevant only for purposes of comparing the relative accuracy of different models.

The Ramberg-Osgood function is a three-parameter one which is expressed in the form :

$$\frac{\emptyset}{\emptyset_o} = \frac{M}{M_o}\left[1 + \left|\frac{M}{M_o}\right|^{n-1}\right] \qquad (3.4)$$

where

n = shape parameter,

M_o = reference moment, and

$\emptyset_o$ = reference rotation.

The cubic B - spline curve-fitting procedure requires that the range of connection rotations be divided into a finite number of smaller ranges. Then the cubic B - spline routines are employed, in conjunction with the experimental data points and a list of the ranges to determine the cubic B - spline coefficients, to fit a curve to the data.

The Richard function expresses moment in terms of rotation as follows:

$$M = \frac{(S-S_p)\emptyset}{\left(1 + \left|\frac{(S-S_p)\emptyset}{M_o}\right|^n\right)^{1/n}} + S_p\emptyset \qquad (3.5)$$

where

S = initial slope or stiffness,

n = shape parameter,

M_o= reference moment, and

S_p= plastic modulus.

The initial slope of the moment-rotation curve can be represented as:

$$S = \frac{M_o}{\phi_o} \tag{3.6}$$

Equation (3.5) has four parameters namely, S, S_p, M_o, and n. However, if ϕ_1 and M_1, the coordinates of the final data point on the curve, are used,

$$S_p = \frac{M_1 - M_o}{\phi_1} \tag{3.7}$$

Then, Equation (3.5) involves only the three independent parameters S, M_o, and n.

By substituting Equation (3.6) into Equation (3.5) and rearranging, the Richard function is expressed in dimensionless form as:

$$\frac{M}{M_o} = \frac{\phi}{\phi_o}\left[\frac{1 - \frac{S_p\phi_o}{M_o}}{\left(1 + \left|\left(\frac{1}{\phi_o} - \frac{S_p}{M_o}\right)\phi\right|^n\right)^{1/n}} + \frac{S_p\phi_o}{M_o}\right] \tag{3.8}$$

In the curve fitting procedure using the least squares

method, convergence was most rapid when the dimensionless form of the Richard function was used. The dimensionless form of the Richard function is illustrated in Figure 3.5 for a particular positive value of S_p and three different values of n. It can be seen that the sharpness of the "knee" on the curve increases with an increase in n.

In evaluating the modelling functions as described above, the experimental data used represented connections in which the columns did not contribute to the overall deformations of the connections. The function of choice, the Richard function, and the other functions considered cannot model the steeply rising portion of the moment-rotation curve which occurs after the beam and column flanges make contact. This is not a severe limitation however, since the rotation values at which contact is made lie well beyond service load range.

3.3 STANDARDIZATION OF MODELLING FUNCTIONS

Attiogbe, Morris and Onuah (1989) developed a multiple regression analysis procedure to standardize the Richard function.

Richard function parameters, $\emptyset_o$, M_o , n and S_p, are assumed to be related to the connection size parameters as follows:

$$\emptyset_o = \prod_{j=1}^{m} q_j^{a_j} \; ; \; M_o = \prod_{j=1}^{m} q_j^{b_j} \; ; \; n = \prod_{j=1}^{m} q_j^{c_j} \; ; \; S_p = \prod_{j=1}^{m} q_j^{d_j} \qquad (3.9)$$

In Equation (3.9), m is the number of connection size parameters, q_j is the j^{th} size parameter, and a_j, b_j, c_j and d_j are exponents which indicate the effect of the j^{th} size parameter. Taking logarithms of both sides of Equation (3.9) yields:

$$\log \phi_o = a_1 \log q_1 + a_2 \log q_2 + a_3 \log q_3 + \ldots + a_m \log q_m$$

$$\log M_o = b_1 \log q_1 + b_2 \log q_2 + b_3 \log q_3 + \ldots + b_m \log q_m \qquad (3.10)$$

$$\log n = c_1 \log q_1 + c_2 \log q_2 + c_3 \log q_3 + \ldots + c_m \log q_m$$

$$\log S_p = d_1 \log q_1 + d_2 \log q_2 + d_3 \log q_3 + \ldots + d_m \log q_m$$

Multiple regression analysis is applied to Equation (3.10) to obtain the coefficients a_j, b_j, c_j, and d_j. These coefficients are the exponents required in Equation (3.9). Once the exponents have been obtained, the Richard function parameters are computed using Equation (3.9).

In this latter standardization procedure, all available test data for a given connection type can be used. This makes the procedure more general than that used by previous investigators, where only a limited number of the available sets of test data could be used.

The procedure developed by Attiogbe, Morris and Onuah (1989) is used in this study. The results for double web

angle connections are presented in chapter 6.

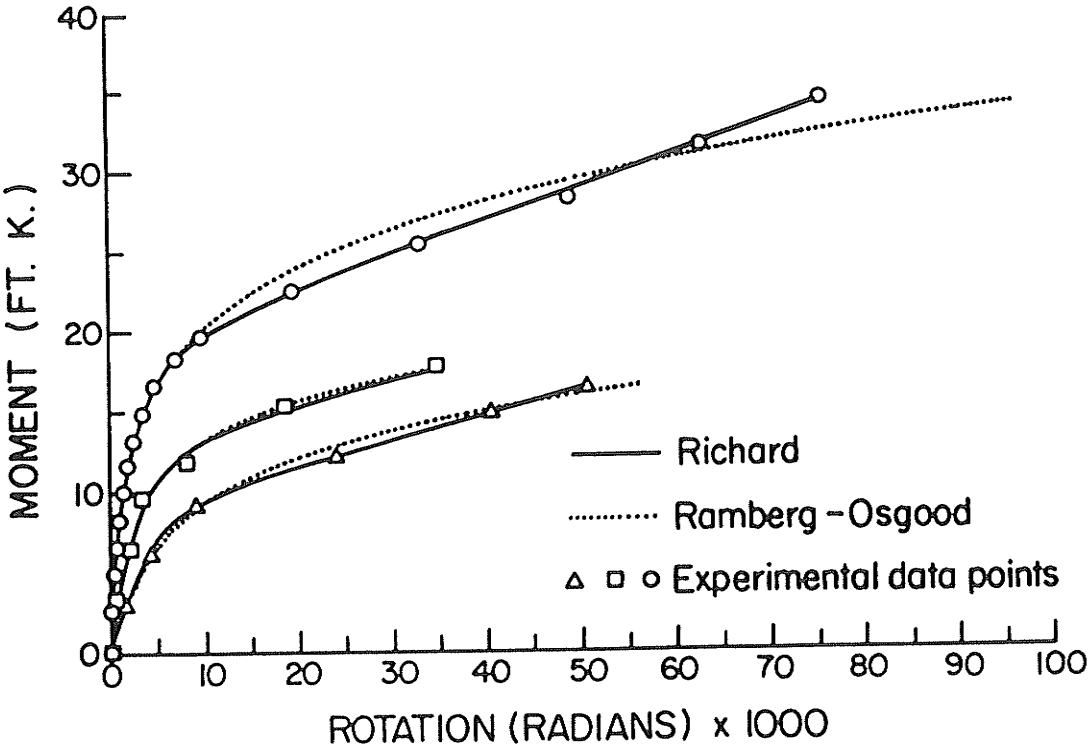

Figure 3.1: Moment-Rotation Curves - Double Web Angle Connections.

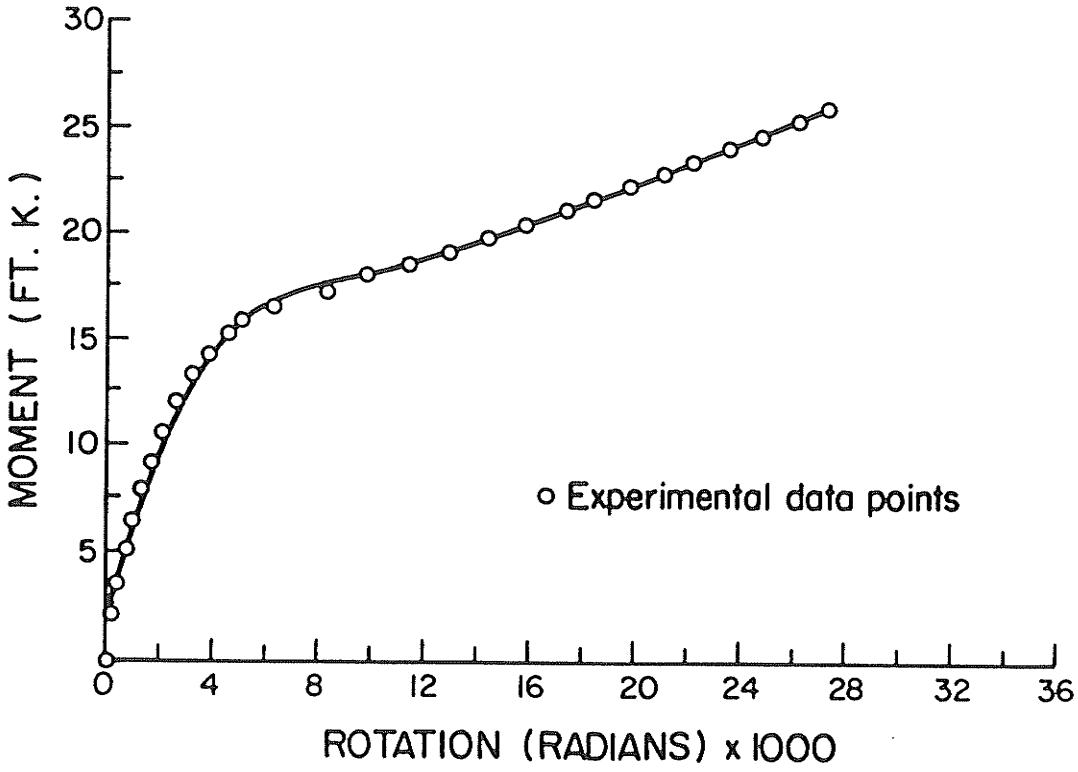

Figure 3.2: Cubic B - Spline Fit.

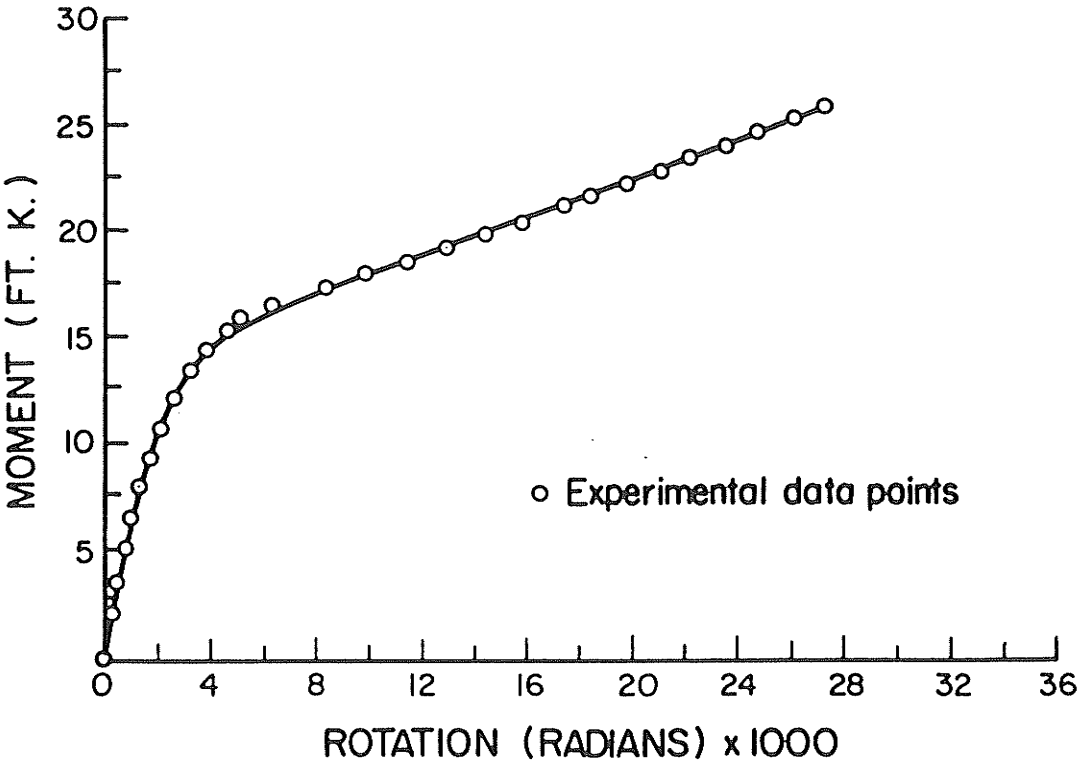

Figure 3.3: Richard Function Fit Using Nonlinear Least Squares Method.

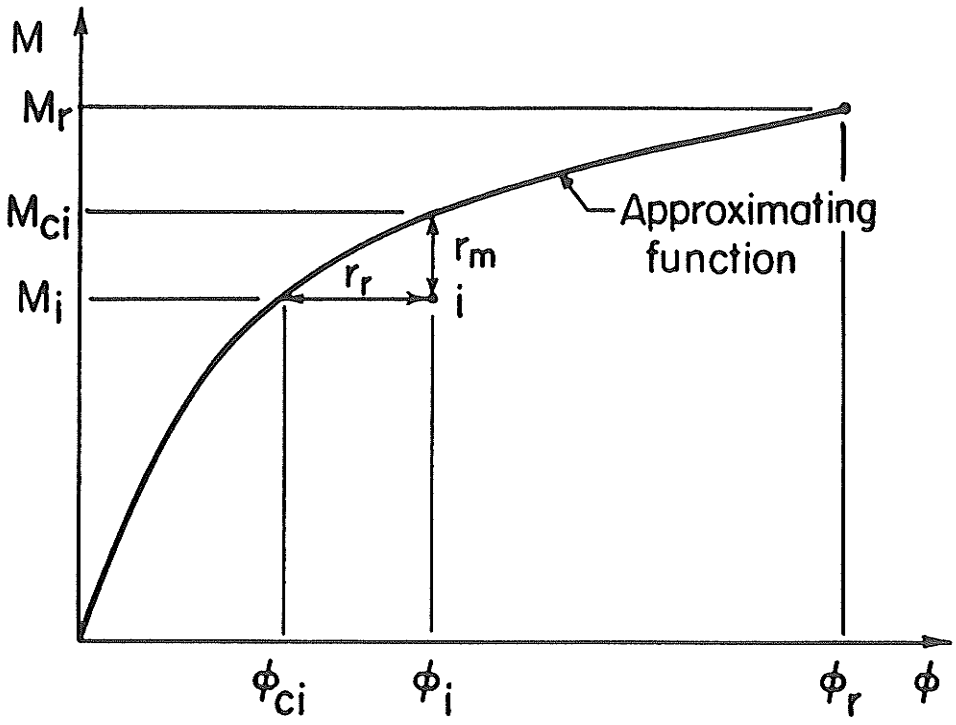

Figure 3.4: Quantities Used in Computation of Error of Approximation.

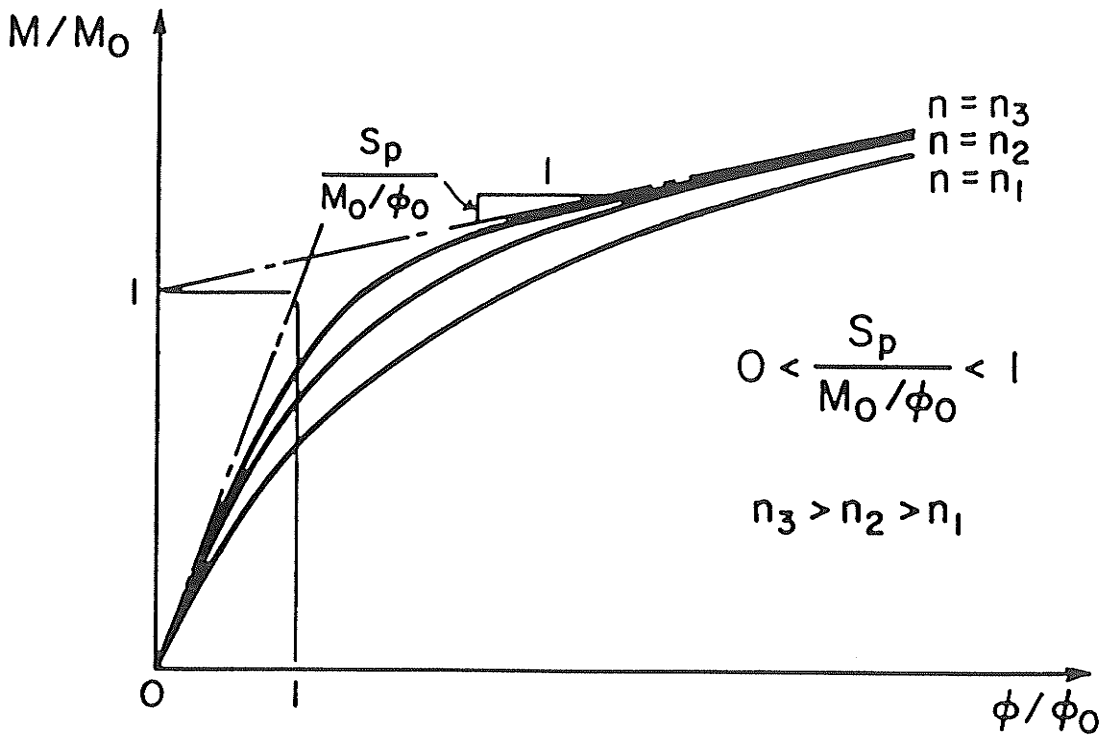

Figure 3.5: Dimensionless Form of Richard Function.

CHAPTER 4
EXPERIMENTAL PROGRAM

4.1 GENERAL

The purpose of the experimental program was to evaluate the moment-rotation behaviour of bolted beam-to-column double web angle connections and to determine the effect on that behaviour of the pertinent geometric parameters for that connection type.

4.2 TEST SPECIMENS

Twenty specimens, designated 1A, 1B, 2, 3, ... 19, as indicated in Table 4.1, were tested. The geometry and loading of a typical test specimen are illustrated in Figure 4.1. The test specimen arrangement consisted of two beam segments (EAST and WEST as shown in Figure 4.1), which were attached to the flanges of a column stub by pairs of bolted web angles. The bolt diameter was 3/4 in. (19.05 mm). ASTM A325 bolts were used for all specimens except 6 and 6A, which employed ASTM A307 bolts.

The beam span lengths were chosen so as to keep the span-to-depth ratio the same for all of the test specimens. Each beam segment was used in two tests, once with one end connected to the column and once with the other end so connected. Cap plates were welded to the top and bottom of all column stubs. Table 4.1 summarizes the member sizes and dimensions of the test specimens. The pertinent connection size parameters are defined in Figure 4.2. The test

specimens were designed to permit the evaluation of the effect of each primary variable on the moment-rotation behaviour of the connection. The primary variables in the study were the angle thickness, t, the gauge on the column, g, the number of bolts per angle leg, b, and the beam depth, d. All of the connections tested in this study had only one vertical line of bolts per angle leg. Figure 4.3 shows the ranges of the primary variables incorporated into the test specimens.

All beam and column sections and all connection angles conformed to CSA G40.21-M grade 300W. The required bolt holes were drilled at both ends of each beam segment prior to delivery, and were 1/16 in. (2 mm) larger than the nominal bolt diameter. The specimens were assembled in the structures laboratory at the University of Manitoba.

The assembly of the test specimens consisted of attaching a pair of beam sections to a centrally positioned column stub using the particular double web angles to be investigated in a given test. The web angles were bolted to the flanges of the column stub and to the webs of the beams. The bolts were used in the "as received" condition. They were installed with the nuts and washers to the inside of the column flange, and finger tightened. After the specimen was assembled, extra care was taken to attain proper alignment of the connection components before final torqueing was done with a spud wrench. The " turn-of-nut " method was used to tighten the A325 high strength bolts

whereas the " full effort of a man " was used to tighten the A307 common bolts. These practices conform to the rcommendations outlined in clauses 21.2 and 22.5.1 of CSA specification CAN3-S16.1-M84 (1984).

To prevent possible torsional displacements at the beam supports, welded-plate angles as shown in Figure 4.4, were bolted to the ends of the beam segments through pairs of 100x100x16 mm angles. The sizes of the two plates used to fabricate the welded-plate angles were 250x750x25 mm and 250x380x25 mm. The fasteners were 3/4 in. (19.05 mm) diameter, three-inch (76.20 mm) long A325 high strength bolts. Slotted holes at a pitch of 80 mm were used in the 250x750x25 mm plates to facilitate the use of the welded-plate angles in all tests.

A previous study (Munse, Bell and Chesson 1959) showed that the deformations of the column flange and web can contribute significantly to the total rotational deformation of a connection. In this study, to exclude the contribution of the column deformations from the total joint rotations, heavy sections, W250x89 and W250x101, were used in nineteen of the tests. A lighter section, W250x49, was used in specimen 4 in order to study the effect of using a column with a small flange thickness. A total of eight column stubs were used. Each of the heavy sections was reused until there was some evidence of flange deformation.

The clearances between the beam and column flanges were measured in each test. Values of these clearances ranged

from 8 mm to 14 mm. A clearance of 10 mm is called for by the Canadian Standards Association (CSA 1984) specification.

4.3 LOADING APPARATUS AND INSTRUMENTATION

As illustrated in Figure 4.5, a 2670 kN (600 kip) capacity Universal Testing Machine, Baldwin 600 XWHV - 1010 model with servo-controlled and hydraulically actuated ram, was used to apply load to the column stubs of the test specimens. The X-Y recorder of the testing machine was used to obtain load-displacement records for all tests.

Nine LVDTs were installed at various locations, as shown in Figure 4.6, in order to monitor the vertical and horizontal deformations in the connections. Three of the LVDTs, numbers 6, 7 and 9, were used to monitor the vertical deflection of the column stub. Four others, numbers 1,3,5 and 8 measured the horizontal displacements of the beam flanges relative to the column faces. The remaining two, numbers 2 and 4, were used to measure the vertical displacements of the top flanges of the beams at the connections relative to the column stub. The positioning of LVDT number 9, on the centre line of the column stub, is illustrated in Figure 4.7.

Eight dial gauges, as illustrated in Figure 4.8, were used to measure bolt slip during loading. Four of them, numbers 1 and 2 in the figure and the corresponding ones on the opposite side of the specimen, measured the slip between the column flanges and the column legs of the angles, and

the remaining four, numbers 3 and 4 and those symmetrically opposite them, measured the slips between the beam legs of the angles and the beam webs. Two of the dial gauges that were used to measure the slip between the column leg and the column flange, and that between the beam leg and the beam web, are shown in Figure 4.7.

Small brackets which were welded to the flanges of the column stub and the beam segments, were used to support the LVDTs. Also, small metal plates with holes, which were welded to the under side of the top flanges of the beam segments, provided supports for the dial gauges that were used to measure the slip between the angle legs and the beam webs. The small plate which supported one of the dial gauges is shown in Figure 4.7. Small screws which were welded along the thickness of the column flanges, provided anchorage for the dial gauges that were used to measure the slip between the flanges of the column stub and the column legs of the angles.

4.4 TESTING PROCEDURE

The support arrangement for a typical test specimen is shown in Figure 4.9. The assembled specimen was mounted on rocker supports which were clamped to the flange of a heavily stiffened girder. The whole assembly was placed in the testing machine. To minimize the effect of friction between the two steel plates at each support, two pieces of teflon were placed between them, as illustrated Figure 4.9.

A final check of the specimen alignment in the testing machine was performed to ensure that the span lengths were correct.

The specimen was white-washed at the connection in order to permit observation of yield patterns. Then the dial gauges and the LVDTs were placed in their appropriate locations. The LVDTs were connected to the data acquisition system, adjusted to utilize their full travel, and then initialized to zero. The data acquisition system was equipped with an Epson LX-80 printer. LVDT readings were taken at two-second intervals and were stored on the hard disk unit of the data acquisition system. The dial gauges were also adjusted and their initial readings were taken. The X-Y recorder of the testing machine was set to the desired scales. The same scales were used for all tests.

All specimens except for numbers 5 and 6A were subjected to static (monotonic) loading only. The specimens were loaded continuously at an initial rate of about 6.0 mm per minute. This rate could not be maintained throughout the test since the Universal Testing Machine is not equipped with a stroke controller. Each test was terminated shortly after contact was made between the column flange and the beam compression flange on one or both sides of the column stub. The maximum values of rotation and vertical deflection attained in each test were at least 0.035 radians and 80 mm, respectively. Before unloading the specimen, the maximum load attained was held constant while the dial gauges were

read. LVDT readings were also taken during the unloading portion of the tests.

Specimens 5 and 6A were subjected to four cycles of loading and unloading, as shown in Table 4.1. Specimen 5 employed A325 high strength bolts while specimen 6A had A307 common bolts. Initially, load was applied until the column stub had experienced a vertical deflection of 20 mm. The load was then reduced to zero and the specimen was reloaded until a new 20 mm vertical deflection of the column stub was attained. The process of loading and unloading was carried through four cycles.

The average duration of test for the specimens subjected to monotonic loading was 40 minutes while that for the specimens subjected to repeated loading was 50 minutes.

TABLE 4.1: TEST SPECIMEN DIMENSIONS.

Specimen number	Beam section	Column section	Angle length l (mm)	Angle size (mm)	Height of col. H (mm)	Angle thickness (mm)	Bolt		Column gauge g (mm)	Bolt rows	Bolt type	Beam span L(m)
							Length	Pitch P (mm)				
1A	W460X82	W250X101	390	100X100X10	810	10	2 1/4	80	140	5	A325	1.50
1B	W460X82	W250X101	390	100X100X10	810	10	2 1/4	80	140	5	A325	1.50
2	W460X82	W250X101	390	100X100X8	810	8	2 1/4	80	140	5	A325	1.50
3	W460X82	W250X101	390	100X100X12	810	12	2 1/4	80	140	5	A325	1.50
4	W460X82	W250X49	390	100X100X10	660	10	2 1/4	80	140	5	A325	1.50
5*	W460X82	W250X101	390	100X100X10	810	10	2 1/4	80	140	5	A325	1.50
6	W460X82	W250X101	390	100X100X10	810	10	2 1/4	80	140	5	A307	1.50
6A*	W460X82	W250X101	390	100X100X10	810	10	2 1/4	80	140	5	A307	1.50
7	W460X82	W250X101	390	100X90X10	810	10	2 1/4	80	130	5	A325	1.50
8	W460X82	W250X101	390	100X75X10	810	10	2 1/4	80	100	5	A325	1.50
9	W310X52	W250X101	230	100X100X10	810	10	2 1/4	80	140	3	A325	1.00
10	W310X52	W250X101	230	100X100X8	810	8	2 1/4	80	140	3	A325	1.00
11	W310X52	W250X101	230	100X100X12	810	12	2 1/4	80	140	3	A325	1.00
12	W460X82	W250X101	230	100X100X10	810	10	2 1/4	80	140	3	A325	1.50
13	W460X82	W250X89	230	100X100X8	810	8	2 1/4	80	140	3	A325	1.50
14	W460X82	W250X89	230	100X100X12	810	12	2 1/4	80	140	3	A325	1.50
15	W460X82	W250X89	310	100X100X10	810	10	2 1/4	80	140	4	A325	1.50
16	W610X101	W250X89	390	100X100X10	810	10	2 1/4	80	140	5	A325	2.00
18	W610X101	W250X89	470	100X100X8	810	8	2 1/4	80	140	6	A325	2.00
19	W610X101	W250X89	470	100X100X12	810	12	2 1/4	80	140	6	A325	2.00

NOTE:

* Repeated Loading.

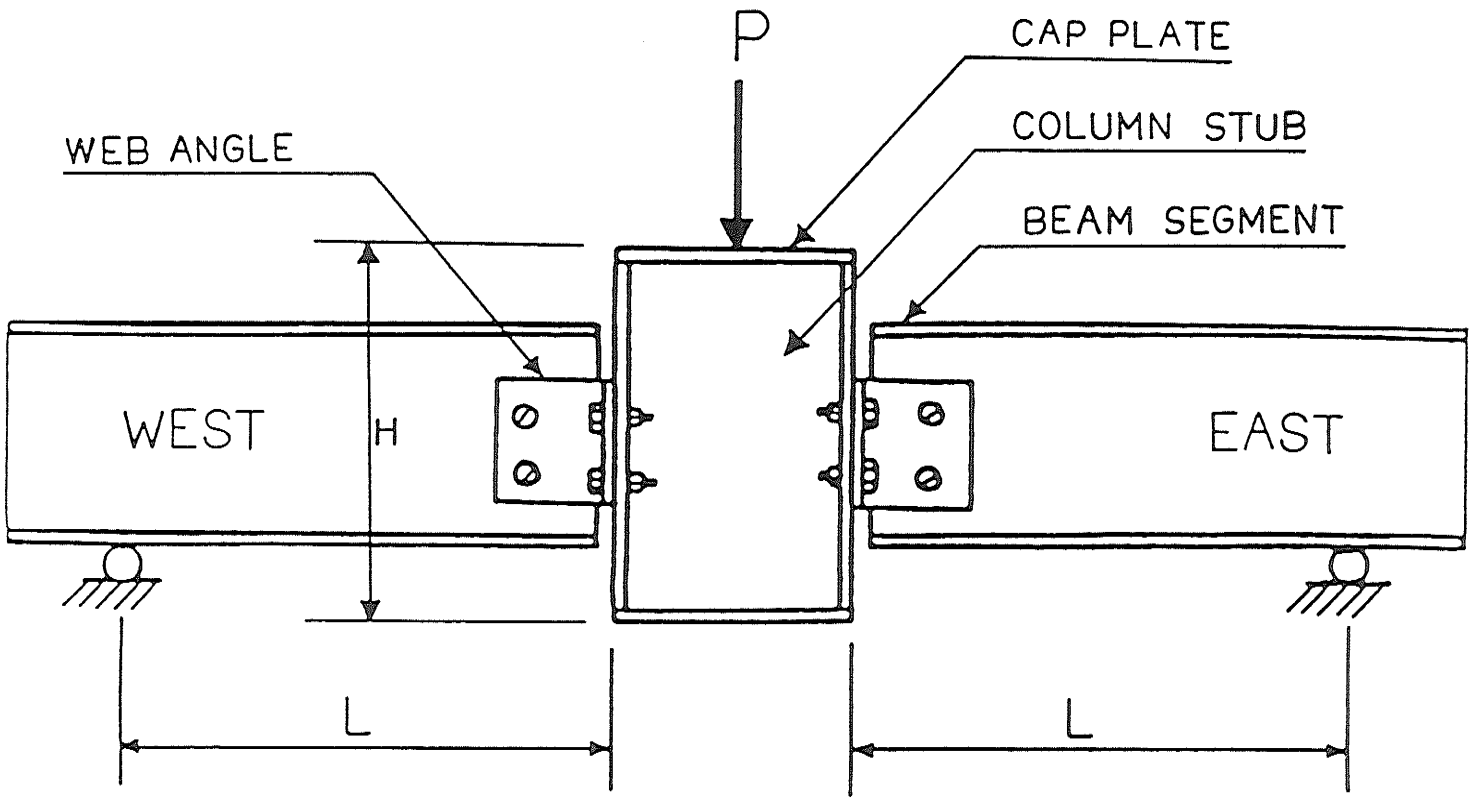

Figure 4.1: Test Specimen Arrangement.

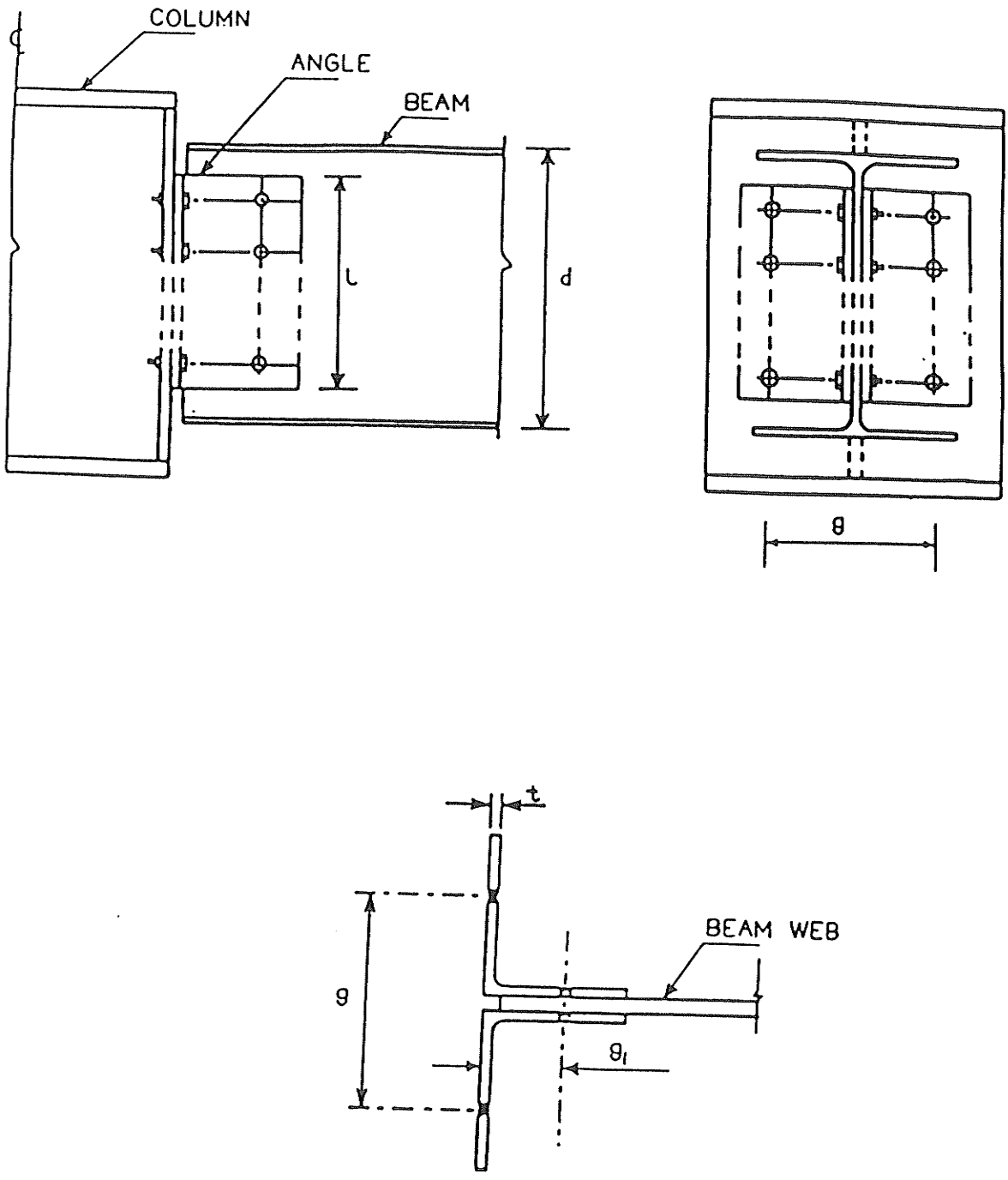

Figure 4.2: Definitions of Connection Size Parameters.

FIGURE 4.3: TEST DETAILS.

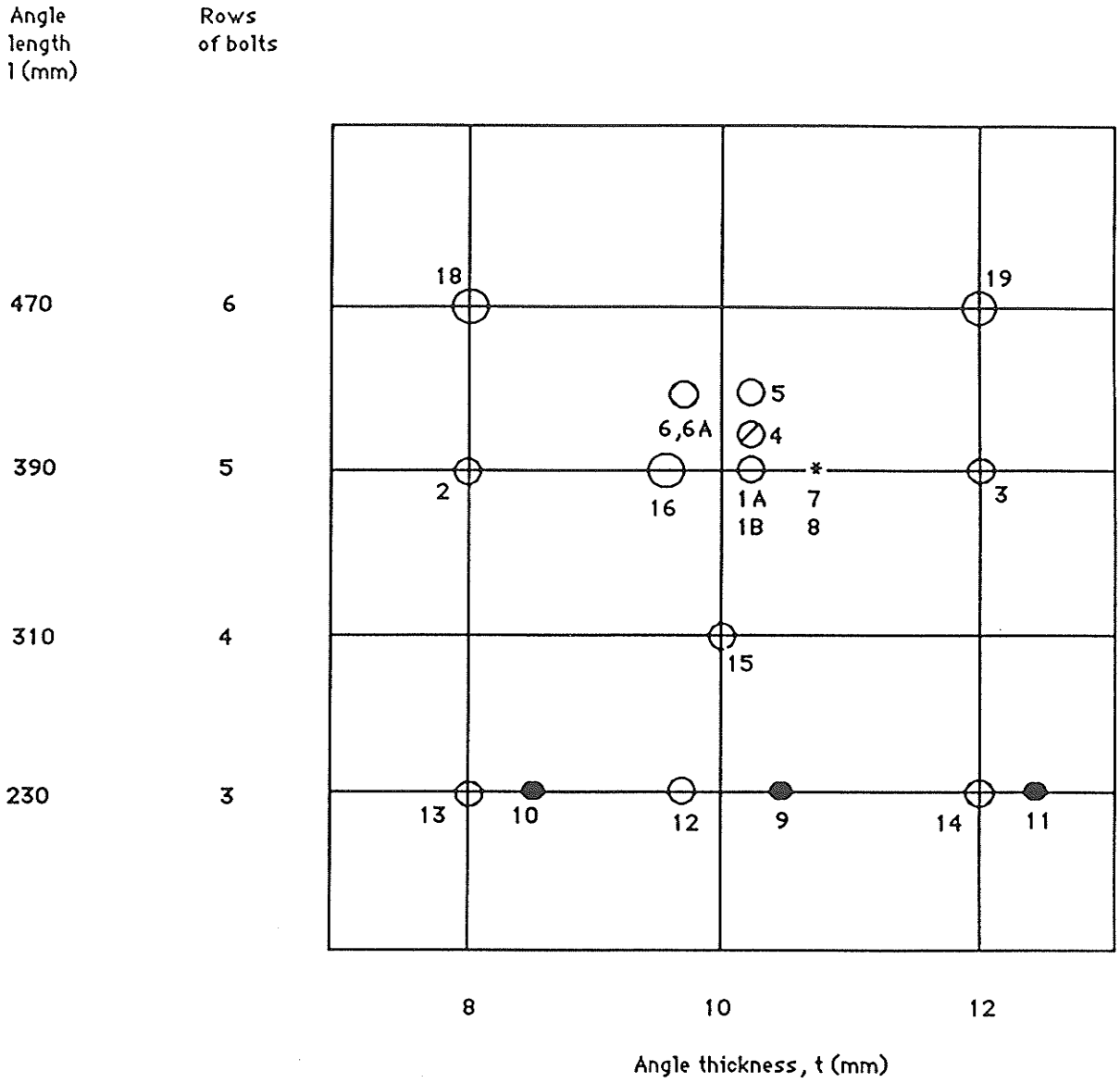

Bolts: 3/4 in. (19.05 mm) ASTM A325 and A307.

Beam sizes: ● = W310X52; ○ = W460X82; ◯ = W610X101.

Gauge on beam, g1 = 65 mm.

Gauge on column, g = 140 mm, except as noted *.
* - 2 specimens, g = 100 mm and 130 mm.

Column sizes: W250X101 and W250X89 except ⊘ with size of W250X49.

NOTE: The numbers within the grid are the test specimen numbers.

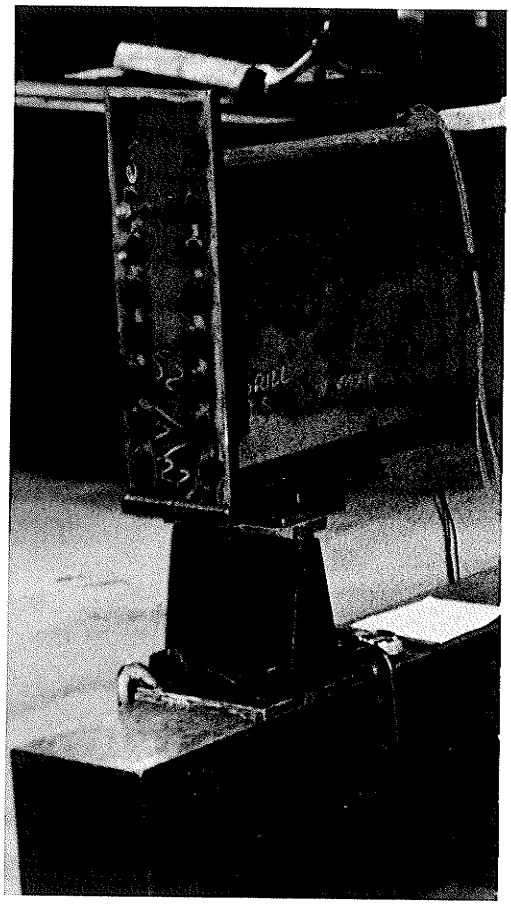

Figure 4.4: Welded-Plate Angle Fastened to the End of the Beam Segment.

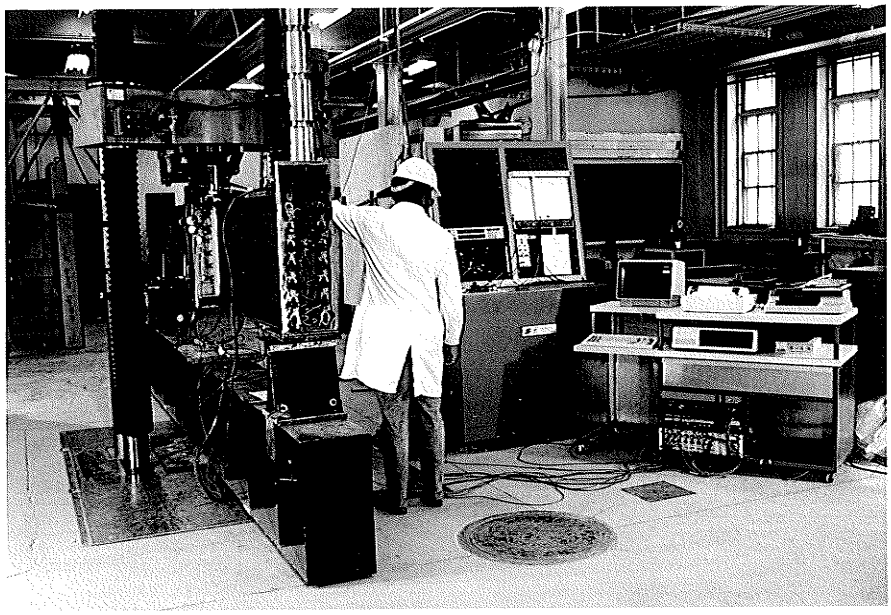

Figure 4.5: Test Set-Up.

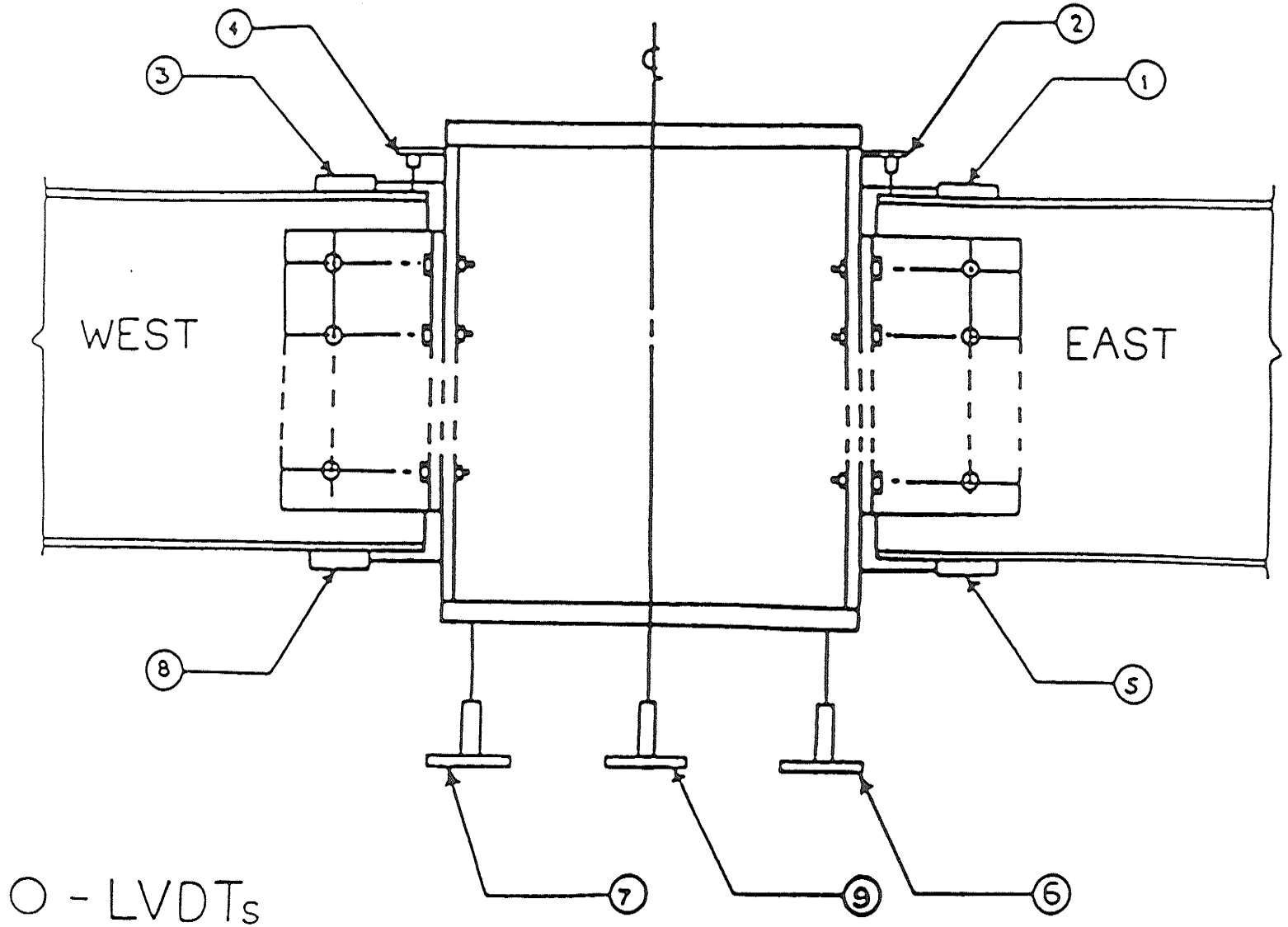

Figure 4.6: Locations of LVDTs.

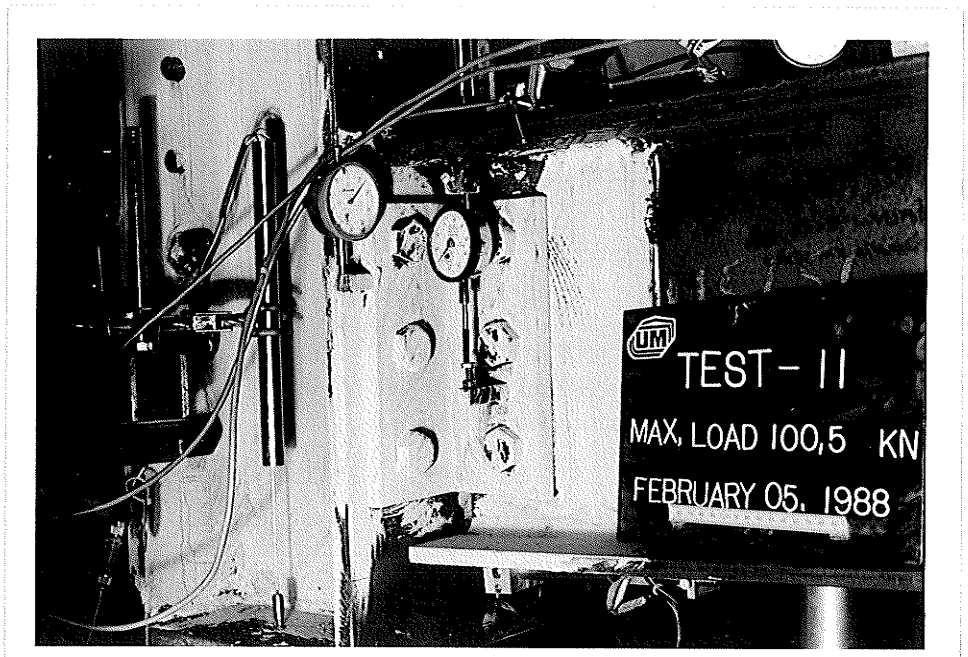

Figure 4.7: LVDT on the Centre Line of Column Stub and two Dial Gauges on the Column Flange and Beam Web.

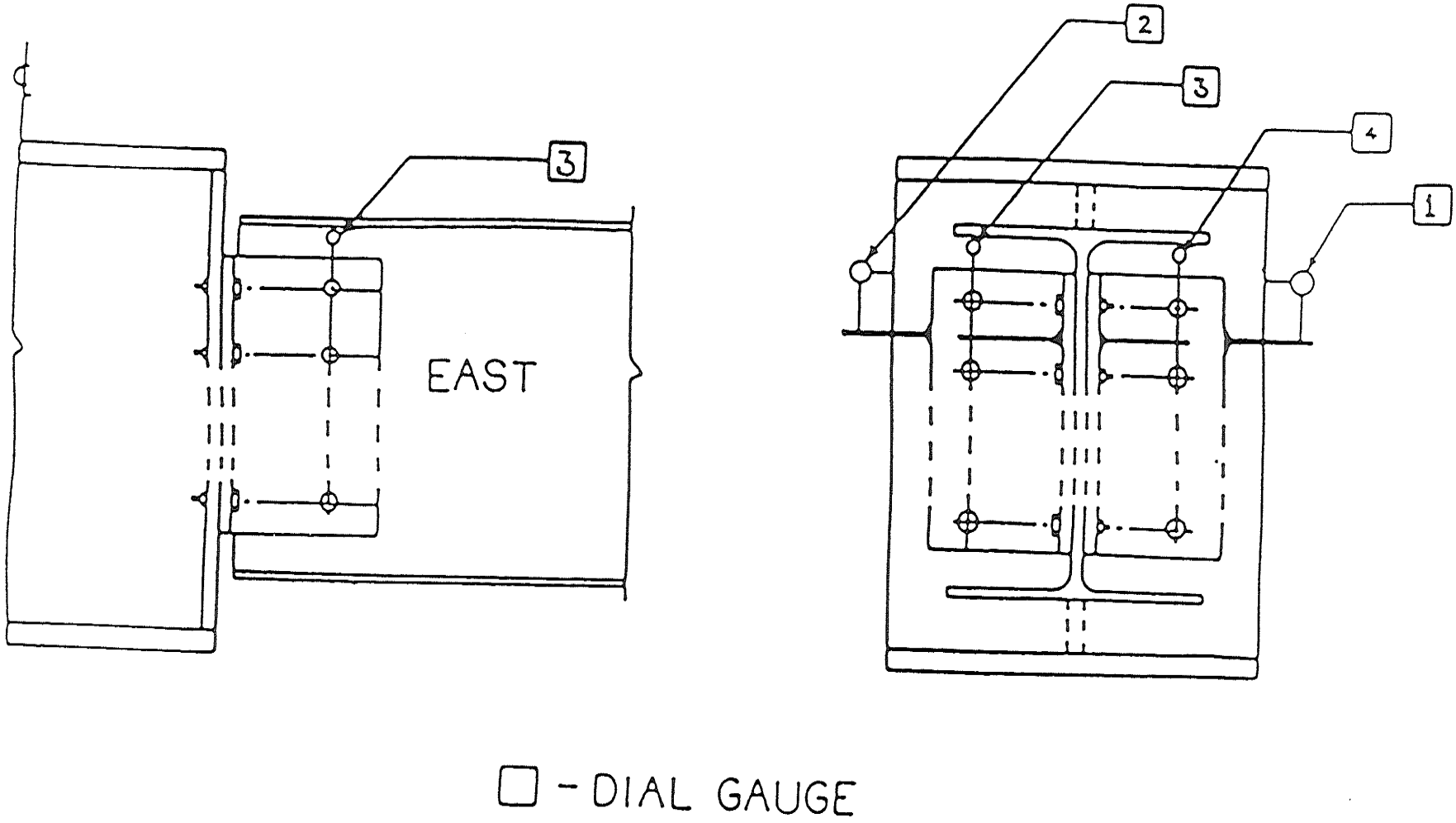

Figure 4.8: Locations of Dial Gauges.

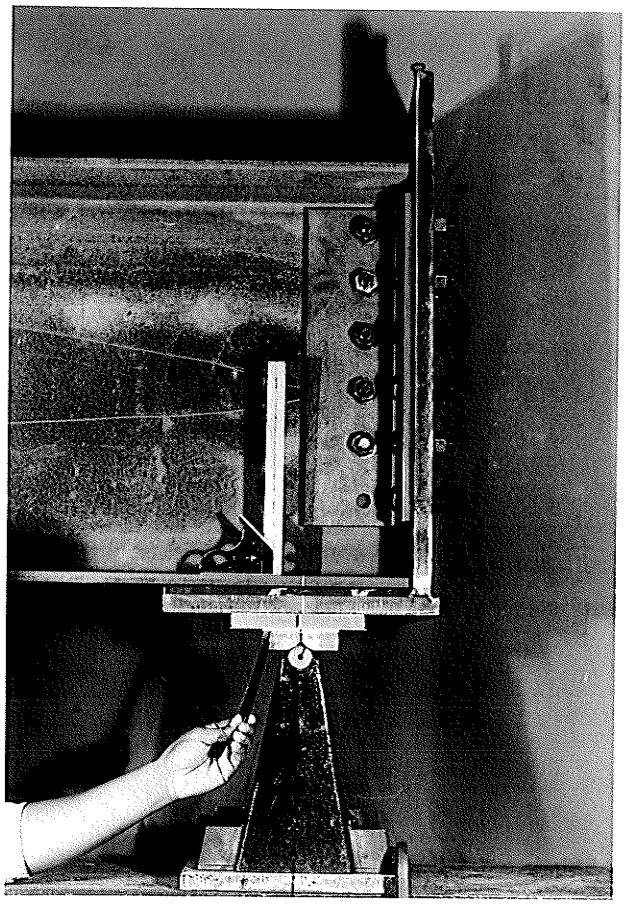

Figure 4.9: Support Arrangement.

CHAPTER 5

TEST RESULTS AND DISCUSSIONS

5.1 GENERAL

In this chapter, the test results are presented in tabular and graphical form. The general behaviour, common to all specimens, is described. Then the behaviour under test of each specimen in turn is discussed. Finally, comparisons are drawn among specimens, and the effects of the significant connection parameters are discussed.

5.2 GENERAL SPECIMEN BEHAVIOUR

In the discussion which follows, the term tension region is used to describe that portion of the connection in which the beam is pulling away from the column flange. The compression region is that area where the beam is displacing toward the column flange. The legs of the connecting angles that are bolted to the column flange are referred to as the "column legs" and those that are bolted to the beam web are referred to as the "beam legs".

Data on the behaviour of all of the test specimens are summarized in Table 5.1. The data include the initial slope of the moment-rotation curve (obtained graphically from the moment-rotation plots), the applied moment corresponding to a rotation of 0.024 radians, the maximum moment sustained, the maximum rotation sustained, and the mode of failure. The rotation of 0.024 radians is the maximum allowable for semi-rigid connections, according to North American steel design

specifications (Canadian Standards Association 1984, American Institute of Steel Construction 1983).

The connection moments were calculated by multiplying the span length by one-half of the applied load, on the assumption that the applied load was distributed equally to the two beam supports. The rotations were calculated twice. In the first method, the relative horizontal displacements between the top and bottom beam flanges and the column flange were summed and divided by the beam depth to give a measure of the rotational deformation in the connection. The second method employed the vertical displacements of the column stub, and the slope-deflection procedure employed by Ostrander (1970) and derived in Appendix A. The method gives the following equation for rotation as a function of deflection and applied load.

$$\phi = \frac{\Delta}{L} - \frac{PL^2}{6EI} \qquad (5.1)$$

where

ϕ = connection rotation,

Δ = vertical deflection,

L = span length,

P = applied load,

E = modulus of elasticity, and

I = second moment of area of the beam about its bending axis.

In the application of Equation (5.1), the load values corresponding to the occurrence of major bolt slip and to the contact between the beam and column flanges were not used.

The moment-rotation (M-Ø) curves, computed from horizontal displacement measurements, for all test specimens are presented in Figures 5.1 through 5.20 for the two sides, east and west, of the column stub. The close match between the curves for east and west is the result of the good agreement that was observed between the rotation values for the two sides. This suggests that the assumption of equal load distribution to the beam supports, used in calculating the moments, is justified.

Figures 5.21 and 5.22 each show two moment-rotation diagrams, one of which uses rotations computed from horizontal displacement measurements, as described above, the other of which uses rotations computed from vertical displacement measurements. The diagrams in Figure 5.21 are for Specimen 1B and those in Figure 5.22 are for Specimen 10. In both cases, the very good agreement between the curves is apparent. Comparisons showing similar good agreement between the two types of curves for the remaining test specimens are presented in Appendix B. Subsequent discussions and analysis involving the experimental moment-rotation curves are based on the curves computed from vertical displacement measurements.

Load-deflection curves obtained using three vertical LVDTs located on the centre line and below the two flanges of the stub column for Specimen 1B are shown in Figure 5.23. The curves are plotted up to the full travel of LVDTs 6 and 7, which were located beneath the column flanges. LVDT 9, which was located on the centre line of the column stub, had a larger travel. The three curves are virtually identical, indicating that there was very little rotation of the column during loading.

In all tests, relative rotational displacement, as illustrated in Figure 5.24, was observed between the beam legs of the connecting angles and the beam webs. After testing and dismantling of the test specimens, it was observed that the bolts in the tension region had experienced large shearing deformation. This is illustrated in Figures 5.25 and 5.26, which show A325 bolts and A307 bolts, respectively, removed from two of the test specimens.

All of the test specimens exhibited yielding along the bolt lines of the column legs of the angles, in the tension region. It is evident in Figure 5.27. The yielding was due to "prying action" in the column legs, restrained by the column flange bolts, as illustrated in Figure 5.28. Neither the column web nor the column flanges showed evidence of yielding, except in Specimen 4, the specimen which involved a light column section.

Vertical movements of the angle legs relative to the column flange and to the beam webs, which are usually

referred to as bolt slip, are summarized in Table 5.2. These data on bolt slip were recorded at the end of each test.

Figures 5.29 and 5.30 show typical plots of applied load versus vertical displacement of the column stub. The sharp drops in load on the curve in Figure 5.30, represent occurrences of bolt slip. The increase in slope at the end of the curves occurred when the beam compression flanges came into contact with the column flanges. Major slip of the bolts was accompanied by a loud noise.

In all tests, relative horizontal displacements occurred between the bottom beam flanges and the supports. For each test, the displacements were nearly the same for the beam segments on either side of the column stub. This was further indication that there was little rotation of the column during the loading of the specimens.

Most of the test specimens exhibited good ductility. However, the ductility of those specimens with A307 bolts was only about 62 percent of that of the specimens with A325 bolts. Figure 5.31 shows A325 and A307 bolts that experienced shear failure during the tests. All bolt failures were accompanied by a loud noise. Figure 5.32 shows a typical specimen after testing. Flexure of the angles was the primary source of failure.

The behaviour of individual test specimens is described below.

SPECIMEN 1A: During the test, major slip of the bolts occurred at moment values of approximately 60 and 78 kN-m. This is evident in Figure 5.1. After testing, the relative horizontal displacements between the bottom flanges of the beams and the supports were 27 mm at the east end and 28 mm at the west end of the beam. Yielding of the beam web was observed adjacent to the second bolt hole in the compression region (the second bolt from the top of the connecting angles). The yield pattern indicated principal compression strains at 45 degrees to the horizontal. Yielding was observed also around the second and third bolt holes in beam legs of the connecting angles. Two bolts in the tension region experienced high shearing deformation. The bolt holes were deformed to an oval shape. Major prying action of the angles in the tension region was observed. Failure of the test specimen was due to yielding of the angles.

SPECIMEN 1B: As is illustrated in Figure 5.2, the test specimen did not show evidence of bolt slip during the test. Yielding was observed in the beam web adjacent to the first bolt hole in the compression region. Yielding occurred along bolt lines in the column legs of the connecting angles in the tension region. Prying action of the angles in the tension region was observed. The specimen failed by yielding of the angles.

SPECIMEN 2: Major bolt slip occurred at moments of approximately 68 and 98 kN-m as shown in Figure 5.3. Yielding was not evident in the beam web. The angles showed evidence of yielding along the bolt lines in the column legs of the connecting angles. Prying action of the angles, in the tension region, was observed. Very large rotational displacement between the beam legs of the angles and the beam webs was observed. The relative horizontal displacements between the bottom flanges of the beams, and the supports, were 30 and 28 mm at the east and west supports, respectively. The failure of the specimen was due to prying action in the angles.

SPECIMEN 3: No evidence of angle yielding was observed. However, slip was evident between the beam web and the beam legs of the connecting angles in the tension region. It can be observed in Figure 5.4 that no sudden slip occurred during the test. Two beam-web bolts from the tension region of the east beam segment, sheared off mid-way through the test. The horizontal displacements of the bottom flanges of the beams relative to the supports were 20 and 25 mm at the east and west ends, respectively. The specimen failed by shearing of bolts in the tension region.

SPECIMEN 4: Major bolt slip occurred at a moment of 85 kN-m, as illustrated in Figure 5.5. The column experienced large flange and web deformation, as can be seen in Figure

5.33. Two of the dial guages used to measure the flange deformation went off range during the test. Yielding was observed around the bolt holes in the column legs of the connecting angles, and also around the bolt holes in the column flange. Yielding was observed on the interior surface of the column flange. Failure was due to extensive yielding of the angles, the column web and the column flange.

SPECIMEN 5: The test specimen was subjected to four cycles of loading and unloading. It can be observed from Figure 5.6 that the stiffness (the slope of the moment-rotation curve) on unloading and reloading was approximately equal to the initial stiffness. Bolt slip occurred at moments of 65 and 95 kN-m. Yielding occurred in the beam web adjacent to the second bolt in the compression region. Yielding of the connecting angles was not evident. The specimen failed by large bolt deformation in the tension region.

SPECIMEN 6: This specimen was assembled with A307 bolts. As is evident in Figure 5.7, bolt slip occurred at a moment of 75 kN-m. There was no apparent yielding of the beam web or the connection angles. Two beam-web bolts in the tension region, and one in the compression region, of the connection on the east side, sheared off. There was large rotational displacement between the beam legs of the

angles and the beam webs. Failure was due mainly to the shearing off of the beam-web bolts.

SPECIMEN 6A: The specimen was assembled with A307 bolts and was loaded through four cycles of loading and unloading. As illustrated in Figure 5.8, the unloading and reloading connection stiffnesses were virtually identical, through three cycles, to the initial stiffness. In the final cycle, the stiffness declined slightly. No bolt slip occurred during the test. There was no evidence of connection angle deformation. However, there was large shearing deformation of the bolts. Two bolts from the tension region on the west side of the specimen sheared off during testing. The specimen failed because of high shearing deformation in the beam-web bolts in the tension region.

SPECIMEN 7: As can be observed in Figure 5.9, bolt slip was not evident. The beam web did not show evidence of yielding, but the column legs of the connecting angles yielded along the bolt lines. Some prying action of the angles was observed. The yielding of the connection angles was the main source of failure.

SPECIMEN 8: Minor bolt slip occurred at moments of 43 and 140 kN-m, as is illustrated in Figure 5.10. The beam legs of the connecting angles experienced visible deformation in the tension region. Large rotational

displacement of the beam legs of the angles relative to the beam web was observed. The column legs showed no evidence of yielding. Large shearing deformation occurred in the bolts in the tension region. Failure was attributed to the shearing of the bolts in the tension region.

SPECIMEN 9: Major bolt slip was observed at moments between 23 and 35 kN-m, as illustrated in Figure 5.11. Yielding was observed in the beam web adjacent to the first bolt in the compression region. The angles developed prying action in the tension region. The specimen failed by yielding of the angles.

SPECIMEN 10: The test specimen showed no evidence of bolt slip. The moment-rotation plot for the specimen is shown in Figure 5.12. One yield line, at 45 degrees to the horizontal axis of the beam segment, appeared on the beam web adjacent to the first bolt in the compression region of the east beam segment. The angles did not show evidence of yielding along the bolt lines on the beam legs, but prying action of the angles was evident in the tension region. Yielding of the angles was the major source of failure.

SPECIMEN 11: As illustrated in Figure 5.13, no sudden bolt slip occurred. Yielding of the beam web was observed adjacent to the first bolt in the compression region. Neither the column legs, nor the beam legs of the

connecting angles showed evidence of yielding. Failure of the specimen was due to bolt shear in the tension region.

SPECIMEN 12: A malfunction of the testing machine occurred during the initial period of loading. However, as evident from the moment-rotation curve in Figure 5.14, major bolt slip occurred at four different moment levels between 20 and 38 kN-m. Yielding was observed in the beam web adjacent to the first bolt in the compression region. The beam legs of the connecting angles showed no evidence of yielding, but the column legs yielded along the bolt line. Prying action of the angles in the tension region was observed. The specimen failed by the yielding of the connection angles.

SPECIMEN 13: As illustrated in Figure 5.15, bolt slip occurred twice, at moments between 20 and 25 kN-m. The beam legs of the angles showed no evidence of yielding. However, yielding was observed in the column legs of the angles. Prying action of the angles occurred in the tension region. The connection failed by the yielding of the angles in the tension region.

SPECIMEN 14: As can be seen from Figure 5.16, bolt slip was not evident during the test. Yielding occurred in the beam web adjacent to the first bolt in the compression region. There was substantial rotational displacement

between the beam legs of the angles and the beam webs. The angles showed no evidence of yielding. The connection failure was due to the shearing of bolts in the tension region.

SPECIMEN 15: Major bolt slip occurred at moments between 42 and 62 kN-m. Minor slip was observed at moments greater than 62 kN-m. These observations are illustrated in Figure 5.17. Yielding was observed along the bolt lines in both the beam legs and column legs of the connecting angles. Prying action of the angles in the tension region was observed. The portion of the beam web adjacent to the first bolt in the compression region showed evidence of yielding. The connection failed by yielding of the connection angles.

SPECIMEN 16: Major bolt slip occurred at moments of 53 and 90 kN-m. This is evident from the moment-rotation curve in Figure 5.18. The beam web did not show evidence of yielding. However, some yielding was observed along the bolt lines in both the beam and column legs of the angles. Prying action occurred in the tension region. Failure was due to a combination of yielding of the angles and shearing deformation of bolts in the tension region.

SPECIMEN 18: As illustrated in Figure 5.19, bolt slip was not evident. As well, no yielding of the connection angles was observed. Small rotational displacement was

observed between the beam legs and the beam webs. Failure was due to the shearing deformation of the beam-web bolts in the tension region.

SPECIMEN 19: As shown in Figure 5.20, no bolt slip was evident. No evidence of yielding was observed, either in the connection angles or in the beam web. Rotational displacement was observed between the beam legs and the beam webs. The first two bolts in the tension region of the connection on the east side sheared off, as illustrated in Figure 5.34. Shearing of bolts was the primary cause of failure.

5.3 EFFECTS OF CONNECTION PARAMETERS

The effects of the pertinent connection parameters are discussed in turn.

5.3.1 BEAM DEPTH

Specimens 10 and 13, 11 and 14, 9 and 12, and 1B and 16, were used to determine the effects of beam depth on the moment-rotation behaviour. The two specimens of each pair were similar except for their beam sections.

Specimens 10 and 13 had W310X52 and W460X82 beam sections, respectively. Both had 8 mm thick angles. Figure 5.35 shows the moment-rotation curves for the two specimens. From Table 5.1, it can be observed that the initial slope, the moment at 0.024 radians, the maximum moment and the

maximum rotation sustained by the Specimen 10 connections were 2,450, 20.9, 35.2 and 0.092, respectively. Specimen 13 connections had 2,780, 19.6, 27.4 and 0.077 for the initial stiffness, the moment at 0.024 radians, the maximum moment and the maximum rotation. The initial stiffness and the moment capacity for the two specimens were not significantly affected by variation in the beam depth. The maximum rotation for the Specimen 10 connections was 19 percent higher than that for Specimen 13. The degradation in the maximum rotation for the Specimen 13 connections was probably due to the occurrence of major slip. The moments at a rotation of 0.024 radians were approximately the same for the two specimens.

Specimens 9 and 12 had W310X52 and W460X82 beam sections, respectively. Both specimens had 10 mm thick angles. Due to a temporary malfunction of the testing machine, the initial stiffness was not determined for the connections of Specimen 12. As a result, a detailed comparison of Specimens 9 and 12 was not possible. However, they both sustained a moment of 26 kN-m at a rotation of 0.024 radians.

Specimen 16 had a W610X101 beam section, while Specimen 1B employed a W460X82. Both had 10 mm thick angles. Figure 5.36 shows the moment-rotation curves for Specimens 1B and 16. It can be observed in Table 5.1 that the initial stiffness, the moment at 0.024 radians, the maximum moment and the maximum rotation sustained by the connections of

Specimen 16 were 20,890, 78.2, 110.8 and 0.067, respectively. The corresponding values for the connections of Specimen 1B were 11,000, 78.2, 124.1 and 0.076. The Specimen 16 connections had slightly larger initial stiffness. However, the Specimen 1B connections sustained larger moment capacity and larger maximum rotation. The moment-rotation behaviour was not significantly affected by the change in depth. For both specimens, a moment of 78.0 kN-m produced a rotation of 0.024 radians.

Specimens 11 and 14 had W310X52 and W460X82 beam sections, respectively. Both specimens had 12 mm thick angles. Figure 5.37 shows the moment-rotation curves for the two. It can be observed in Table 5.1, that the initial slope, the maximum moment, the maximum rotation, and the moment at 0.024 radians, were larger for the connections of Specimen 14 than for those of Specimen 11. Specifically, the connections of Specimen 14 had a 10 percent larger initial stiffness, and a 50 percent larger moment at a rotation of 0.024 radians. The initial stiffness and the moment-rotation were not significantly affected by the change in the beam depth. The maximum rotation for the Specimen 14 connections was 8 percent higher than that for Specimen 11.

In summary, the influence of beam depth on the moment-rotation behaviour of the connection was negligible for those connections with 8 and 10 mm thick angles. For the connections with 12 mm thick angles, the connection

stiffness and moment resistance both increased with an increase in beam depth.

5.3.2 ANGLE THICKNESS

Specimens 13 and 14, 10 and 11, 1B, 2 and 3, and 18 and 19, were used to determine the influence of the angle thickness on the moment-rotation behaviour. The specimens in each group were similar except for their angle thickness.

Specimens 13 and 14 had 8 and 12 mm thick angles, respectively. Both had three bolts per angle leg. The moment-rotation curves for Specimens 13 and 14 are shown in Figure 5.38. The initial stiffness, the moment at 0.024 radians, the maximum moment and the maximum rotation for the Specimen 14 connections, as shown in Table 5.1 were 5,760, 43.0, 57.7 and 0.068, respectively. The corresponding values for the Specimen 13 connections were 2,780, 19.6, 27.4 and 0.077. It can be observed in Table 5.1 that the initial stiffness for the Specimen 14 connections was 107 percent larger than that for Specimen 13. The moment resistance of the connections of Specimen 14 at a rotation of 0.024 radians was 120 percent larger than that for Specimen 13. The maximum rotation was 12 percent smaller than that for Specimen 13. The moment-rotation behaviour was significantly affected by the increase in angle thickness.

Specimens 10 and 11 had 8 and 12 mm thick angles, respectively. The two specimens had three vertical bolts per angle leg. The moment-rotation curves for Specimens 10 and

11 are shown in Figure 5.39. The initial stiffness, the moment at 0.024 radians, the maximum moment and the maximum rotation for the Specimen 11 connections, as shown in Table 5.1, were 3,240, 28.7, 41.1 and 0.063, respectively. Those for the Specimen 10 connections were 2,450, 20.9, 35.2 and 0.092. Thus, the Specimen 11 connections were stiffer than those for Specimen 10 by 32 percent. The maximum rotation sustained by the Specimen 11 connections was, however, smaller than that for the Specimen 10 ones by 31 percent. Specimen 11 connections had 38 percent larger moment at a rotation of 0.024 radians. The moment-rotation behaviour was significantly affected by the change in the angle thickness.

Specimens 2, 1B and 3 had 8, 10 and 12 mm thick angles, respectively. All of the specimens had five bolts per angle leg. The moment-rotation curves for the three specimens are shown in Figure 5.40. The initial stiffness, the moment at 0.024 radians, the maximum moment and the maximum rotation for the Specimen 1B connections as shown in Table 5.1 were 11,000, 78.2, 124.1 and 0.076, respectively. The corresponding values for the Specimen 3 connections were 14,280, 95.8, 126.1 and 0.055. It can be seen that the initial stiffnesses for the connections of Specimen 3 were 85 and 30 percent higher than those for Specimens 2 and 1B, respectively. The moment at 0.024 radians for the Specimen 3 connections was 36 and 23 percent higher than those for Specimens 2 and 1B, respectively. The moment-rotation behaviour was significantly affected by the change in angle

thickness.

Specimens 18 and 19 had 8 and 12 mm thick angles, respectively. Both specimens had six bolts in a vertical line per angle leg. Figure 5.41 shows the moment-rotation curves for the two specimens. The initial stiffness, the moment at 0.024 radians, the maximum moment and the maximum rotation for the Specimen 19 connections, as shown in Table 5.1, were 18,520, 152.5, 174.6 and 0.035, respectively. The corresponding values for the Specimen 18 connections were 20,777, 100.4, 130.3 and 0.041. It can be seen therefore that the Specimen 19 connections had approximately the same initial stiffness as those for Specimen 18, and 52 percent larger moment resistance corresponding to a rotation of 0.024 radians. The maximum moment sustained by the Specimen 19 connections was 34 percent larger than that for Specimen 18. The initial stiffness was not significantly affected. However, a significant effect in the inelastic region of the moment-rotation curve was observed.

In summary, increasing the angle thickness increased both the stiffness and the maximum moment sustained by the connection. The effect of the angle thickness on the moment-rotation behaviour was most pronounced when a thick angle was used in conjunction with a deep beam.

5.3.3 NUMBER OF BOLTS

Specimens 13 and 2, 1B and 15, and 3 and 14, were used to study the effect of the number of bolts per angle leg on

the moment-rotation behaviour. The two specimens of each pair were similar except for the number of bolts in a vertical line per angle leg.

Specimens 13 and 2 had three and five bolts per angle leg, respectively, in a vertical row. Both specimens had 8 mm thick angles. Figure 5.42 shows the moment-rotation curves for the two specimens. The initial stiffness, the moment at 0.024 radians, the maximum moment and the maximum rotation for the Specimen 2 connections, as shown in Table 5.1, were 7,710, 70.4, 106.5 and 0.073, respectively. Those for the Specimen 13 connections were 2,780, 19.6, 27.4 and 0.077, respectively. It can be seen therefore that the Specimen 2 connections were stiffer than those for Specimen 13 by 177 percent. However, the Specimen 13 connections demonstrated slightly greater ductility. The initial stiffness, the maximum moment sustained and the moment-rotation behaviour were significantly affected by the change in the number of bolts per angle leg.

Specimens 1B and 15 had five and four bolts per angle leg, respectively. Both specimens had 10 mm thick angles. Figure 5.43 shows the moment-rotation curves for the two specimens. The initial stiffness, the moment at 0.024 radians, the maximum moment and the maximum rotation for the Specimen 1B connections, as shown in Table 5.1, were 11,000, 78.2, 124.1 and 0.076, respectively. The corresponding values for the Specimen 15 connections were 10,650, 52.8, 94.8 and 0.080. It can be seen therefore that the Specimen

1B connections sustained a 31 percent larger maximum moment than those for Specimen 15. Furthermore, the Specimen 1B connections had a slightly larger initial stiffness. The moment-rotation behaviour was significantly affected by the change in the number of bolts per angle leg.

Specimens 3 and 14 had five and three bolts per angle leg, respectively. Both specimens had 12 mm thick angles. Figure 5.44 shows the moment-rotation curves for the two specimens. The initial stiffness, the moment at 0.024 radians, the maximum moment and the maximum rotation for the Specimen 3 connections, as shown in Table 5.1, were 14,280, 95.8, 126.1 and 0.055, respectively. The corresponding values for the Specimen 14 connections were 5,760, 43.0, 57.7 and 0.068. It can be observed therefore that the Specimen 3 connections had a 48 percent larger initial stiffness than those for Specimen 14. The Specimen 3 connections also had 123 percent larger moment at 0.024 radians than those for Specimen 14. The initial stiffness, the moment capacity and the moment-rotation behaviour were significantly affected by the change in the number of bolts per angle leg.

In summary, the number of bolts per angle leg has a great influence on the moment-rotation behaviour. The maximum moment sustained was increased by 289 percent when the number of bolts per angle leg was increased from three to five.

5.3.4 GAUGE OF COLUMN BOLTS

The specimens used to determine the influence of column gauge on the moment-rotation behaviour were 1B, 7 and 8. The three specimens had similar connection parameters except for the column gauges.

Column gauges of 100, 130 and 140 mm, were used in Specimens 8, 7 and 1B, respectively. The three specimens had five bolts per angle leg and 10 mm thick angles. Figure 5.45 shows the moment-rotation curves for the three specimens. The initial stiffness, the moment at 0.024 radians, the maximum moment and the maximum rotation for the Specimen 8 connections, as shown in Table 5.1, were 11,587, 89.9, 140.7 and 0.084, respectively. The corresponding values for the Specimen 7 connections were 11,011, 70.4, 137.8 and 0.072. The values for the Specimen 1B connections were 11,000, 78.2, 124.1 and 0.076. It can be seen that the Specimen 8 connections had slightly larger initial stiffnesses than those for Specimens 7 and 1B. The stiffnesses of the connections of Specimens 1B and 7 were virtually the same. The Specimen 8 connections sustained larger moment capacity and larger rotation than those for Specimens 1B and 7. The large clearance between the beam flange and the column flange probably was the reason for such differences. It can be seen that a decrease in column gauge from 140 to 100 mm, caused an increase of 13 percent in the maximum moment and virtually no change in the initial stiffness.

The initial stiffness of the connections was not significantly affected by the change in the column bolt gauge. However, a slight increase in the moment capacity can be expected when the gauge is decreased from 140 to 100 mm.

5.3.5 TYPE OF FASTENER

Specimens 5 and 6A, and 1B and 6, were used to study the effects of fasteners on the moment-rotation behaviour. The two specimens of each pair were similar except for the fasteners used.

Specimens 5 and 6A had 10 mm thick angles. The two specimens were subjected to four cycles of loading and unloading. Specimen 5 had A325 bolts whereas Specimen 6A had A307 bolts. The initial stiffness, the moment at 0.024 radians, the maximum moment and the maximum rotation for the Specimen 5 connections, as shown in Table 5.1, were 16,490, 89.5, 137.0 and 0.084, respectively. The values for the Specimen 6A connections were 11,710, 52.8, 74.3 and 0.042. The initial stiffness was not significantly affected. The Specimen 5 connections sustained larger moment capacity and larger rotation than those for Specimen 6A. The different methods of bolt tightening probably contributed to the degradation in the moment and the rotation in the Specimen 6A connections.

Specimens 1B and 6 had 10 mm thick angles and were subjected to a monotonic loading. Specimen 1B had A325 bolts while Specimen 6 had A307 bolts. The initial stiffness, the

moment at 0.024 radians, the maximum moment and the maximum rotation for the Specimen 1B connections, as shown in Table 5.1, were 11,870, 78.2, 124.1 and 0.076, respectively. The corresponding values for the Specimen 6 connections were 12,123, 64.4, 88.0 and 0.041. The maximum rotation and the maximum moment sustained by the Specimen 1B connections were larger than those for Specimen 6 by 86 and 41 percent, respectively. The different methods of bolt tightening probably contributed to the differences. However, the Specimen 6 connections had a 2 percent larger initial stiffness.

The moment-rotation behaviour was significantly affected by the type of bolts used in the connections. The ductility of the connections is increased significantly if A325 bolts, as opposed to A307 bolts, are used.

5.3.6 TYPE OF LOADING

The specimens used to determine the effects of the type of loading on the moment-rotation behaviour were 6 and 6A, and 1B and 5. The two specimens of each pair were similar except for the type of loading.

Specimens 6 and 6A had 10 mm thick angles. Monotonic loading was applied to Specimen 6 while Specimen 6A was subjected to a repeated loading. The initial stiffness, the moment at 0.024 radians, the maximum moment and the maximum rotation for the Specimen 6 connections, as shown in Table 5.1, were 12,130, 64.4, 88.0 and 0.041, respectively. The

values for the Specimen 6A connections were 11,710, 52.8, 74.3 and 0.042. The Specimen 6 connections had 4 percent larger initial stiffness and 22 percent larger moment at 0.024 radians than those for the Specimen 6A. The initial stiffness and the moment capacity were not affected negatively by repeated loading. In fact, the moment capacity for the Specimen 5 connections was higher than that for Specimen 1B. The stiffness after repeated loading was maintained through the testing.

Specimens 1B and 5 had 10 mm thick angles. Specimen 5 was subjected to four cycles of loading and unloading, whereas monotonic loading was applied to Specimen 1B. The initial stiffness, the moment at 0.024 radians, the maximum moment and the maximum rotation for the Specimen 5 connections, as shown in Table 5.1, were 16,490, 89.5, 137.0 and 0.084, respectively. The corresponding values for the Specimen 1B connections were 11,870, 78.2, 124.1 and 0.076. It can be seen that the Specimen 5 connections had a 39 percent larger initial stiffness and 15 percent larger moment at 0.024 radian rotation than those for Specimen 1B. While the moment on the WEST side for the Specimen 6 connections was larger than that for Specimen 6A, the moment-rotation behaviour appeared not to be significantly affected by repeated loading. The slight degradation of stiffness for Specimen 6A after several load cycles was probably due to deformation around bolts.

Repeated loading applied to connections with A325 and A307 bolts do not influence the moment-rotation behaviour significantly.

5.4 SUMMARY OF RESULTS AND CONCLUSIONS

All of the test specimens behaved nonlinearly even at low load levels. The maximum rotations for all connections were between 0.035 to 0.084 radians. The maximum moment ranged from 27 to 174 kN-m. All of the connections were able to sustain a rotation of 0.024 radians, the minimum allowable for semi-rigid connections.

Ten specimens failed by shearing deformations of the beam-web bolts, caused by the high bearing stresses on the bolts by the beam web, as the specimens were loaded, nine by the yielding of the connection angles, and one by the prying action of the angles in the tension region.

In view of the observations discussed above, it can be concluded that the angle thickness and the number of bolts per angle leg had greater influence on the connection behaviour than the other connection parameters considered namely, the beam depth, the gauge of column bolts, the type of fasteners and the type of loading.

TABLE 5.1: SUMMARY OF TEST RESULTS.

Specimen number	Initial Slope of M-Ø curve (kN-m/rad)	Moment at 0.024 radians (kN-m)	Maximum moment (kN-m)	Maximum rotation (radians)	Mode of failure	Remarks
1A	11,020	79.17	105.56	0.0587	Yielding of the connection angles.	-
1B	11,000	78.19	124.13	0.0760	Yielding of the connection angles.	-
2	7,710	70.37	106.53	0.0729	Prying action of the angles.	-
3	14,280	95.78	126.10	0.0546	Bolt-shearing deformation.	Two bolts sheared-off.
4	11,870	78.19	103.60	0.0711	Yielding of the connection angles.	-
5*	13,514	89.51	137.00	0.0841	Bolt-shearing deformation.	-
6	12,130	64.41	87.96	0.0409	Bolt-shearing deformation.	Two bolts sheared-off.
6A*	11,710	52.78	74.29	0.0418	Bolt-shearing deformation.	Two bolts sheared-off.
7	11,011	70.38	137.81	0.0724	Yielding of the connection angles.	-
8	11,587	89.92	140.74	0.0843	Bolt-shearing deformation.	-
9	2,920	26.07	44.31	0.0751	Yielding of the connection angles.	-
10	2,450	20.85	35.19	0.0921	Yielding of the connection angles.	-

TABLE 5.1 (continued)

Specimen number	Initial slope of M-Ø curve (kN-m/rad)	Moment at 0.0024 radians (kN-m)	Maximum moment (kN-m)	Maximum rotation (radian)	Mode of failure	Remarks
11	3,914	28.67	41.05	0.0633	Bolt-shearing deformation.	-
12	-	26.66	34.48	0.0504	Yielding of the connection angles.	-
13	2,780	19.55	27.37	0.0773	Yielding of the connection angles.	-
14	4,277	43.01	57.66	0.0682	Bolt-shearing deformation.	-
15	10,650	52.78	94.80	0.0797	Yielding of the connection angles.	-
16	20,089	78.20	110.77	0.0672	Bolt-shearing deformation.	-
18	20,777	100.35	130.32	0.0412	Bolt-shearing deformation.	-
19	18,520	152.48	174.63	0.0350	Bolt-shearing deformation.	Two bolts sheared-off.

NOTE:

* Repeated Loading.

TABLE 5.2: TOTAL SLIP AT THE END OF TEST.

Specimen number	Slip between column flange and angle leg (mm)		Slip between beam web and angle leg (mm)	
	East	West	East	West
1A	0.02	0.33	0.13	0.13
1B	0.10	0.30	0.25	0.13
2	0.01	0.09	0.23	0.13
3	0.09	0.04	0.00	0.13
4	0.22	0.02	0.00	0.00
5	0.25	0.38	0.38	0.25
6	0.09	0.06	0.43	0.28
6A	0.03	0.04	0.48	0.31
7	0.15	0.46	0.18	0.25
8	0.16	0.20	0.41	0.20
9	0.08	0.41	0.51	0.25
10	0.01	0.01	0.03	0.23
11	0.12	0.06	0.23	0.31
12	0.04	0.09	0.05	0.51
13	0.07	0.01	0.25	0.28
14	0.10	0.08	0.08	0.15
15	0.11	0.21	0.13	0.05
16	0.05	0.07	0.03	0.03
18	0.01	0.05	0.03	0.13
19	0.03	0.11	0.15	0.18

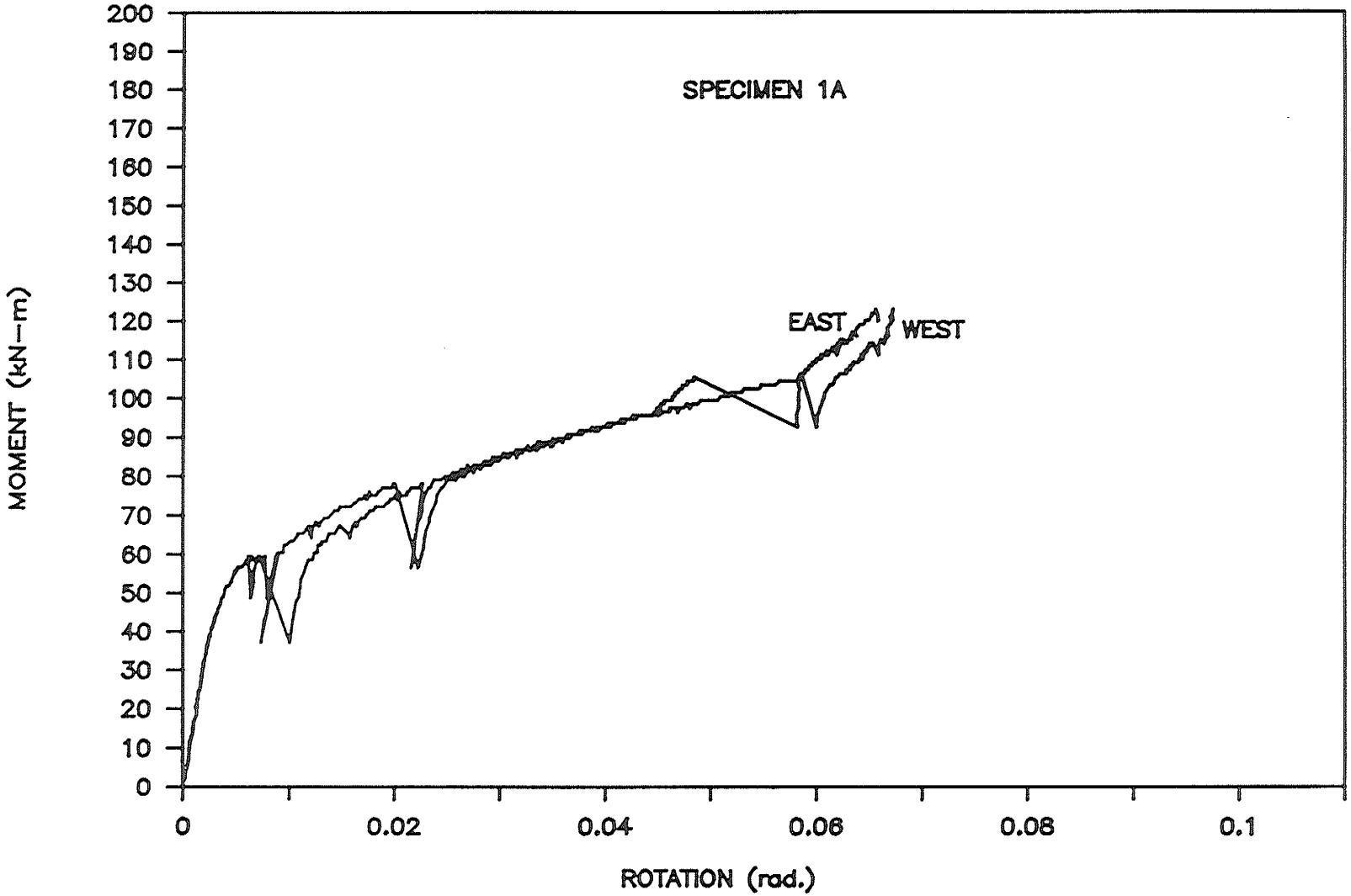

Figure 5.1: Moment-Rotation Curves for Specimen 1A.

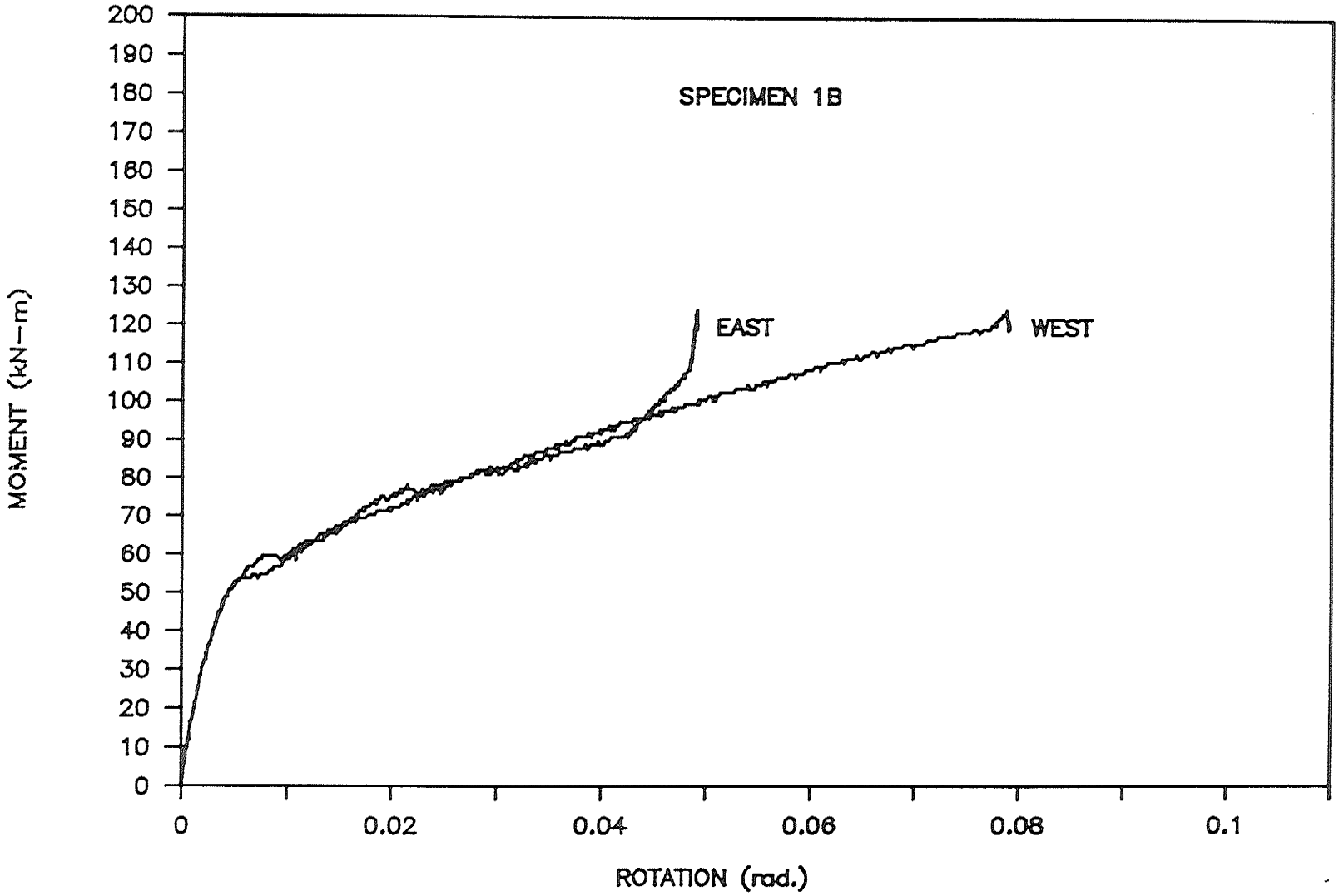

Figure 5.2: Moment-Rotation Curves for Specimen 1B.

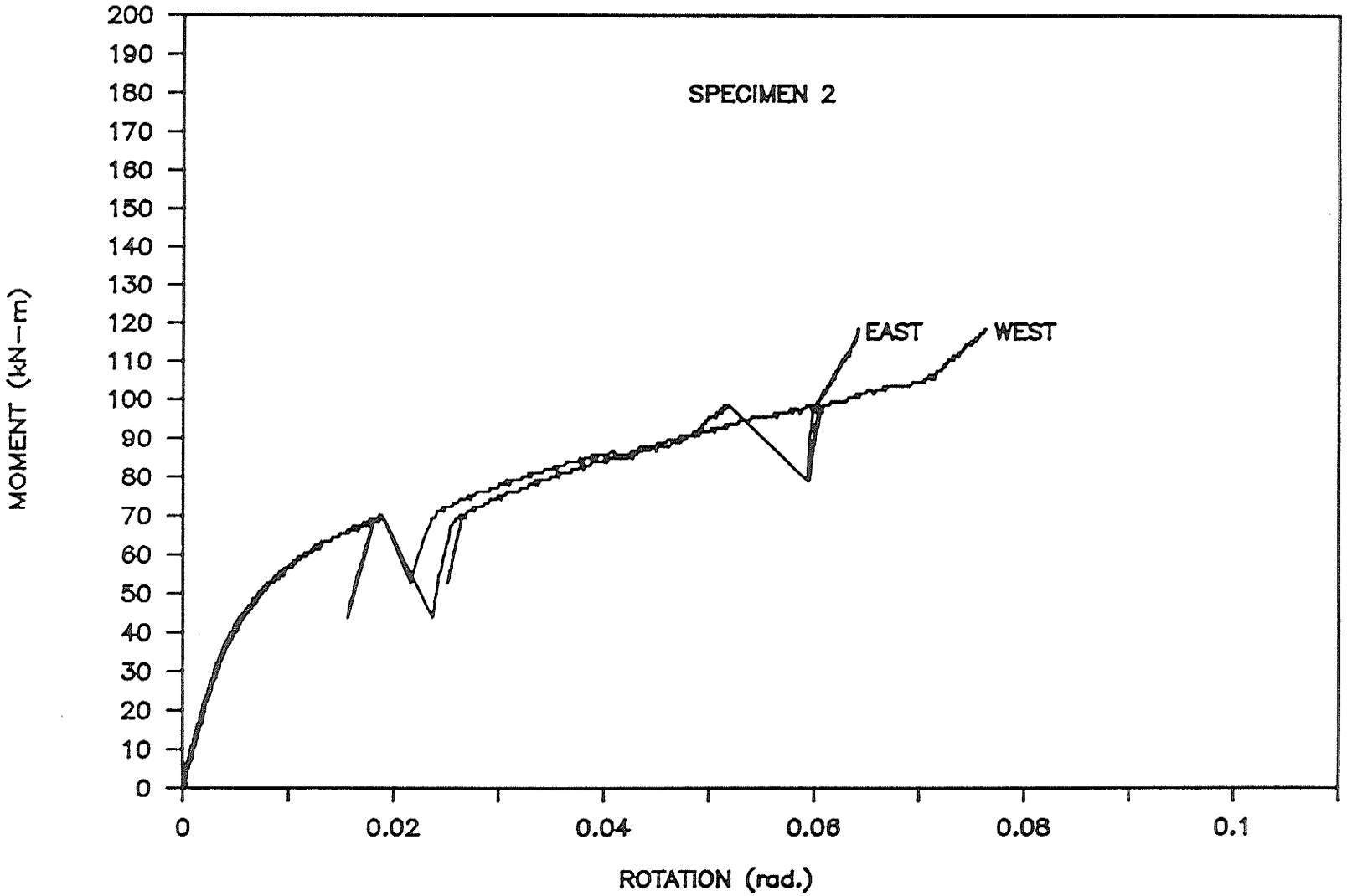

Figure 5.3: Moment-Rotation Curves for Specimen 2.

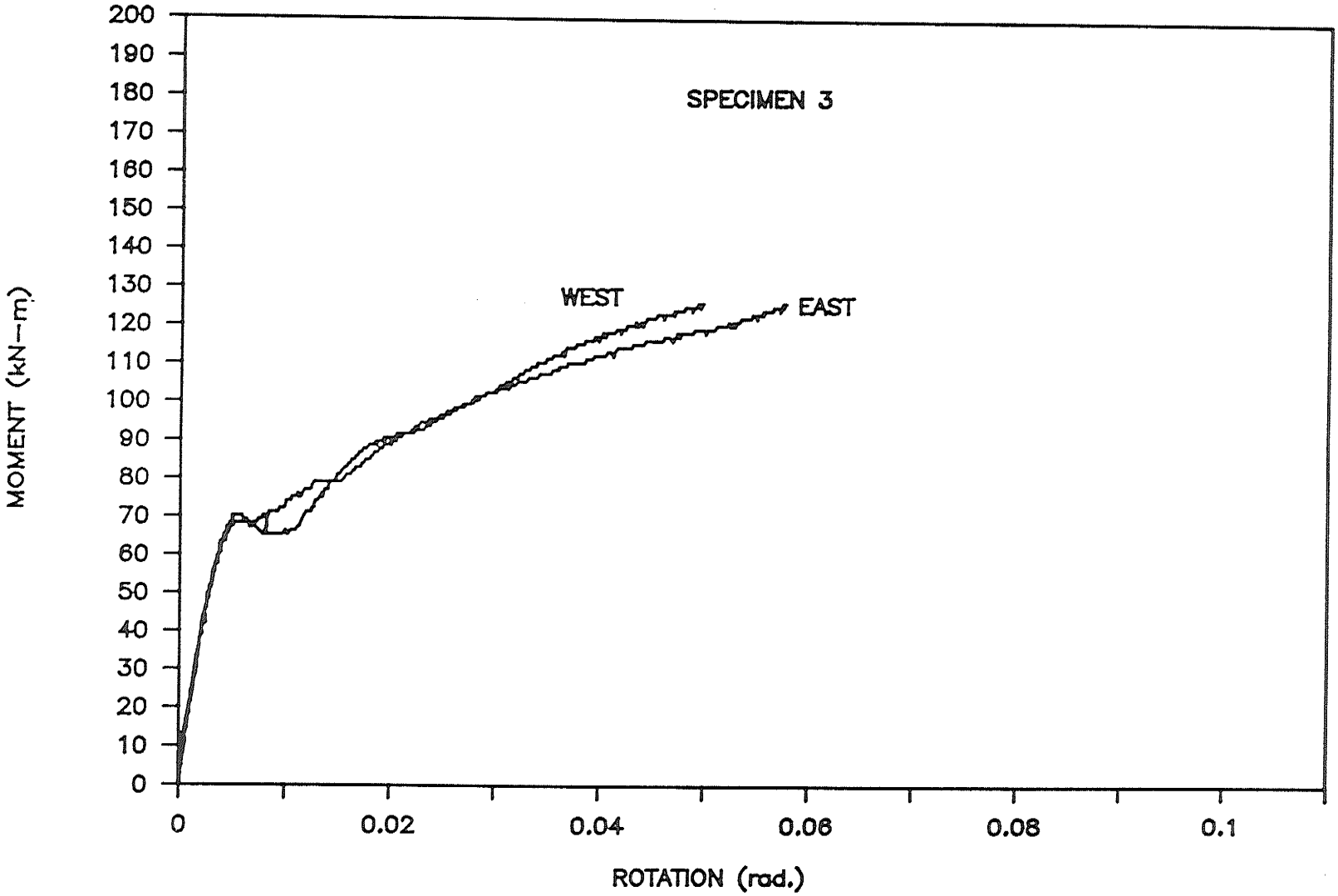

Figure 5.4: Moment-Rotation Curves for Specimen 3.

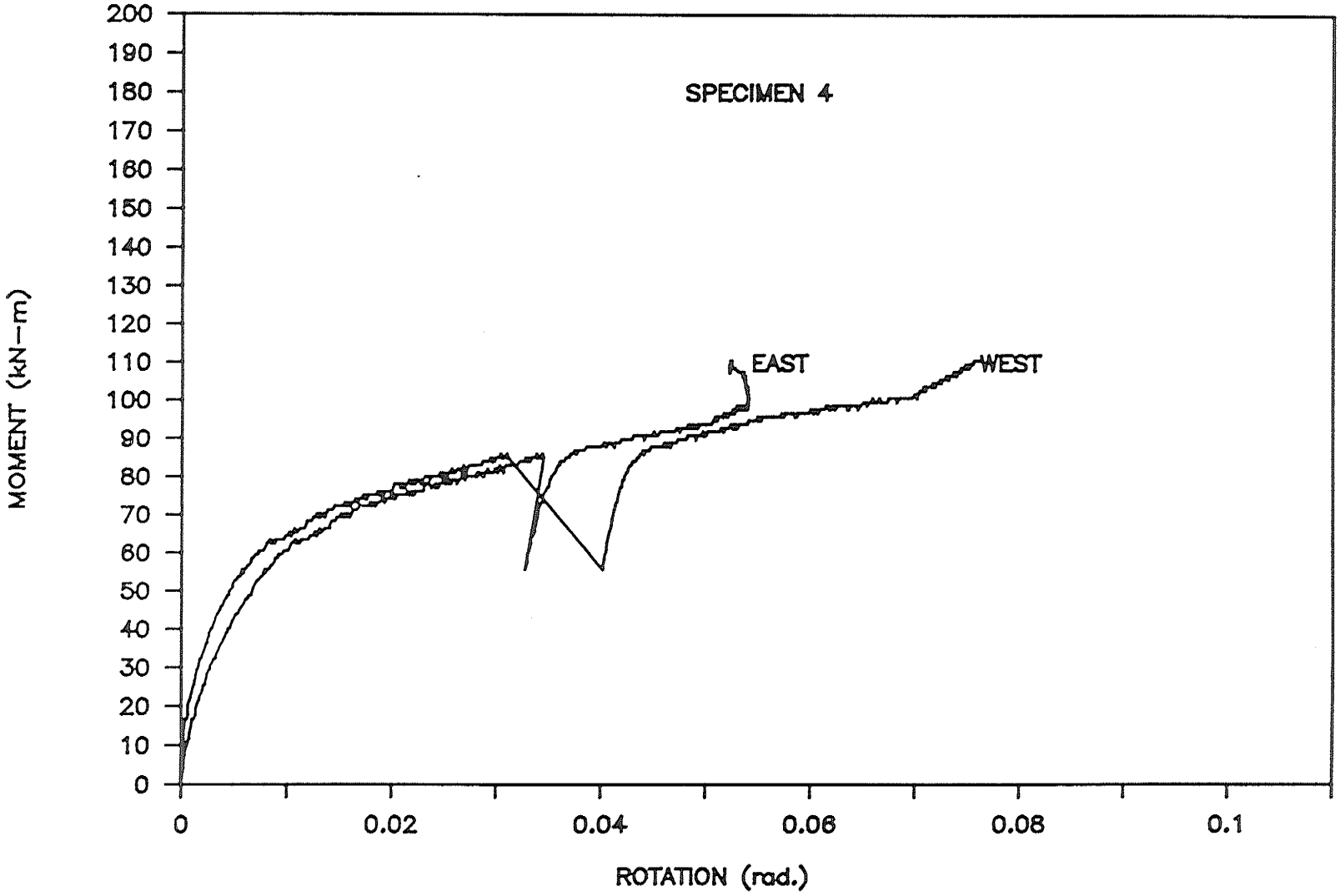

Figure 5.5: Moment-Rotation Curves for Specimen 4.

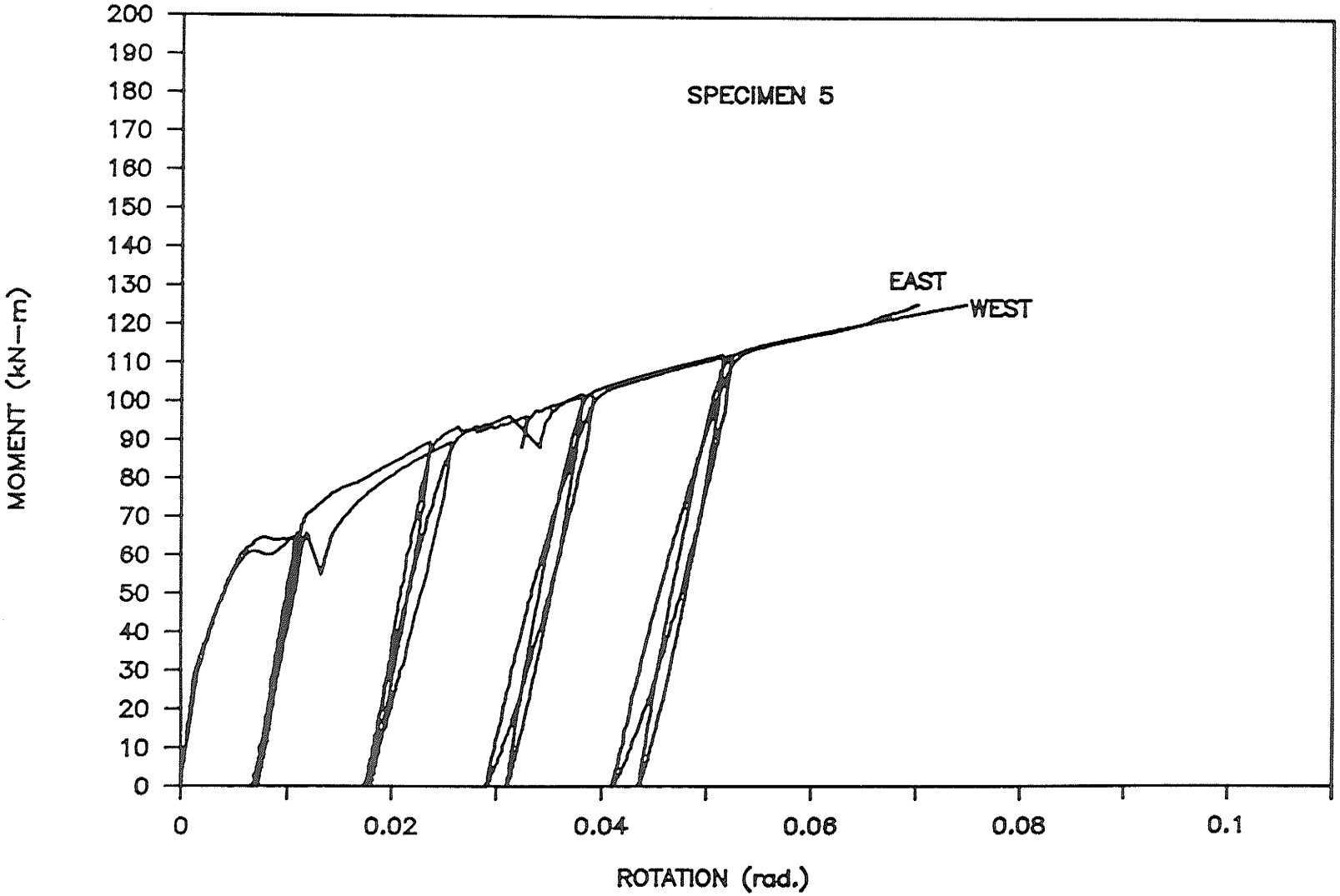

Figure 5.6: Moment-Rotation Curves for Specimen 5.

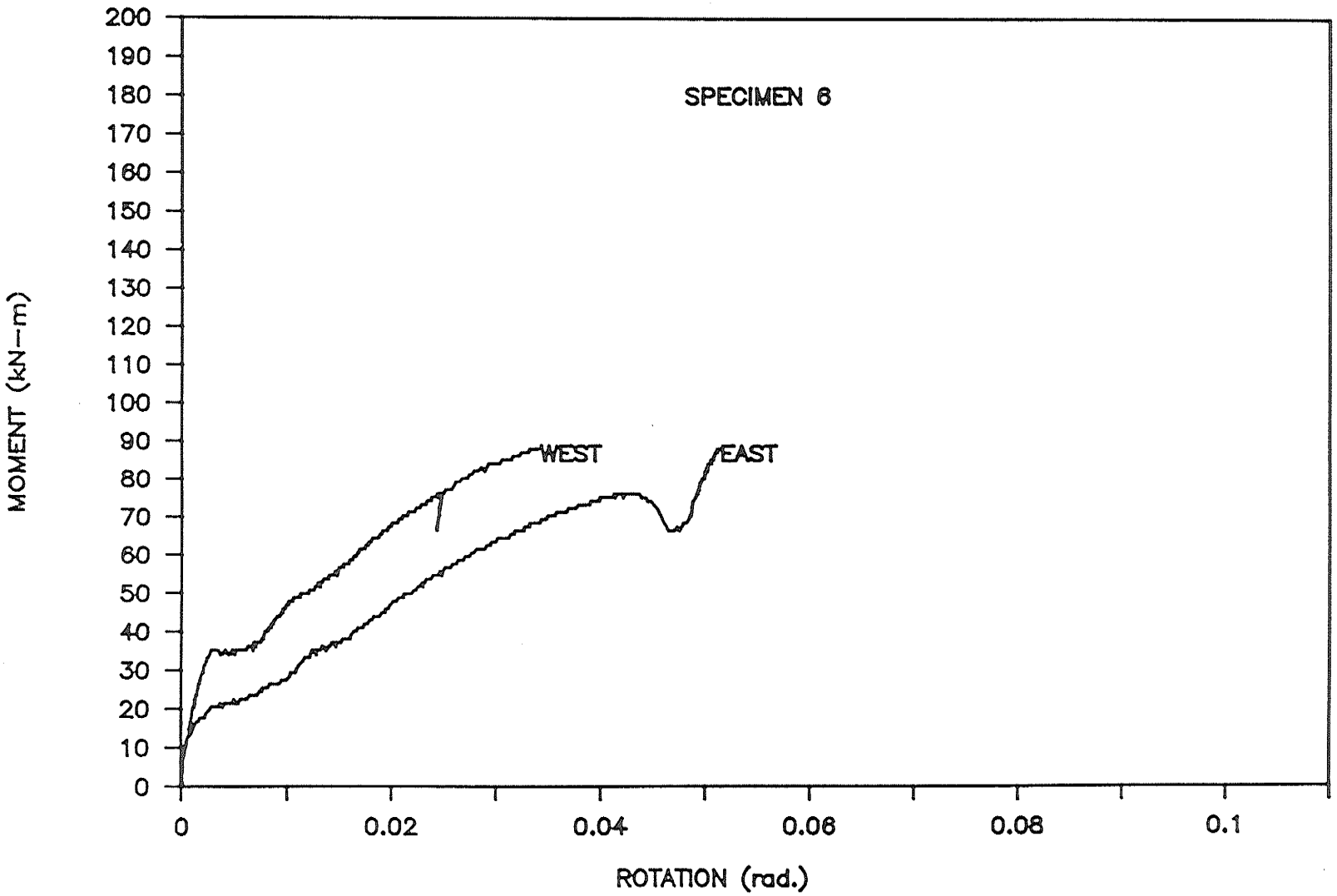

Figure 5.7: Moment-Rotation Curves for Specimen 6.

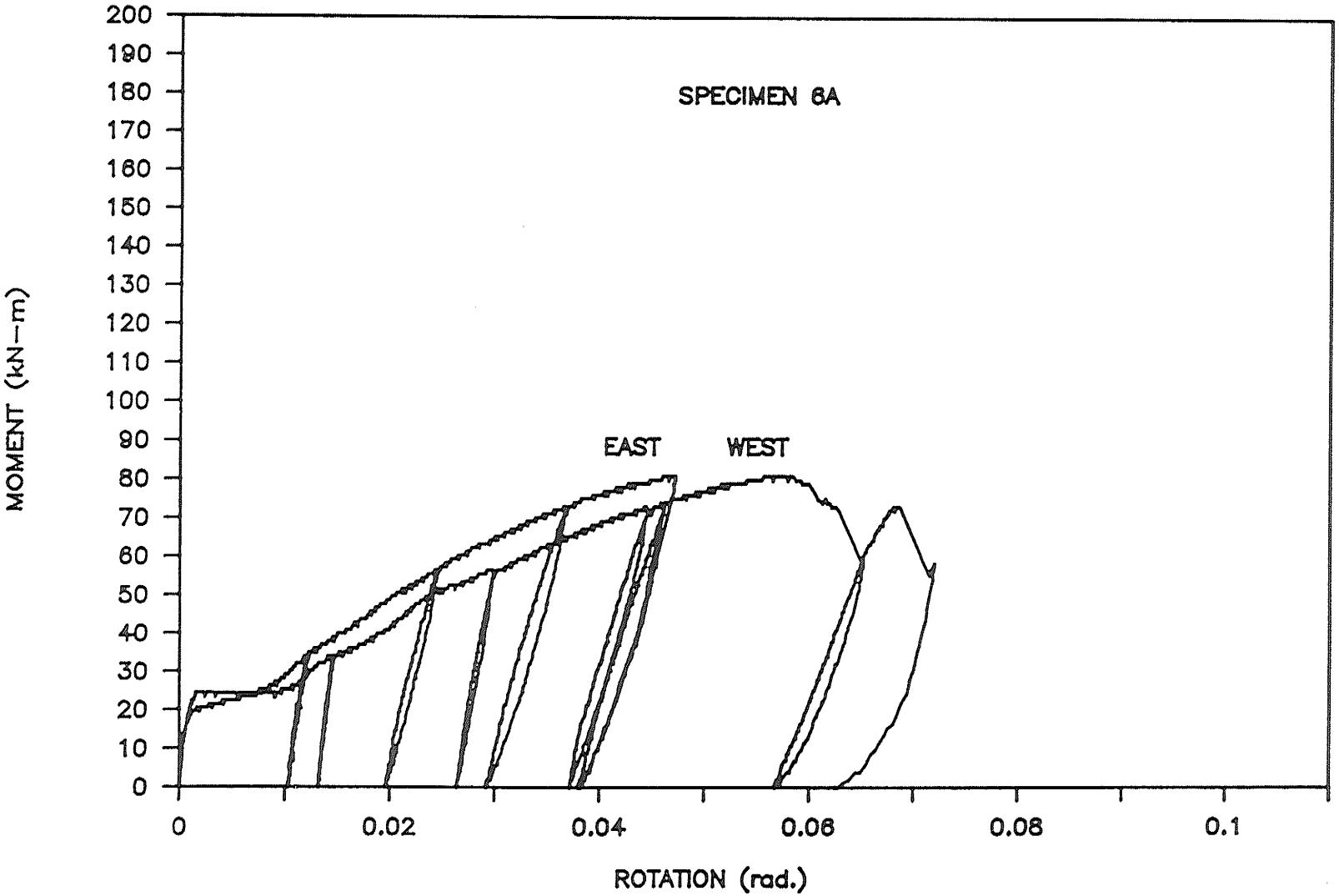

Figure 5.8: Moment-Rotation Curves for Specimen 6A.

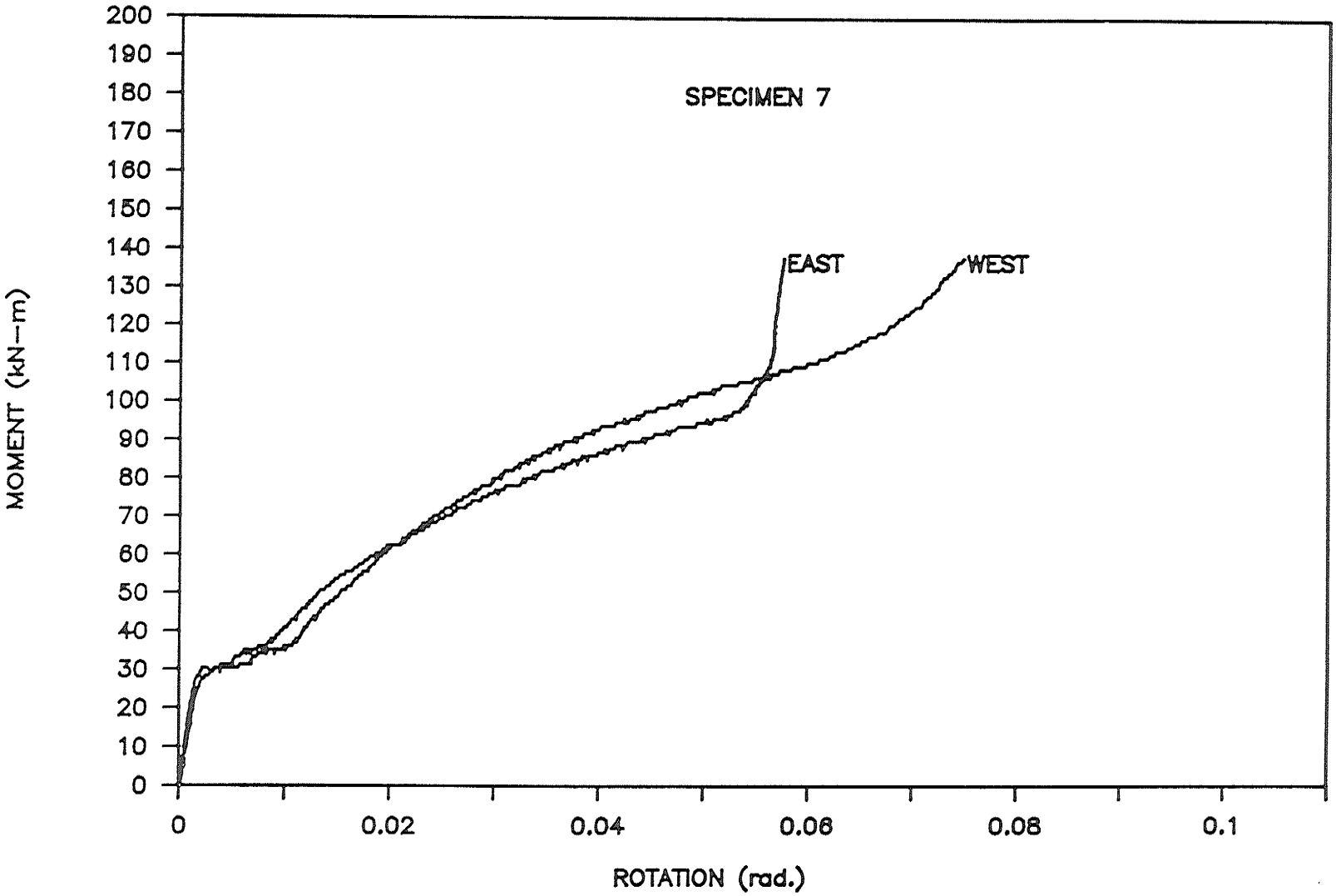

Figure 5.9: Moment-Rotation Curves for Specimen 7.

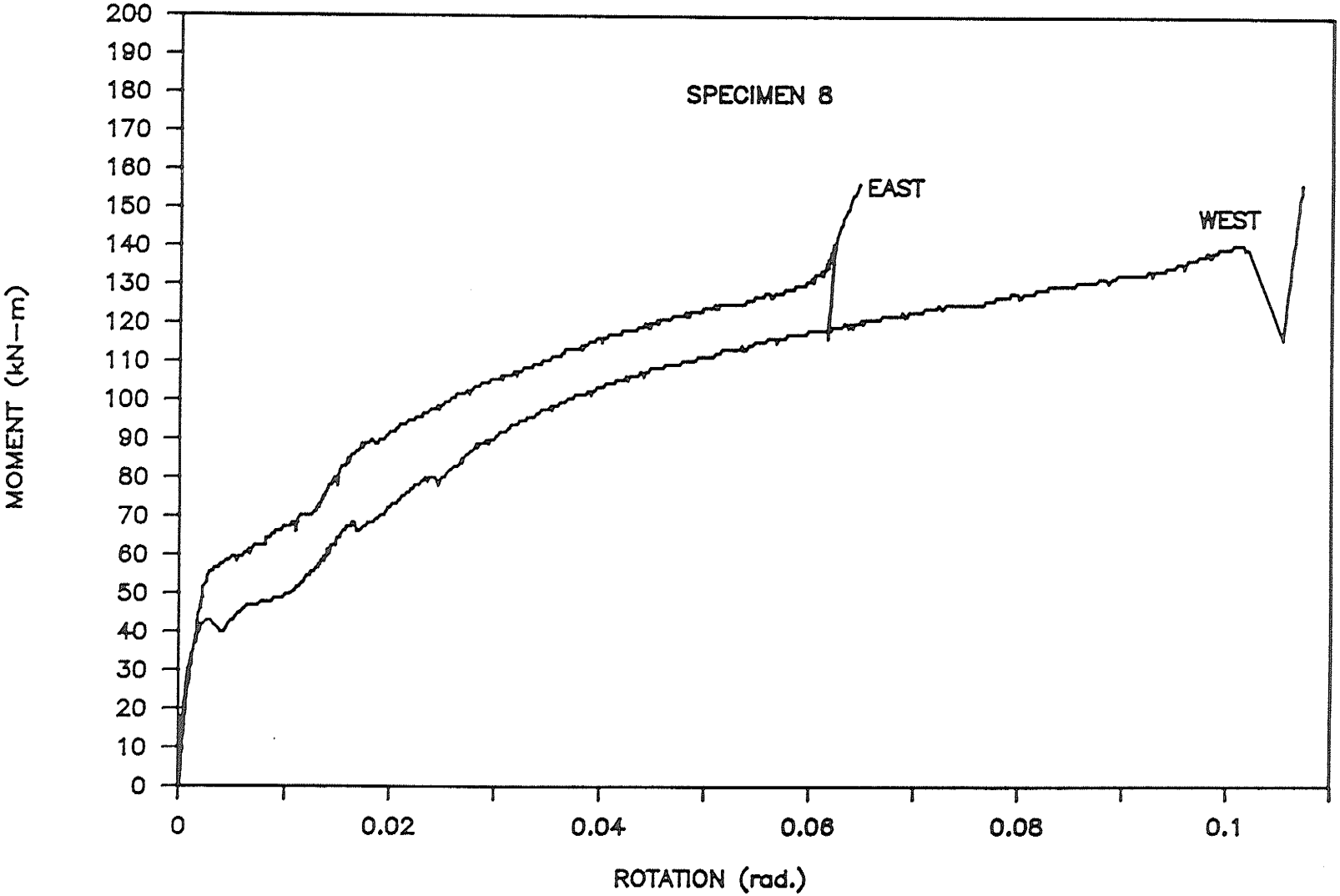

Figure 5.10: Moment-Rotation Curves for Specimen 8.

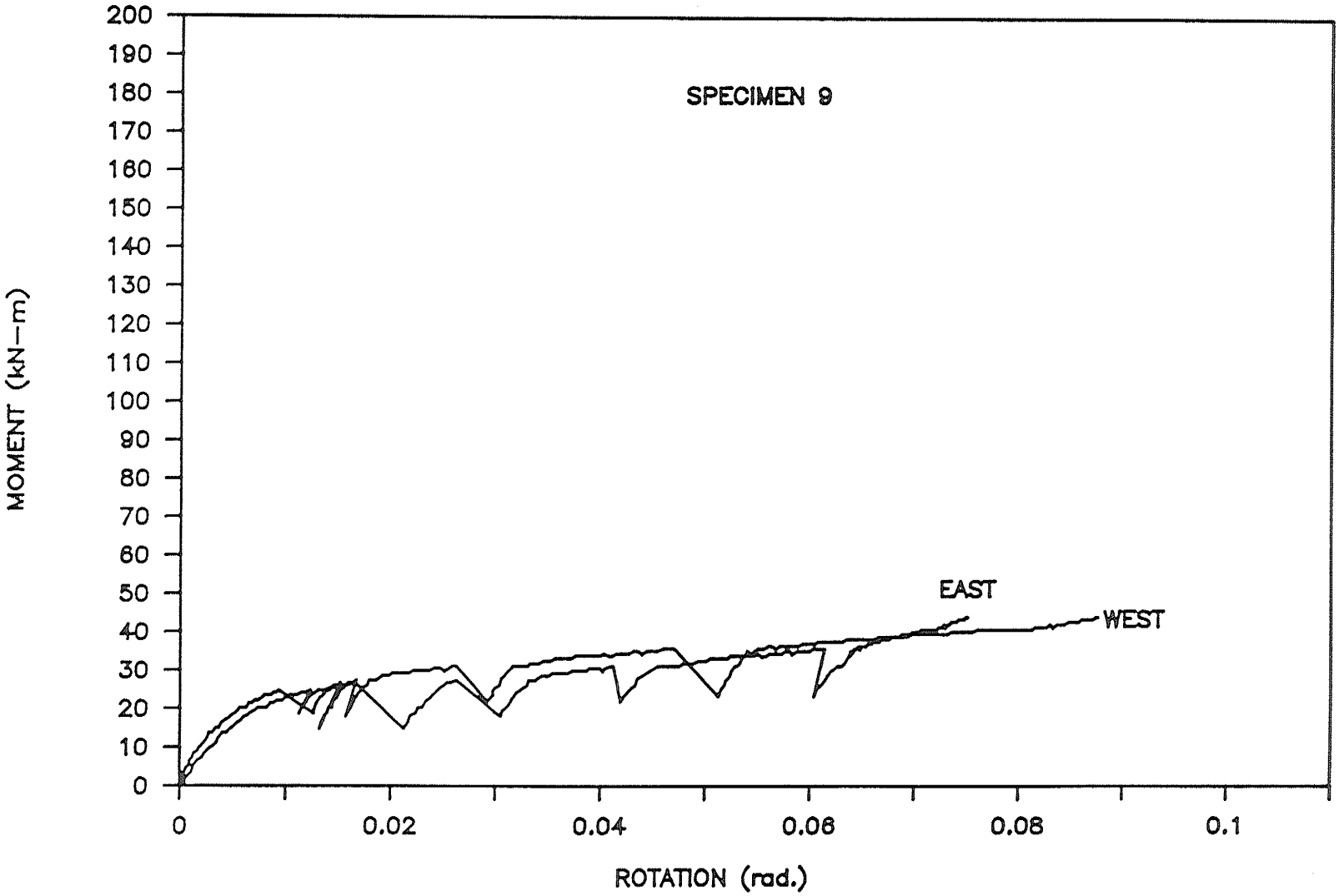

Figure 5.11: Moment-Rotation Curves for Specimen 9.

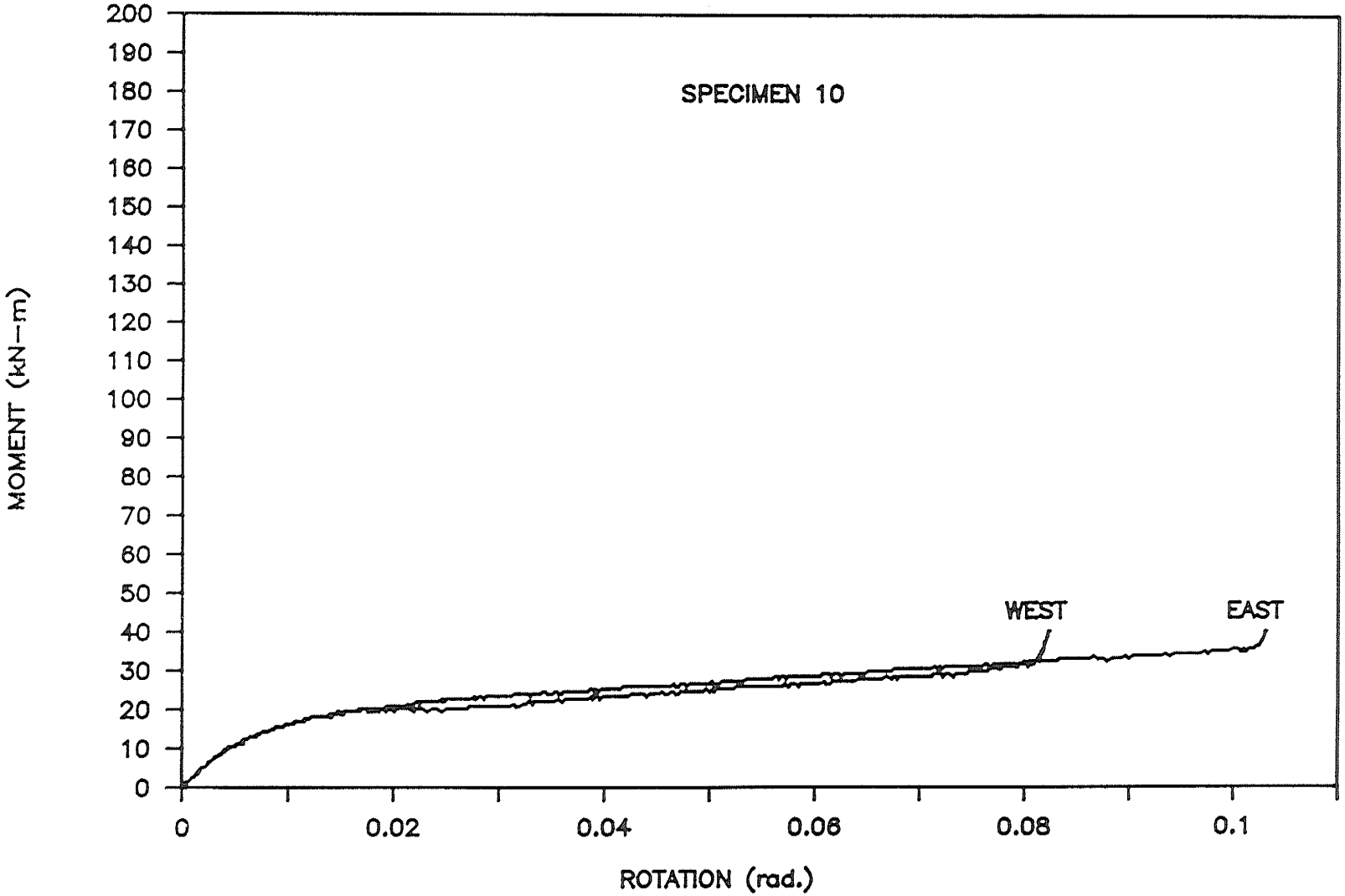

Figure 5.12: Moment-Rotation Curves for Specimen 10.

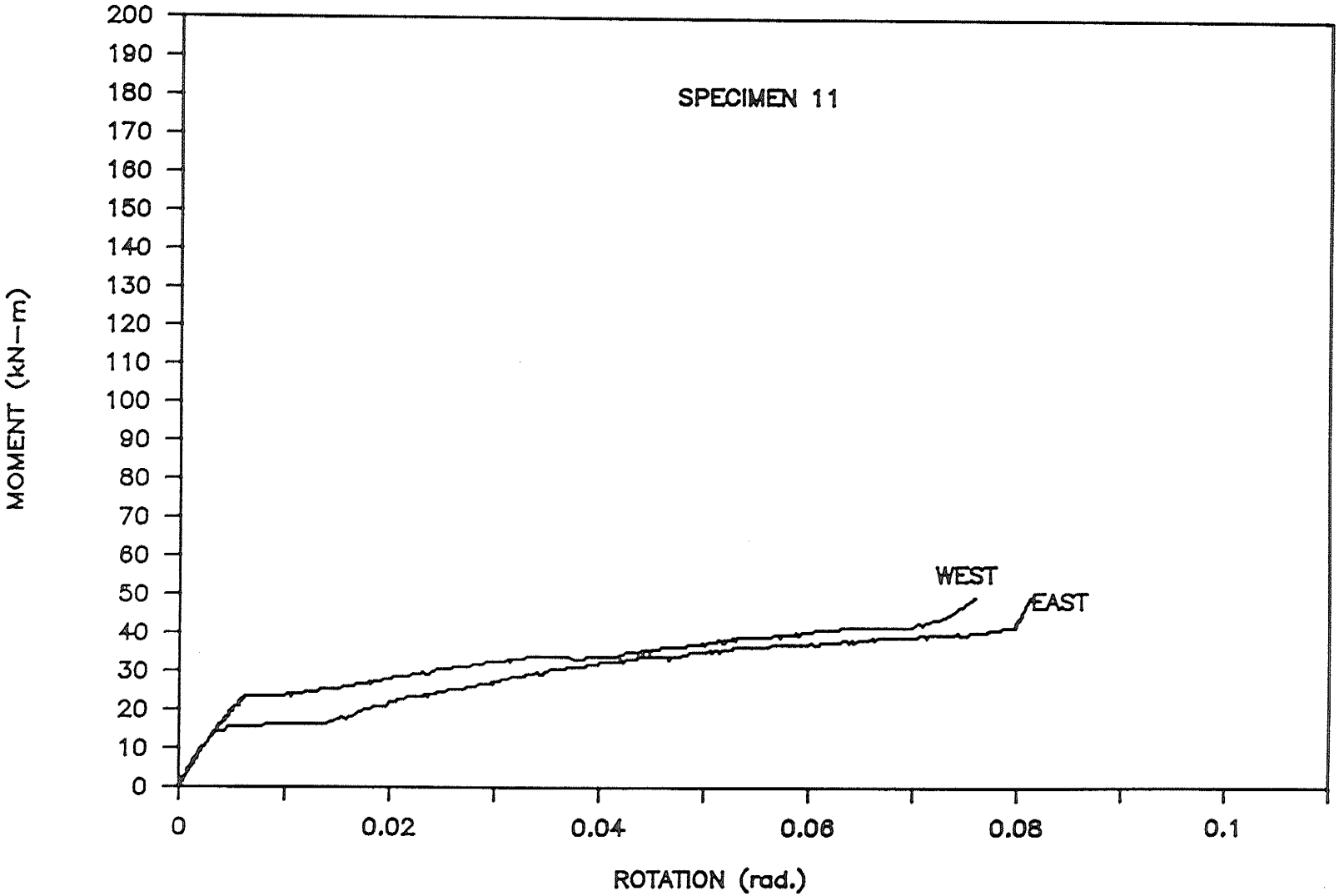

Figure 5.13: Moment-Rotation Curves for Specimen 11.

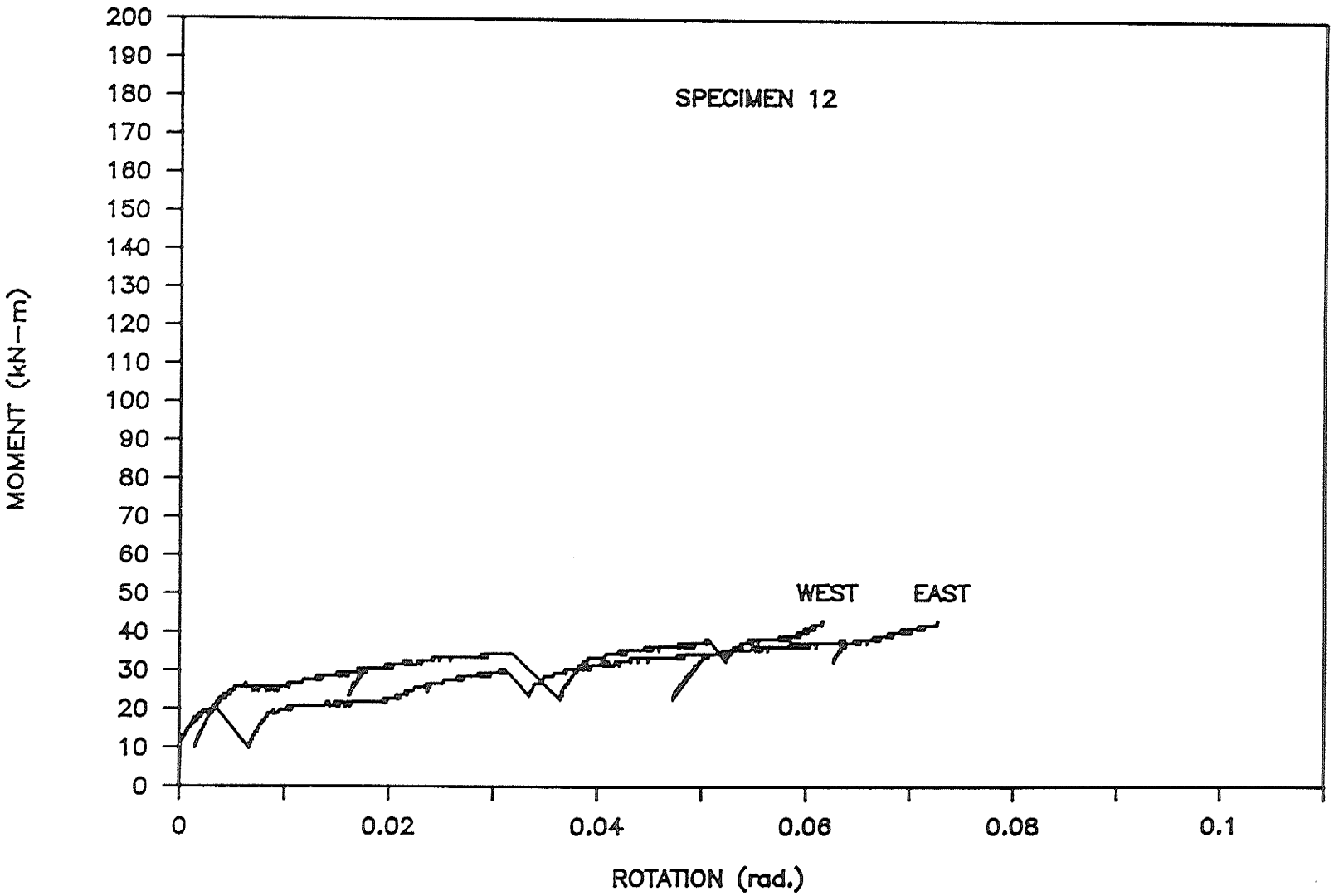

Figure 5.14: Moment-Rotation Curves for Specimen 12.

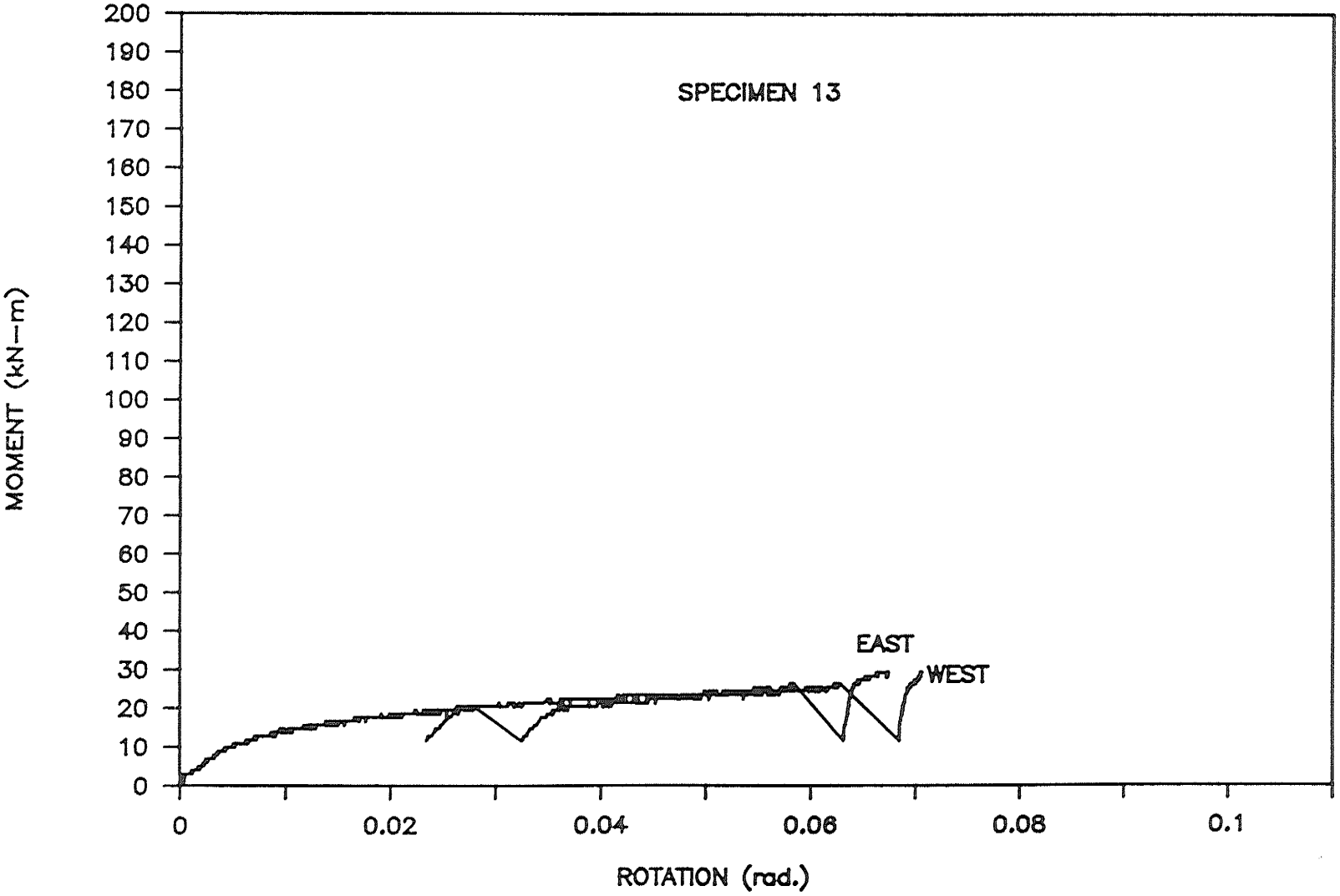

Figure 5.15: Moment-Rotation Curves for Specimen 13.

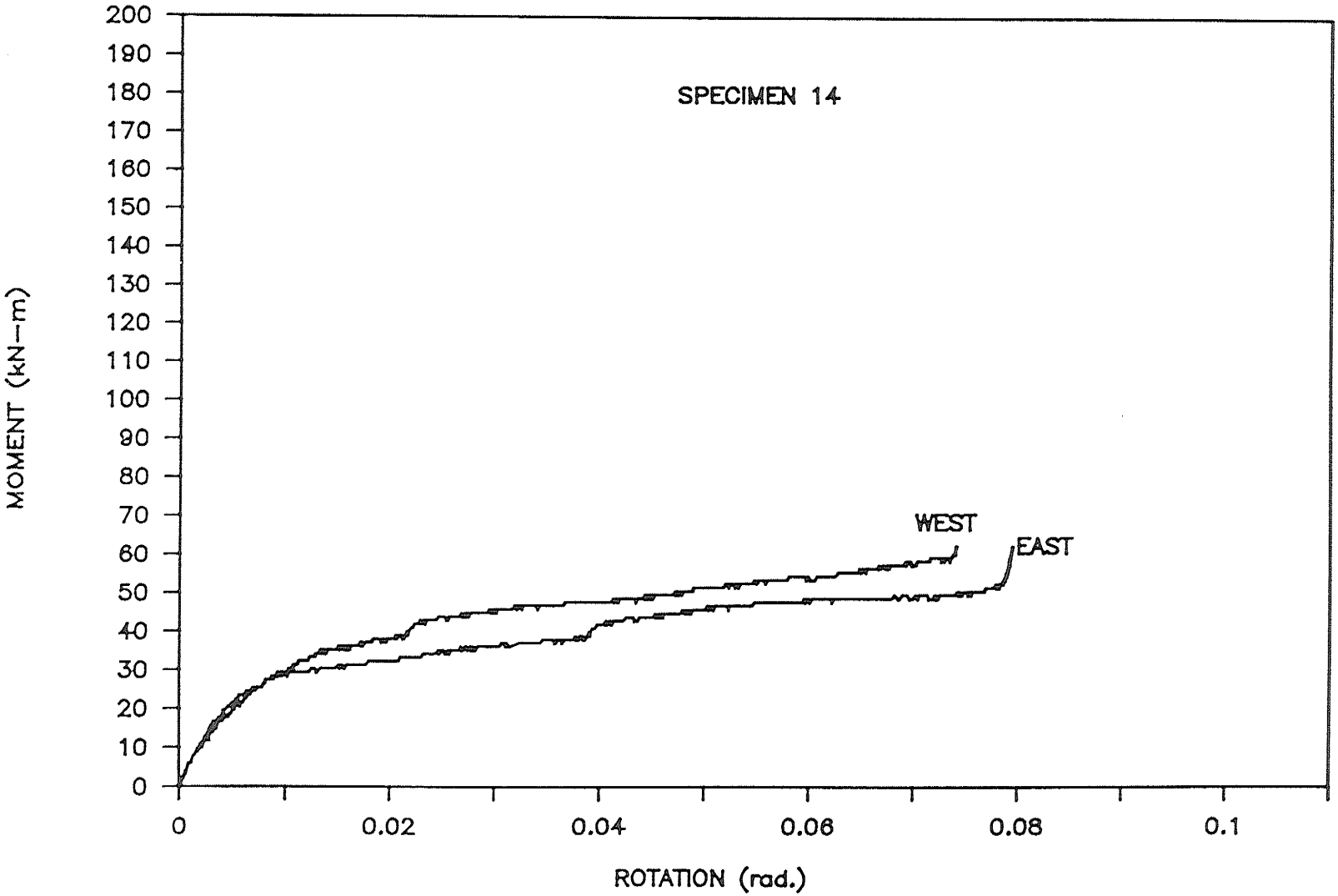

Figure 5.16: Moment-Rotation Curves for Specimen 14.

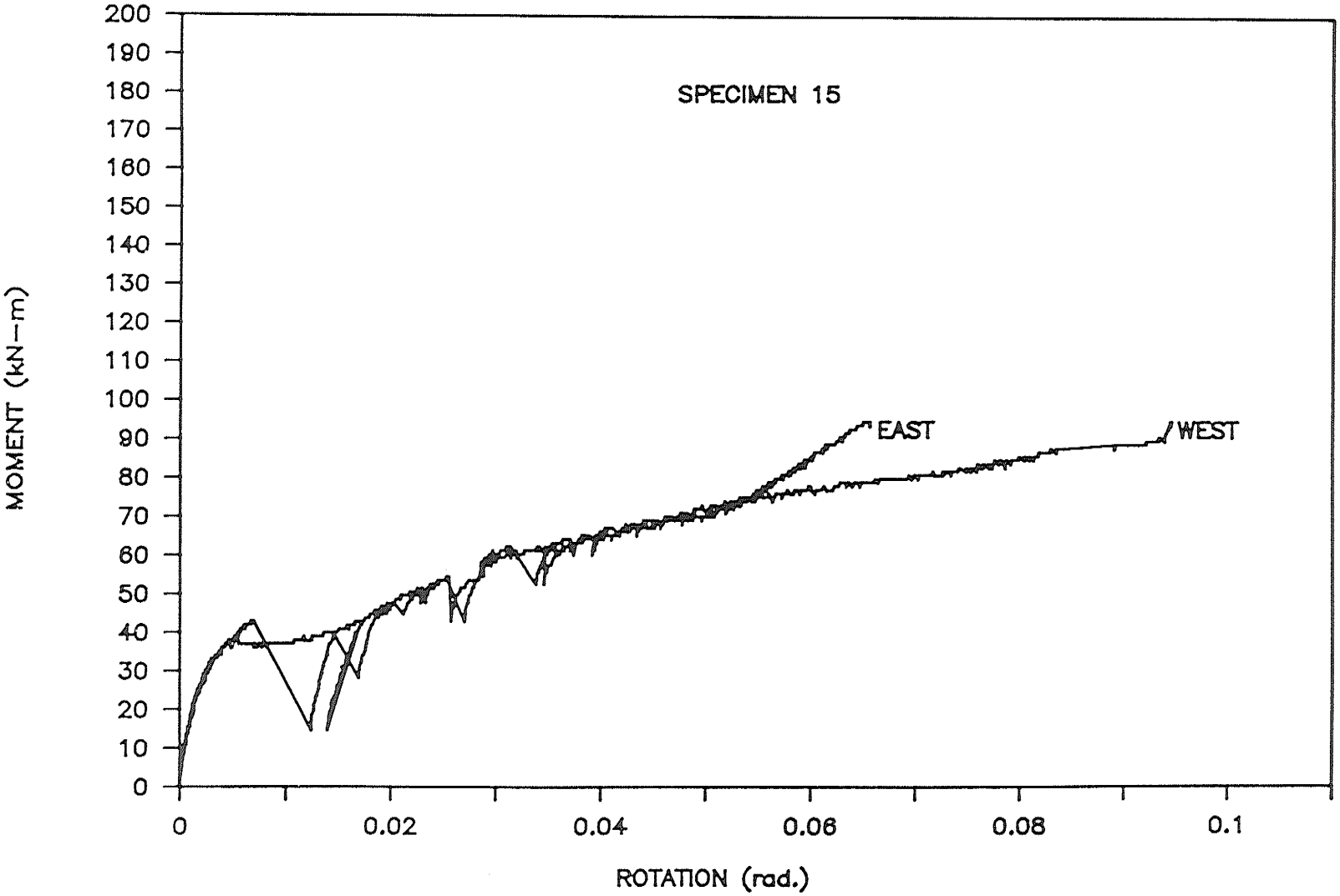

Figure 5.17: Moment-Rotation Curves for Specimen 15.

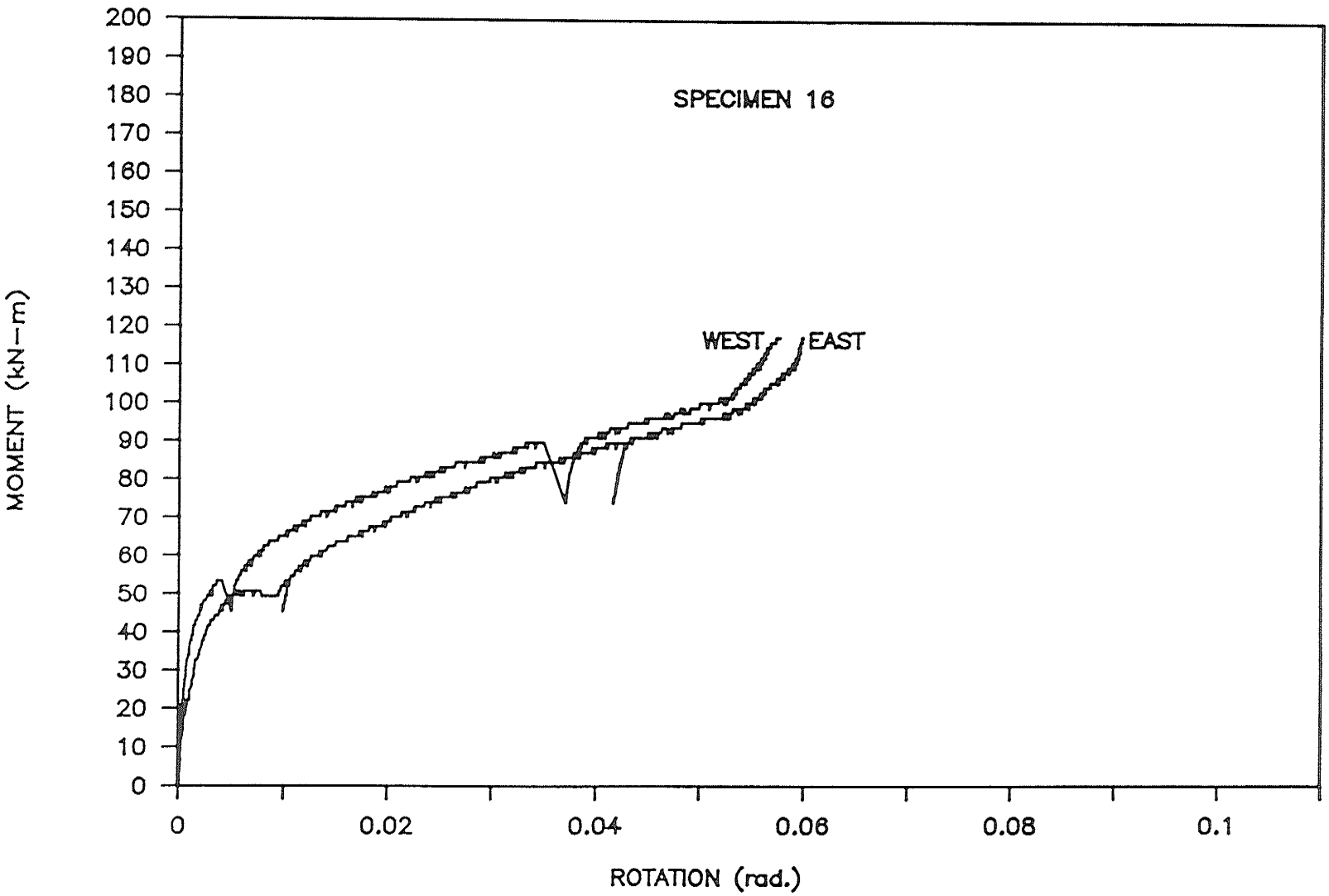

Figure 5.18: Moment-Rotation Curves for Specimen 16.

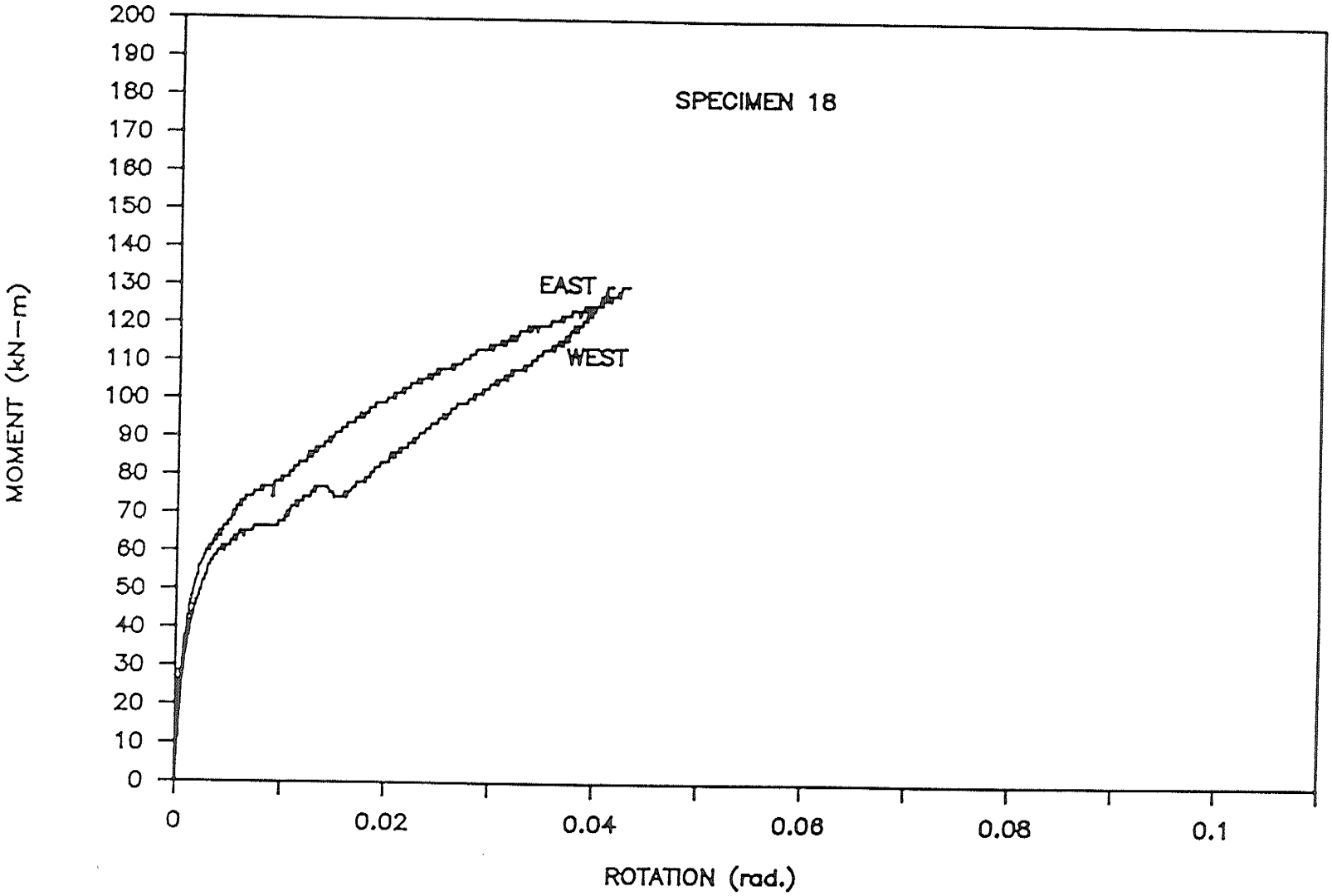

Figure 5.19: Moment-Rotation Curves for Specimen 18.

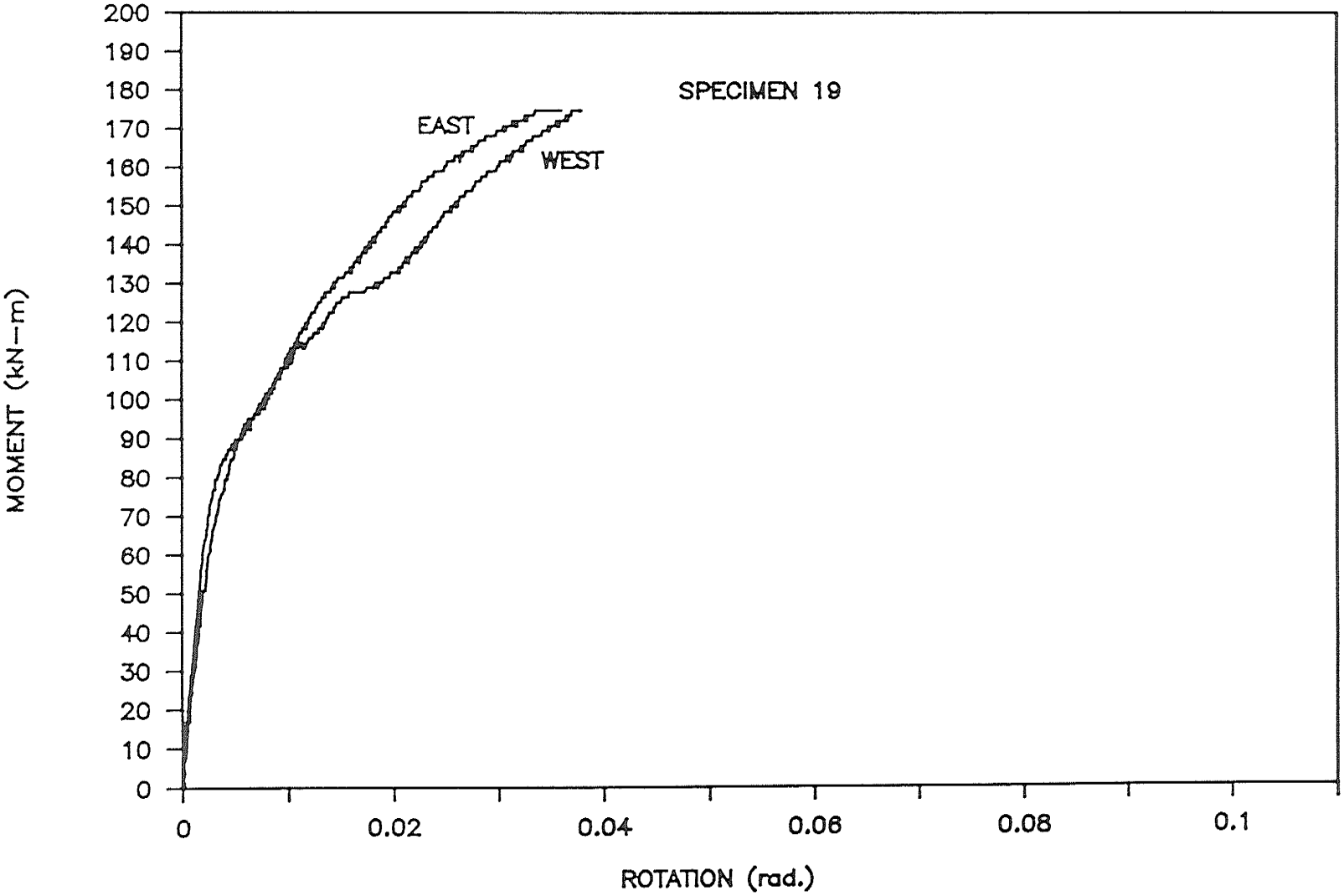

Figure 5.20: Moment-Rotation Curves for Specimen 19.

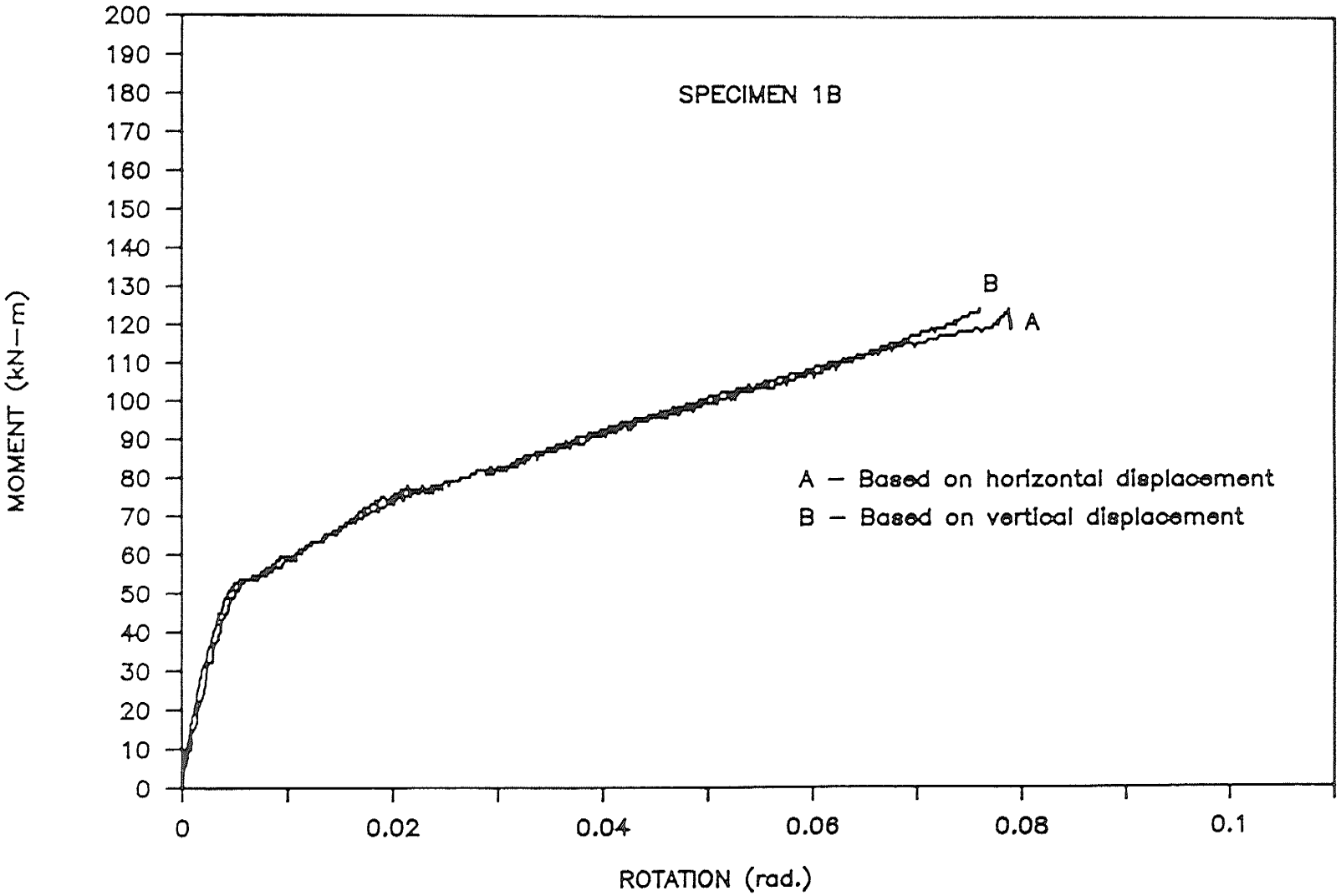

Figure 5.21: Moment-Rotation Curves Based on Horizontal and Vertical Displacements of Specimen 1B.

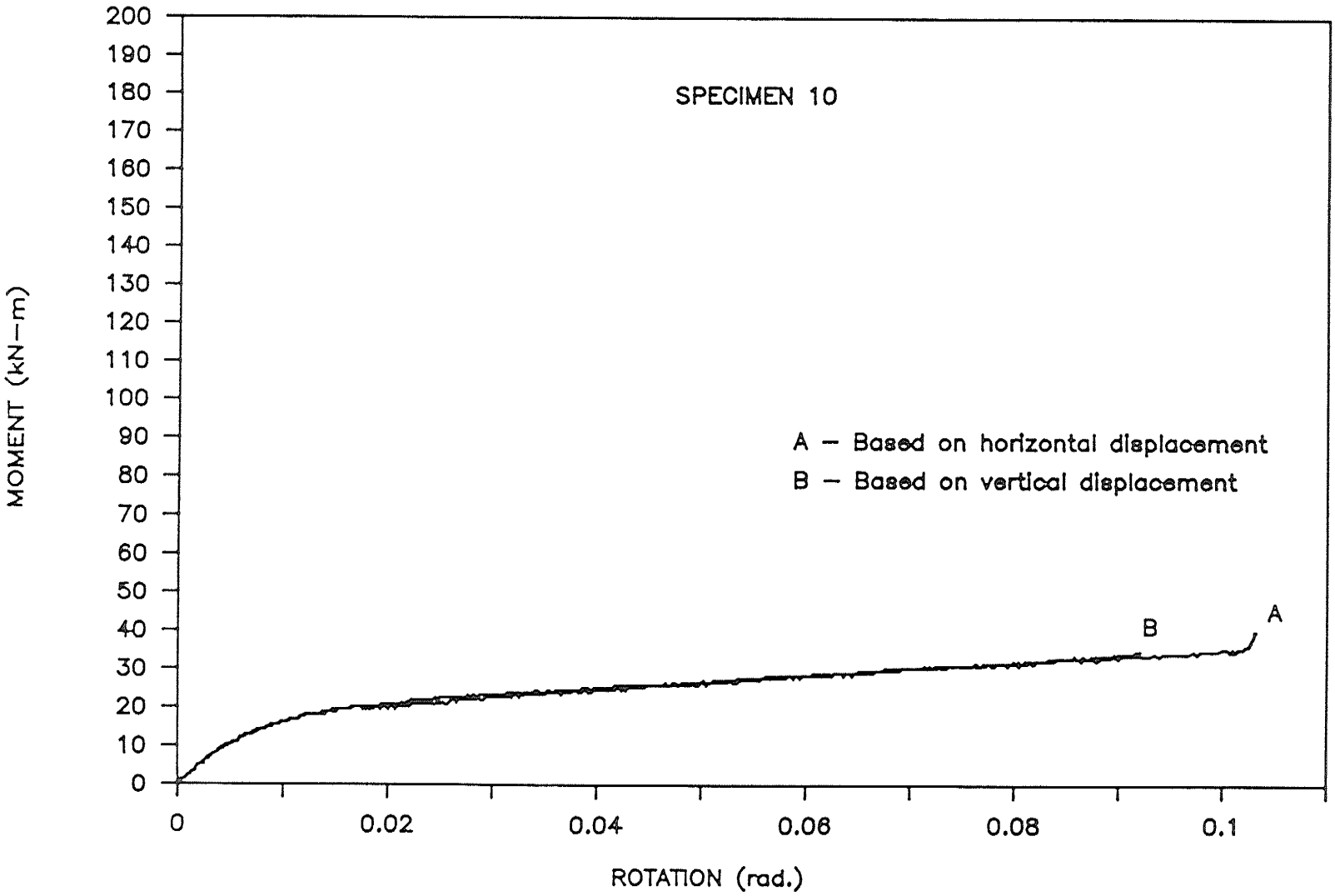

Figure 5.22: Moment-Rotation Curves Based on Horizontal and Vertical Displacements of Specimen 10.

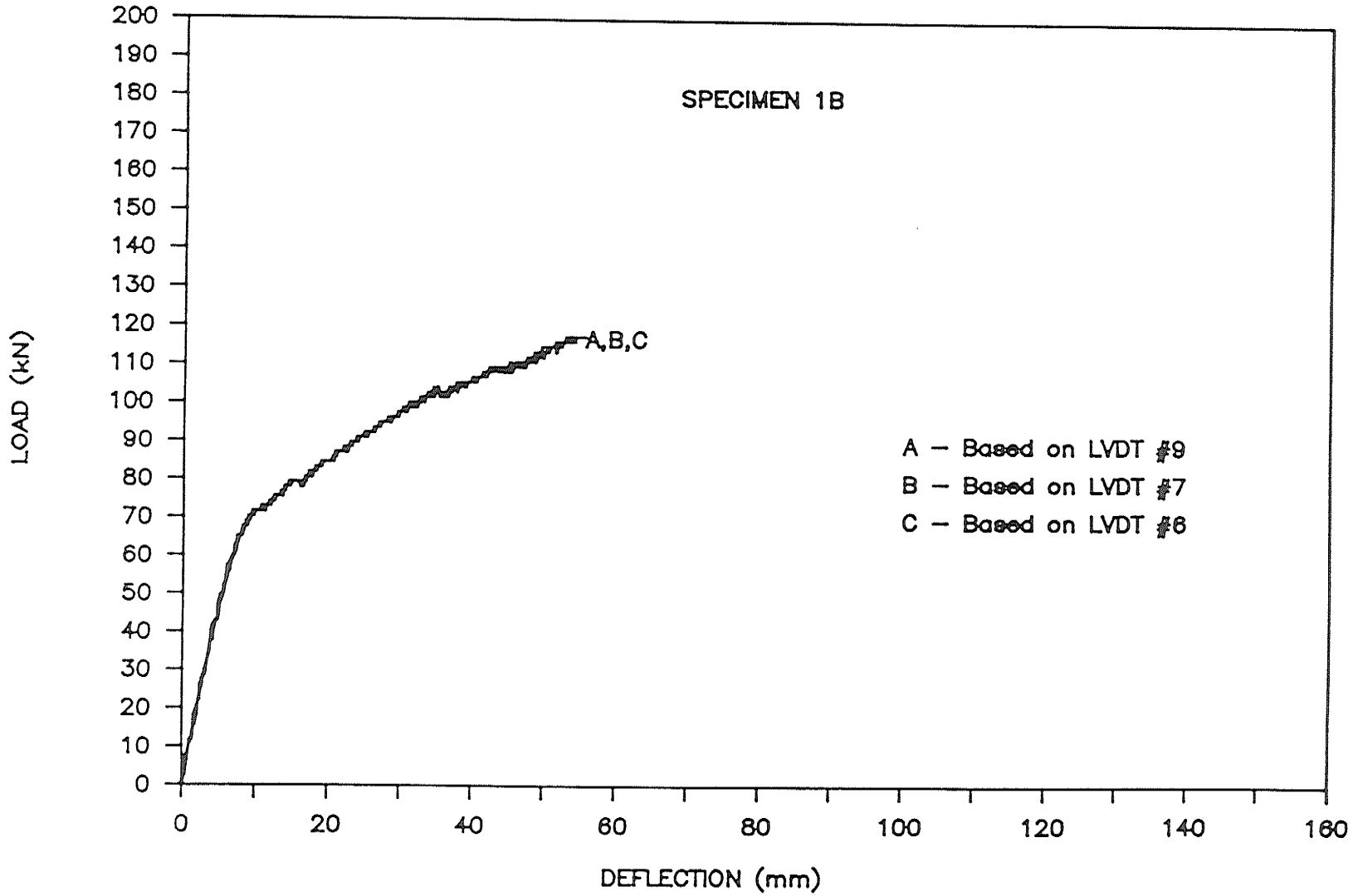

Figure 5.23: Load-Deflection Curves for Specimen 1B Based on Three LVDTs under the Column Stub.

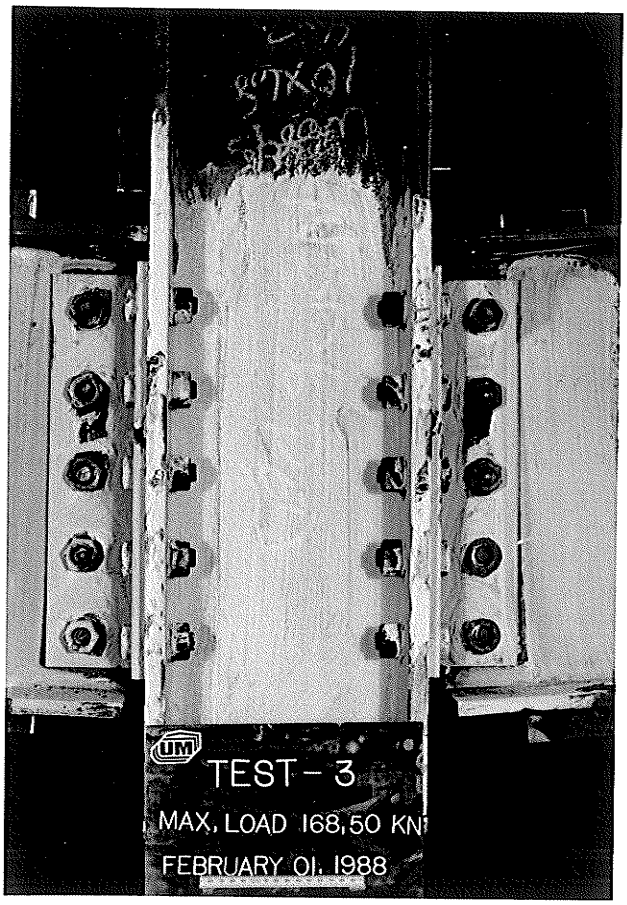

Figure 5.24: Rotational Displacement Between the Angle Leg and the Beam Web in the Tension Region of Specimen 3.

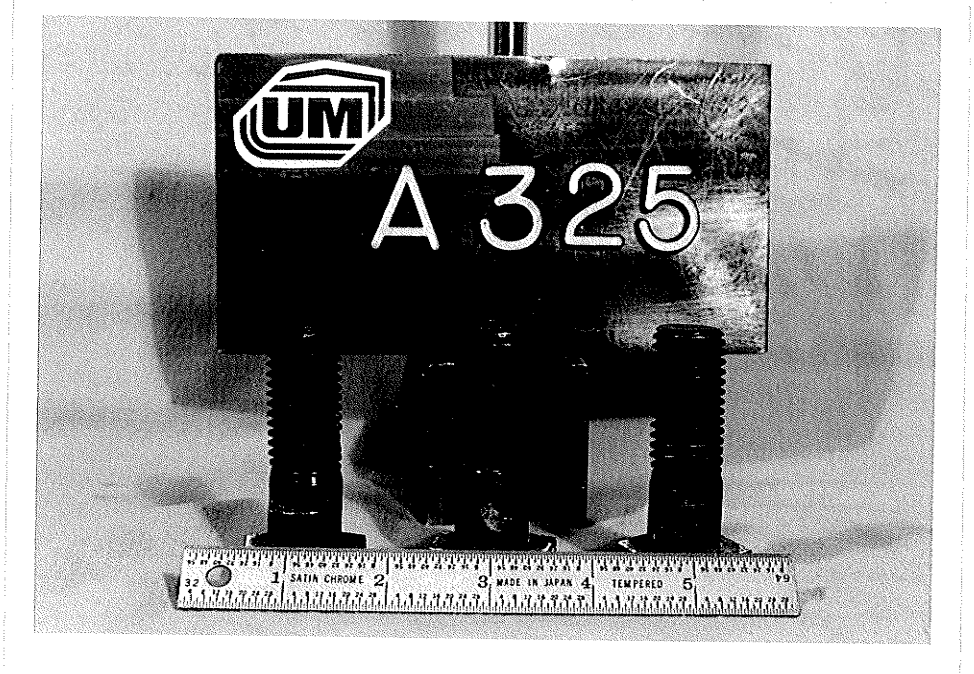

Figure 5.25: Deformed A325 Bolts at the End of a Test.

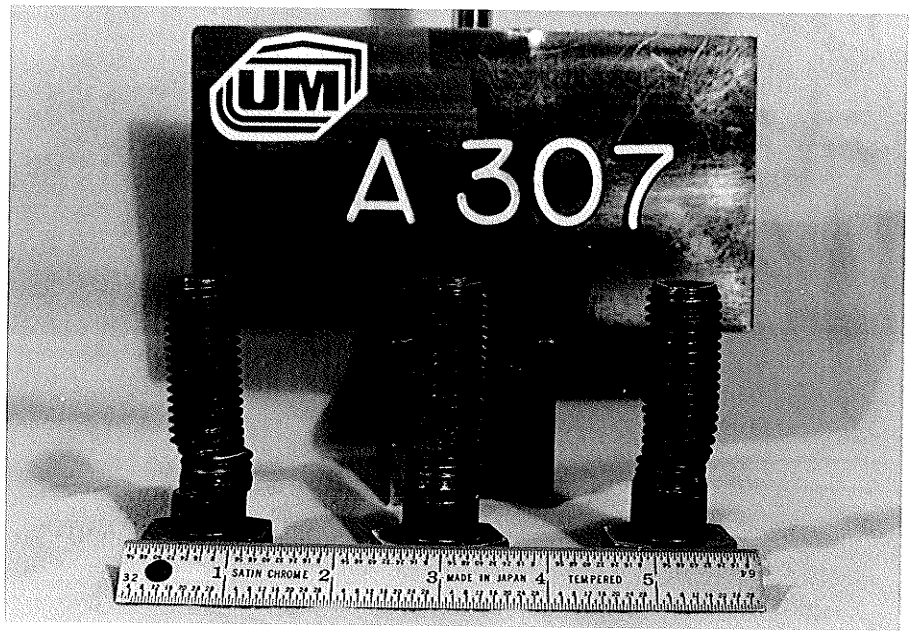

Figure 5.26: Deformed A307 Bolts at the End of Tests.

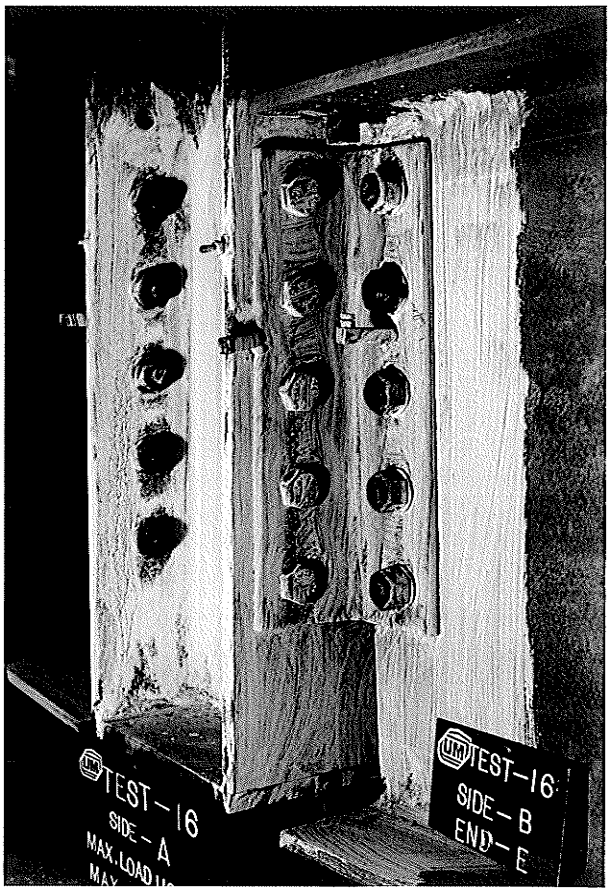

Figure 5.27: Yielding Along the Bolt Lines of the Column Leg of the Angle in the Tension Region of Specimen 16.

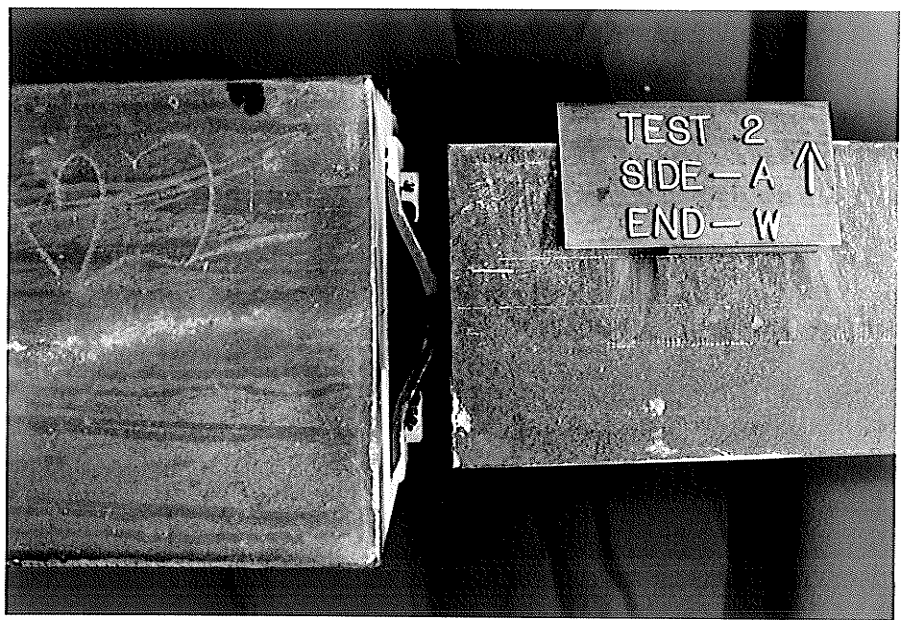

Figure 5.28: Prying Action in Specimen 2.

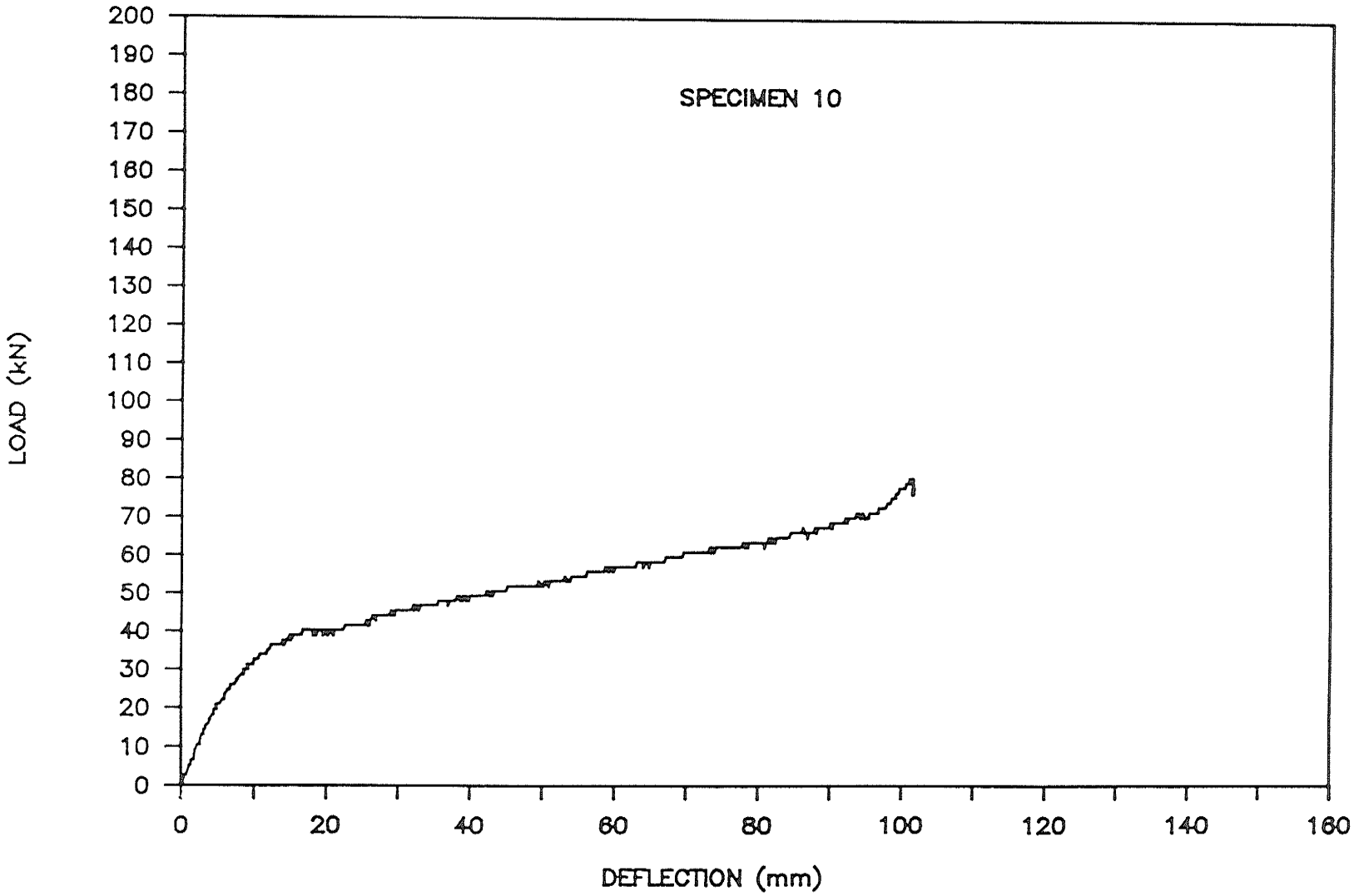

Figure 5.29: Load-Deflection Curve of Specimen 10.

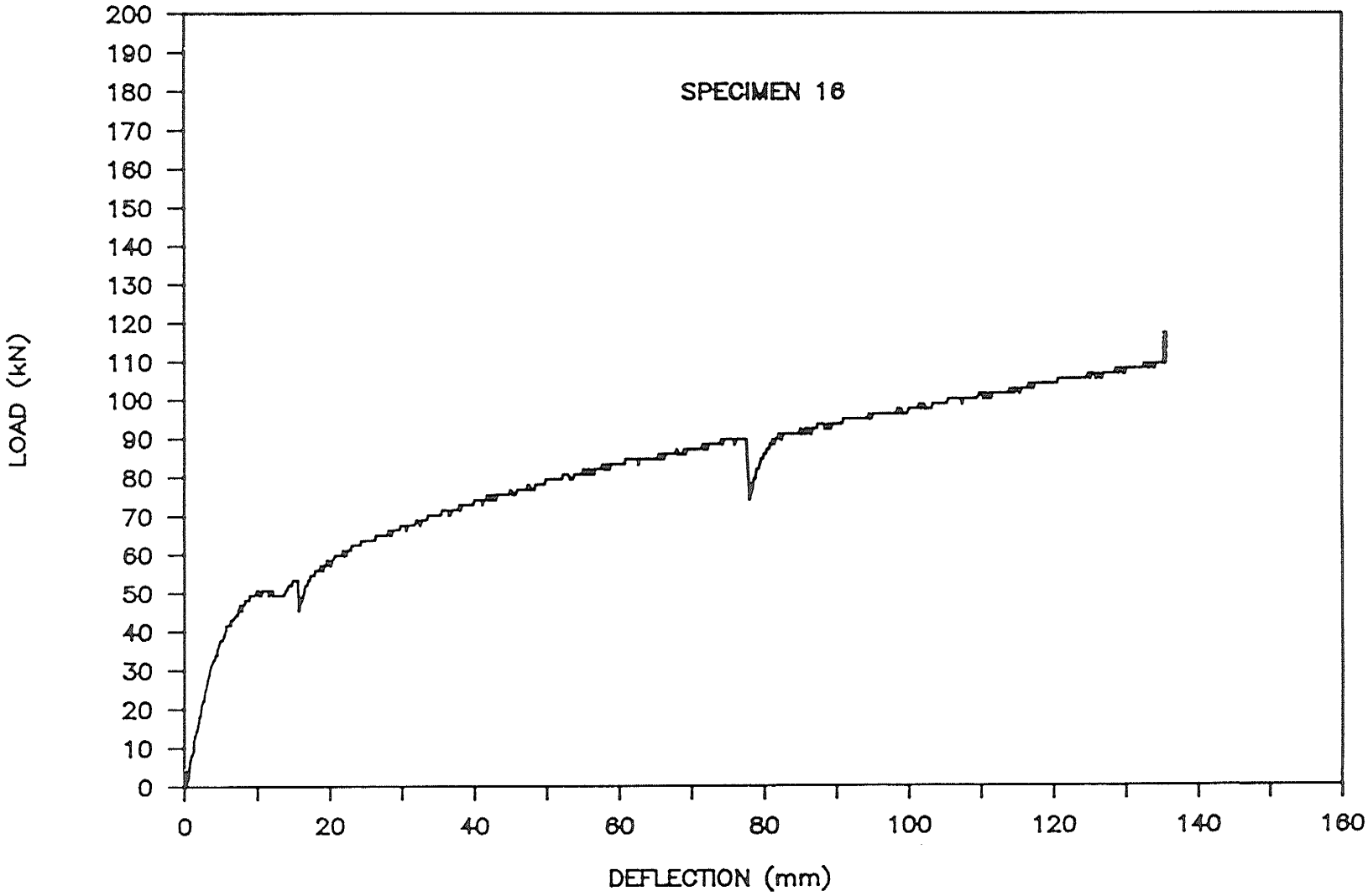

Figure 5.30: Load-Deflection Curve of Specimen 16.

Figure 5.31: Sheared Off Bolts from Specimens which had A325 and A307 Bolts, respectively.

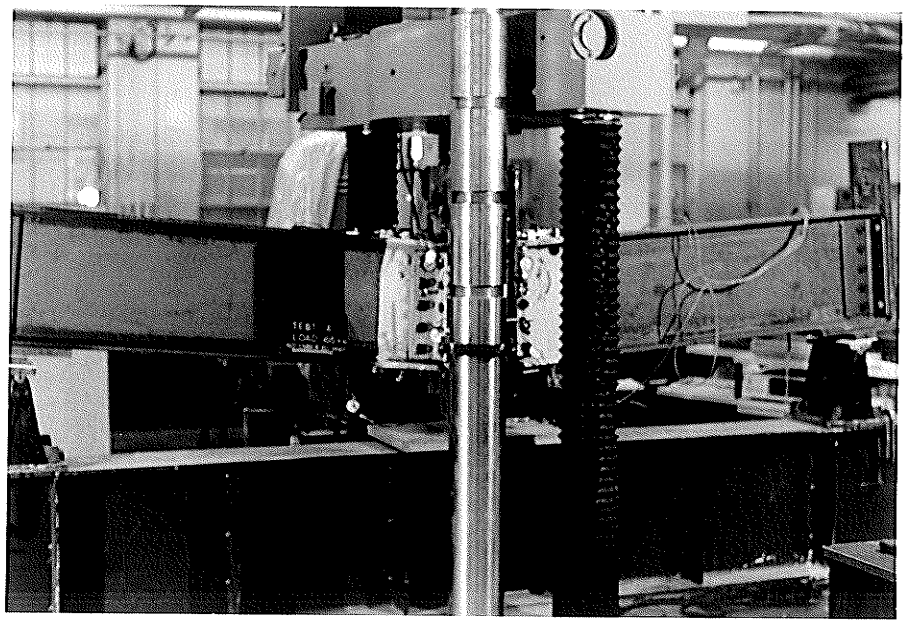

Figure 5.32: Typical Specimen at the End of Test.

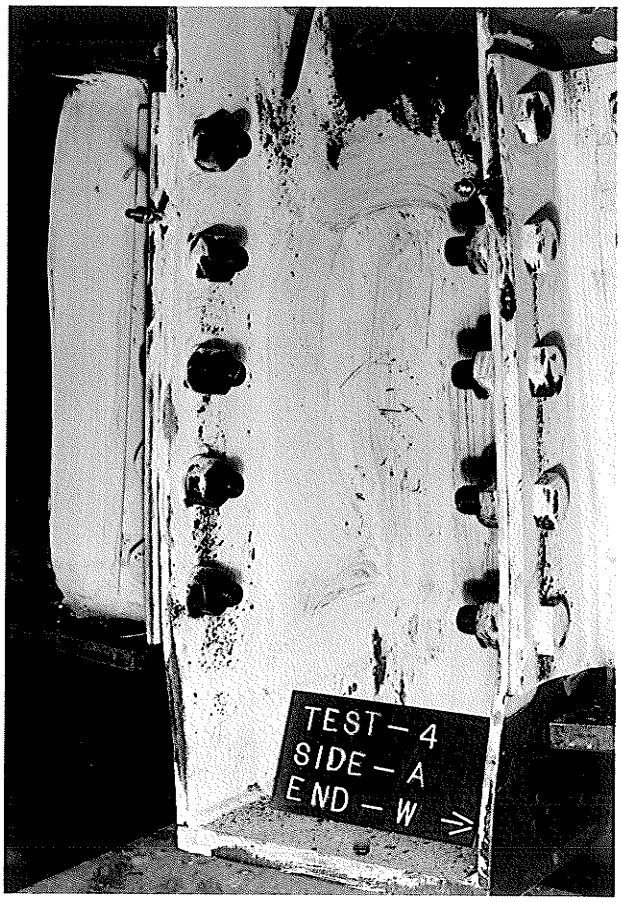

Figure 5.33: Deformation of Both Column Flange and Web in Specimen 4.

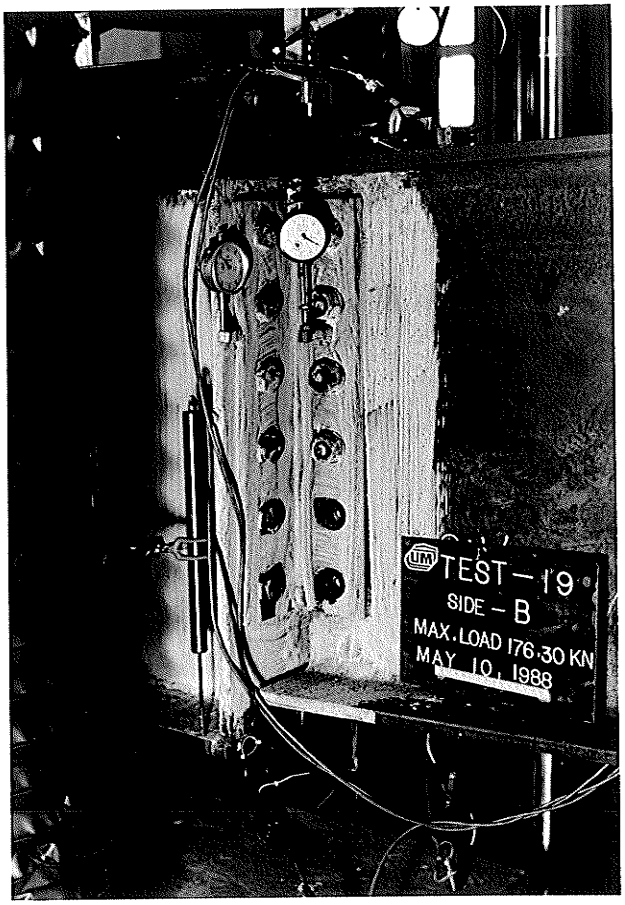

Figure 5.34: Shearing Off of Two Bolts in the Tension Region in Specimen 19.

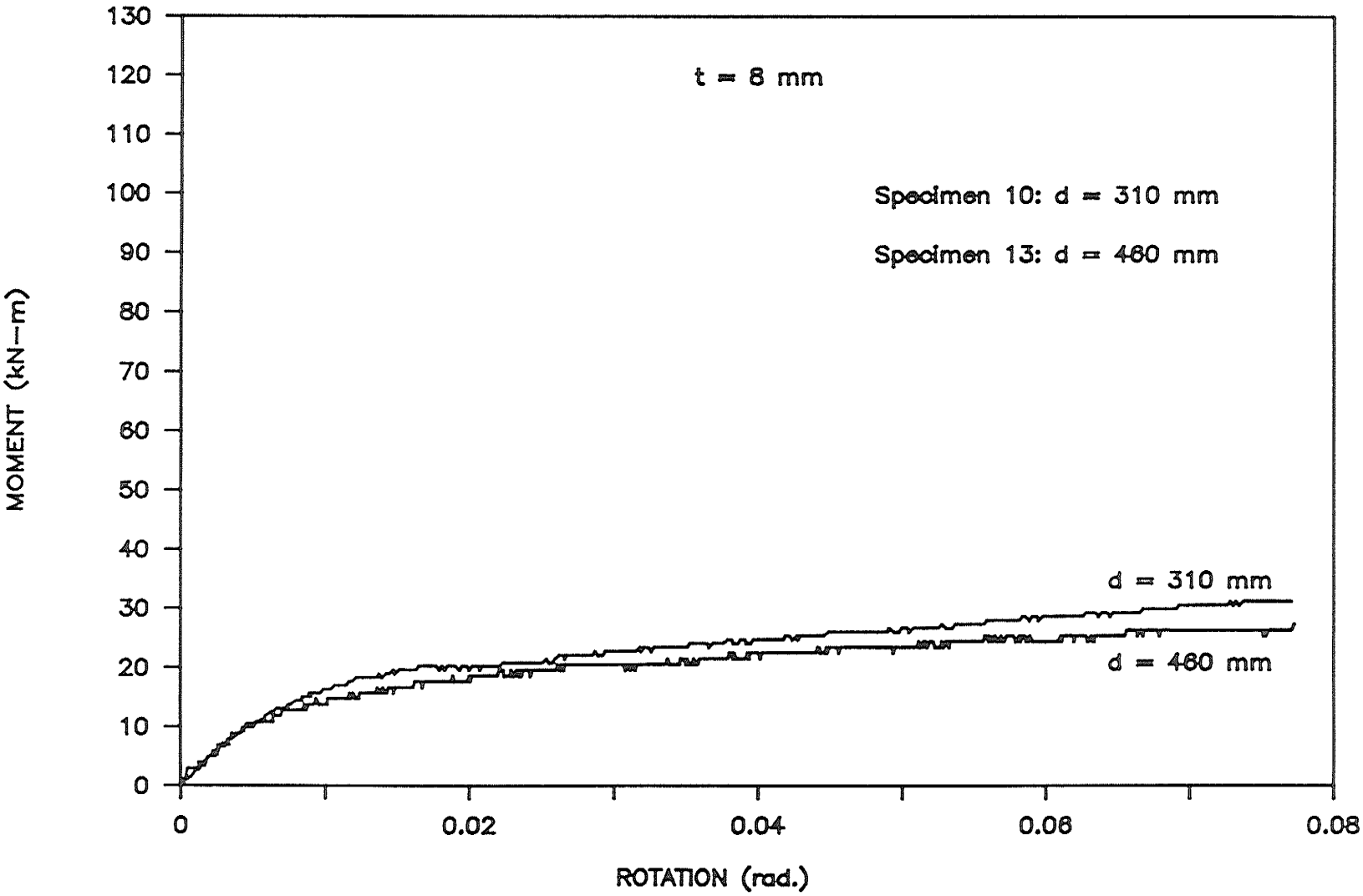

Figure 5.35: Effect of the Beam Depth on the M-Ø Curves of Specimens 10 and 13.

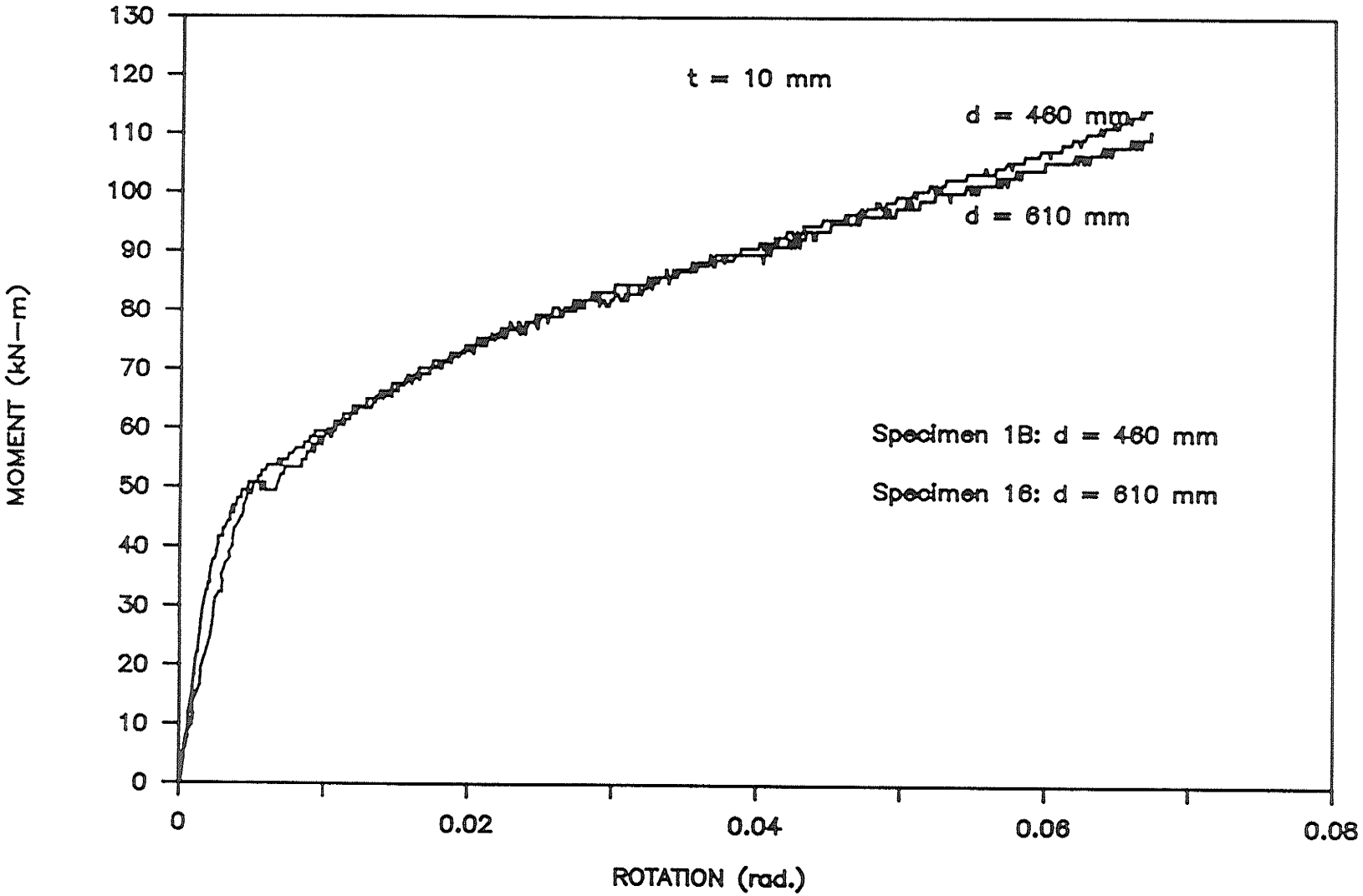

Figure 5.36: Effect of the Beam Depth on the M-Ø Curves of Specimens 1B and 16.

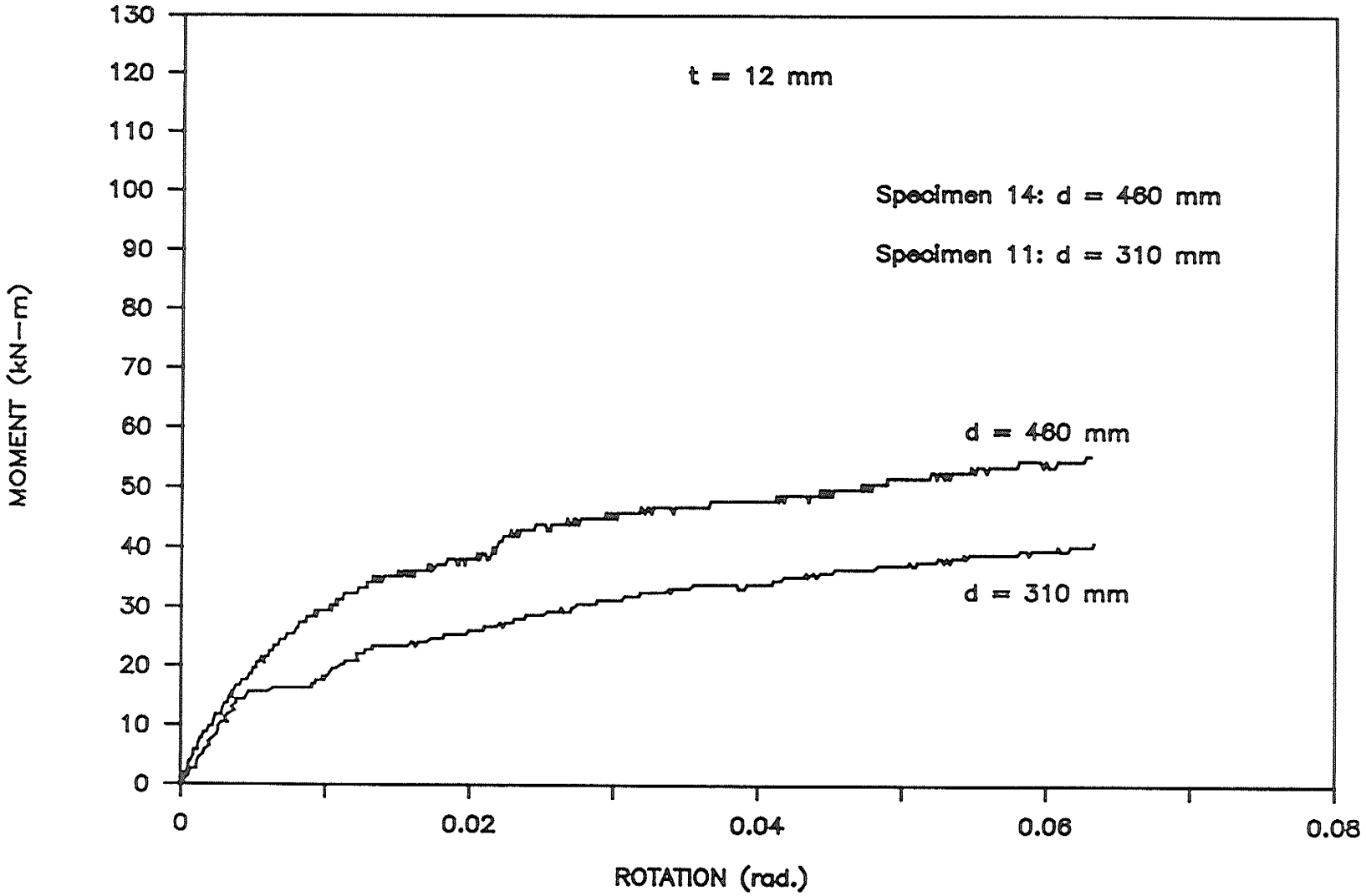

Figure 5.37: Effect of the Beam Depth on the M-Ø Curves of Specimens 11 and 14.

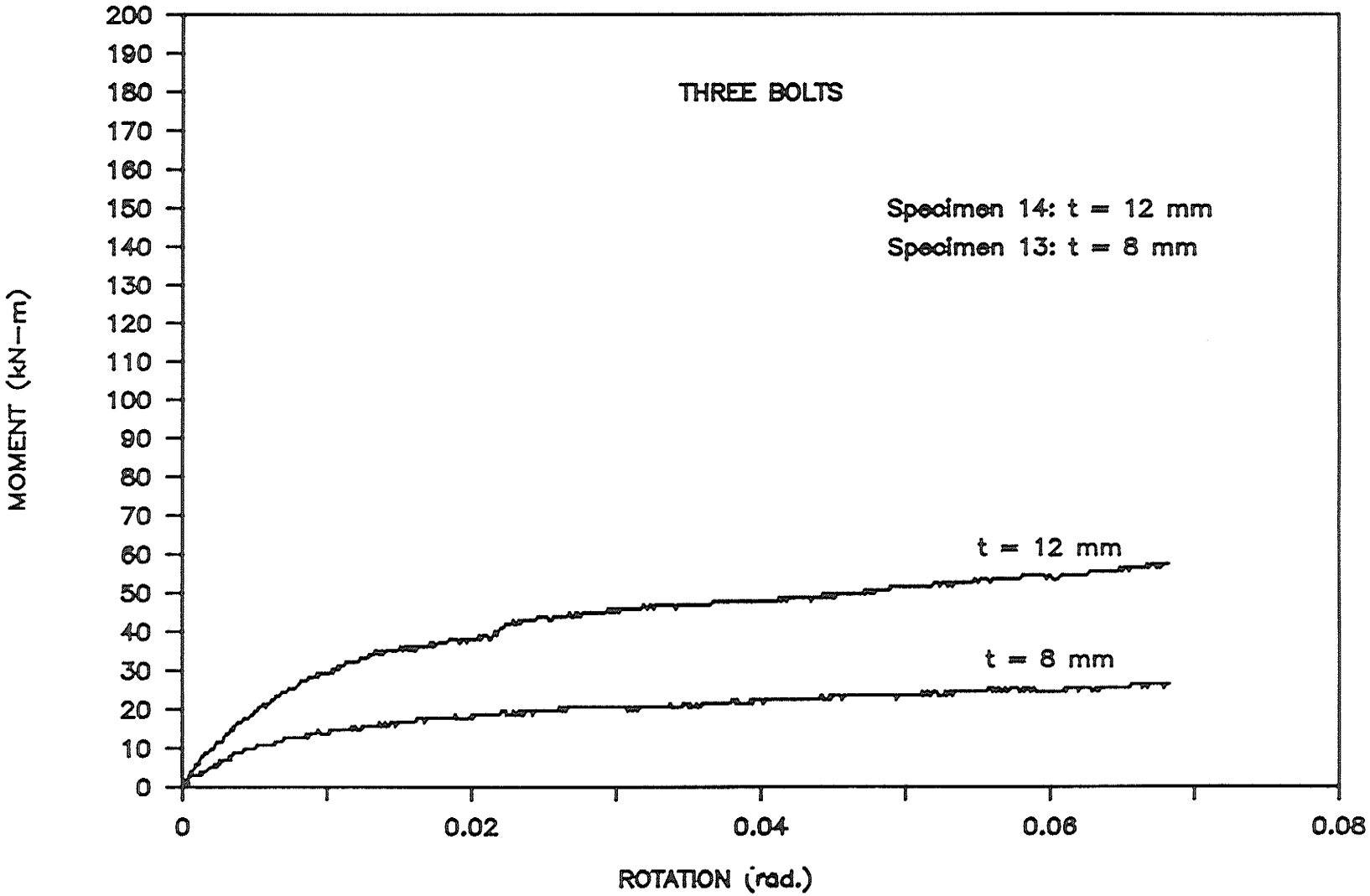

Figure 5.38: Effect of the Angle Thickness on the M-Ø Curves of Specimens 13 and 14.

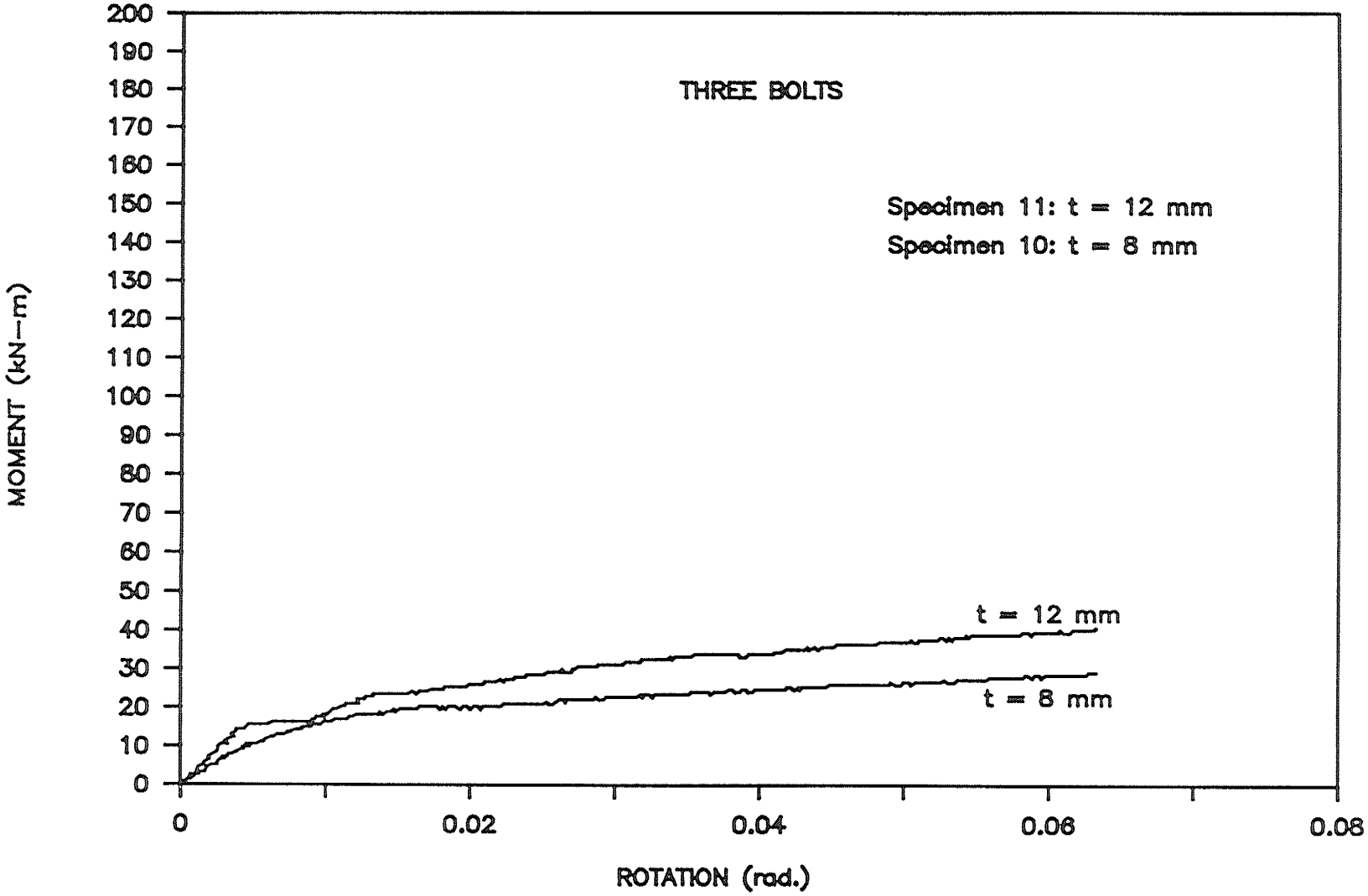

Figure 5.39: Effect of the Angle Thickness on the M-Ø Curves of Specimens 10 and 11.

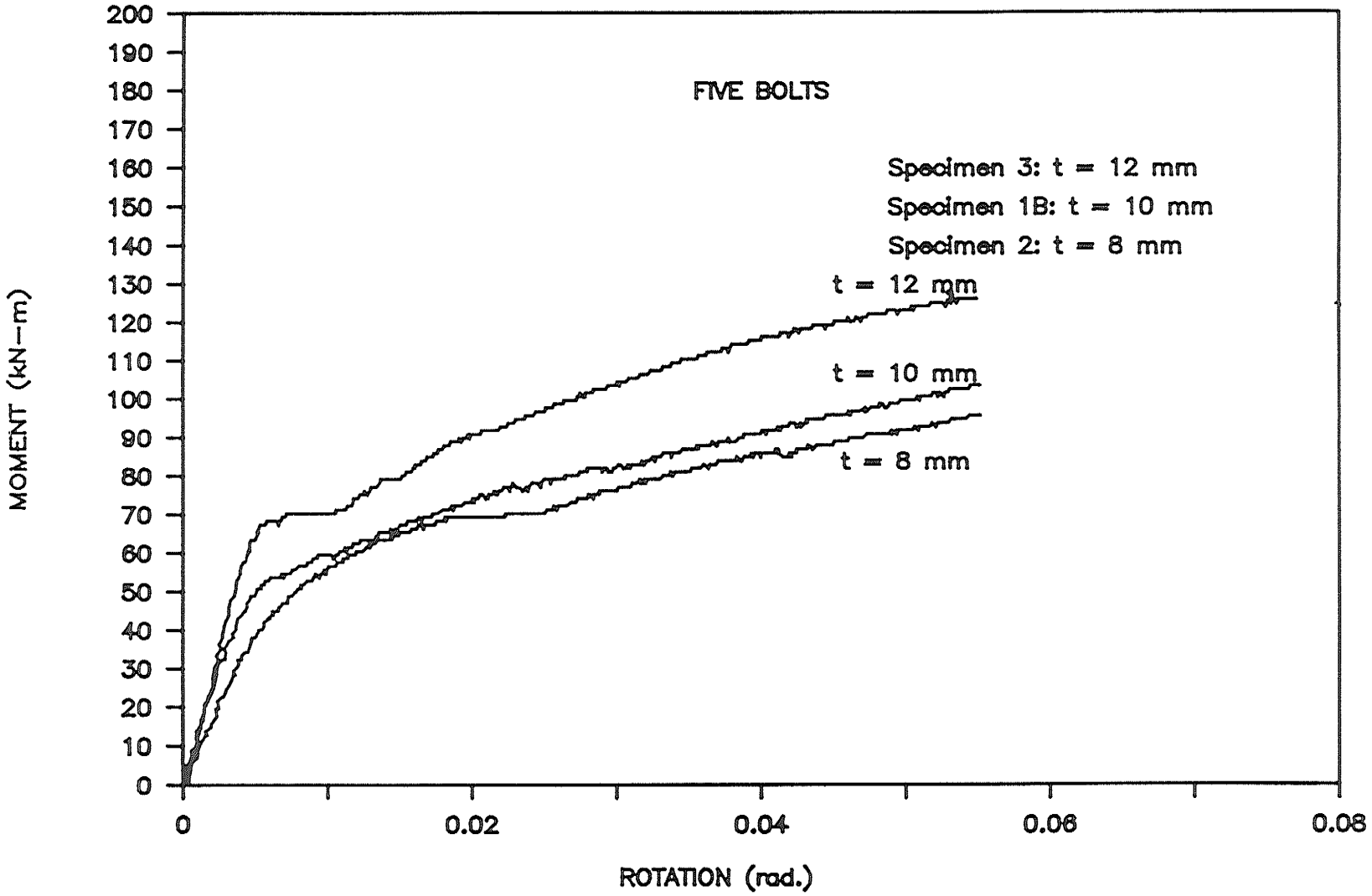

Figure 5.40: Effect of the Angle Thickness on the M-Ø Curves of Specimens 1B, 2 and 3.

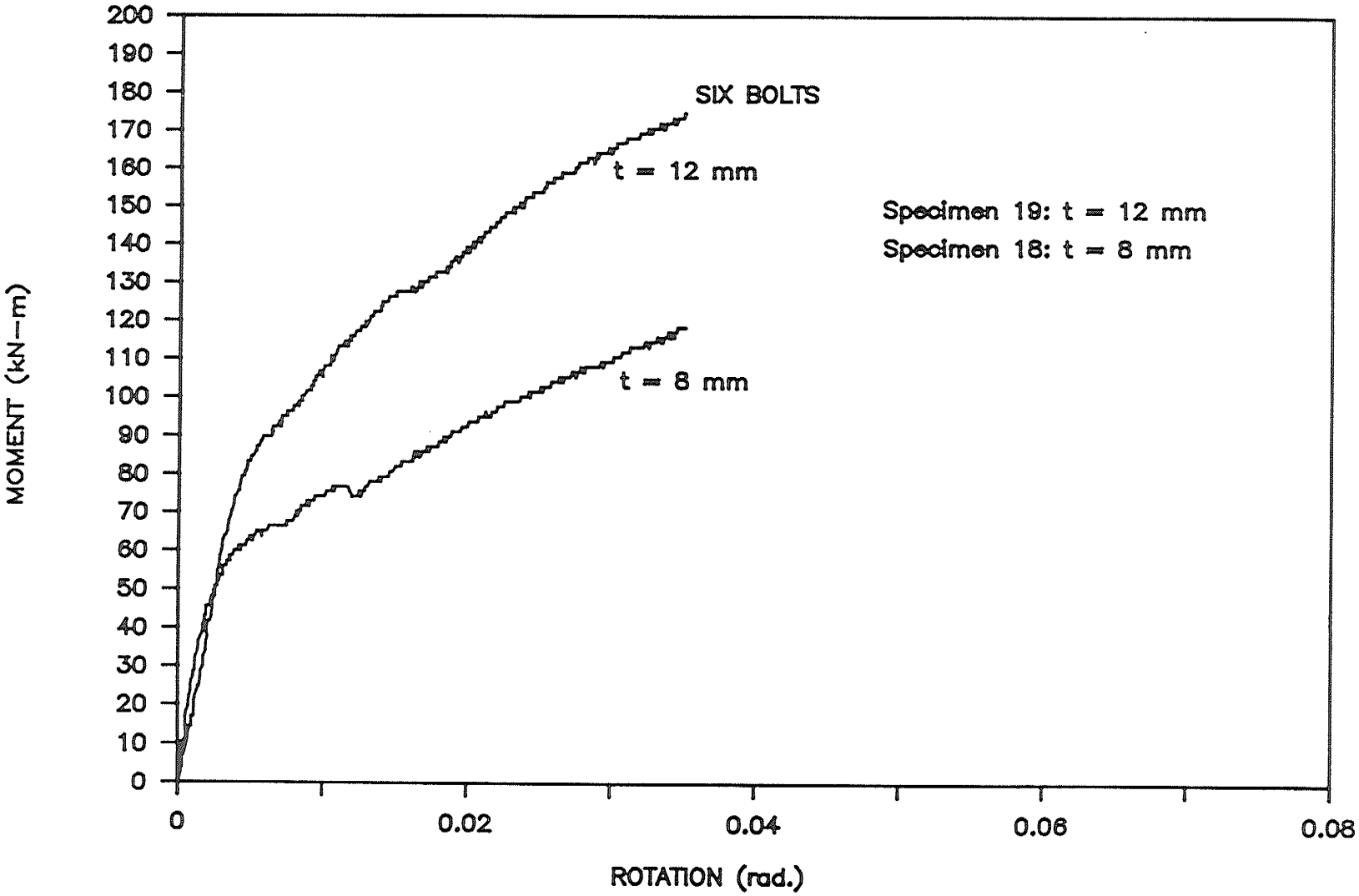

Figure 5.41: Effect of the Angle Thickness on the M-Ø Curves of Specimens 18 and 19.

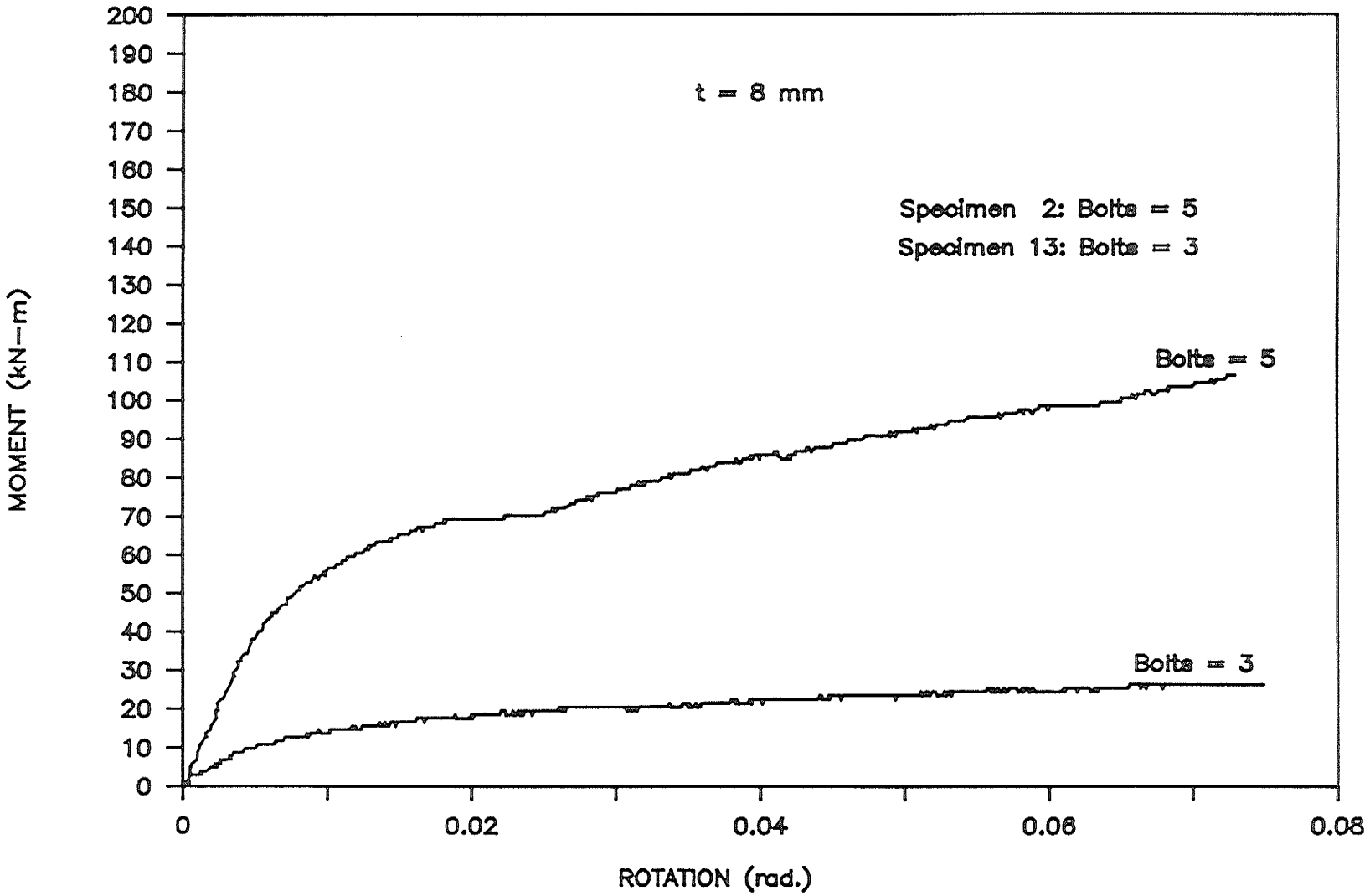

Figure 5.42: Effect of the number of Bolts per Angle Leg on the M-Ø Curves of Specimens 2 and 13.

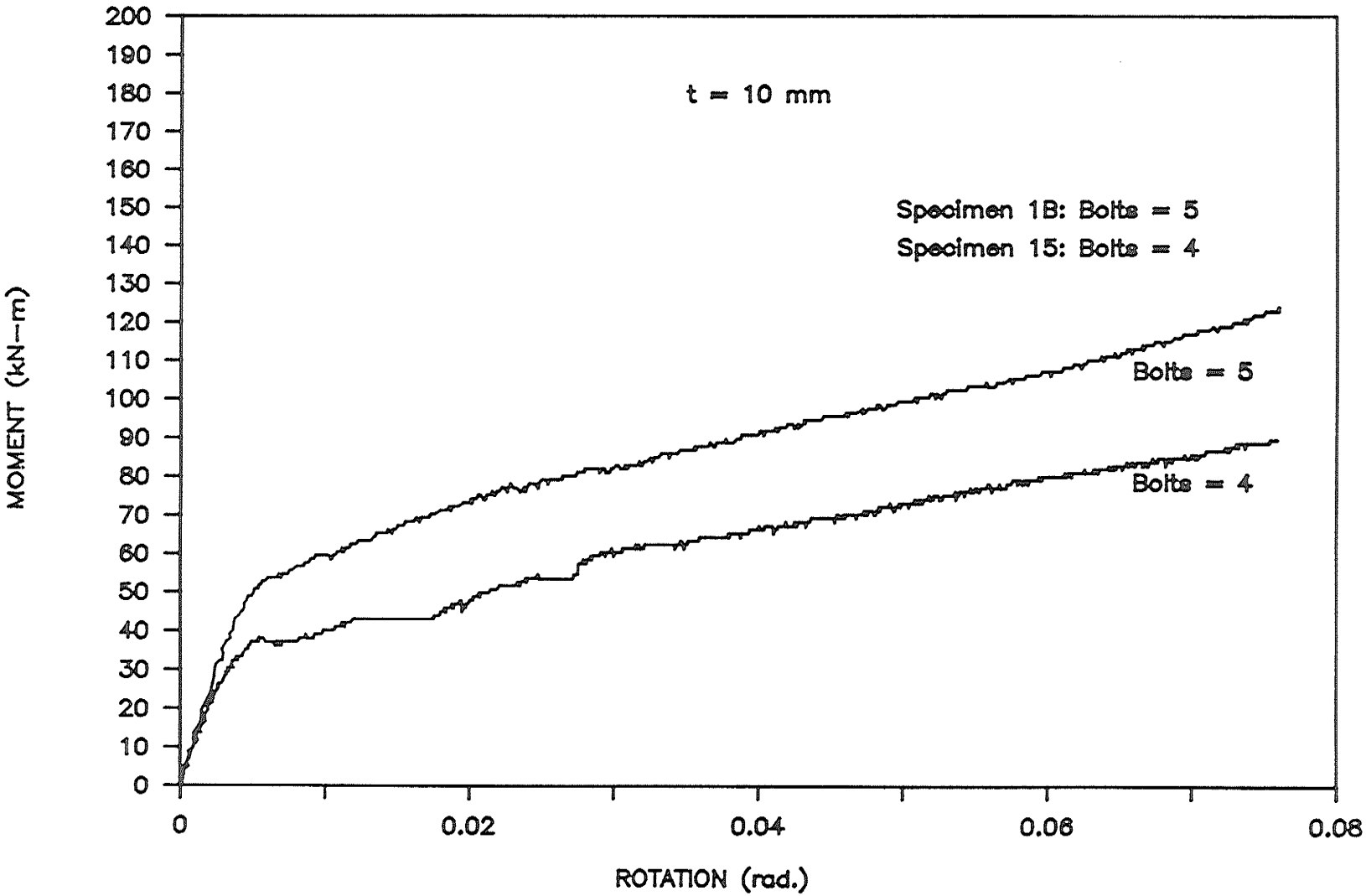

Figure 5.43: Effect of the Number of Bolts per Angle leg on the M-Ø Curves of Specimens 1B and 15.

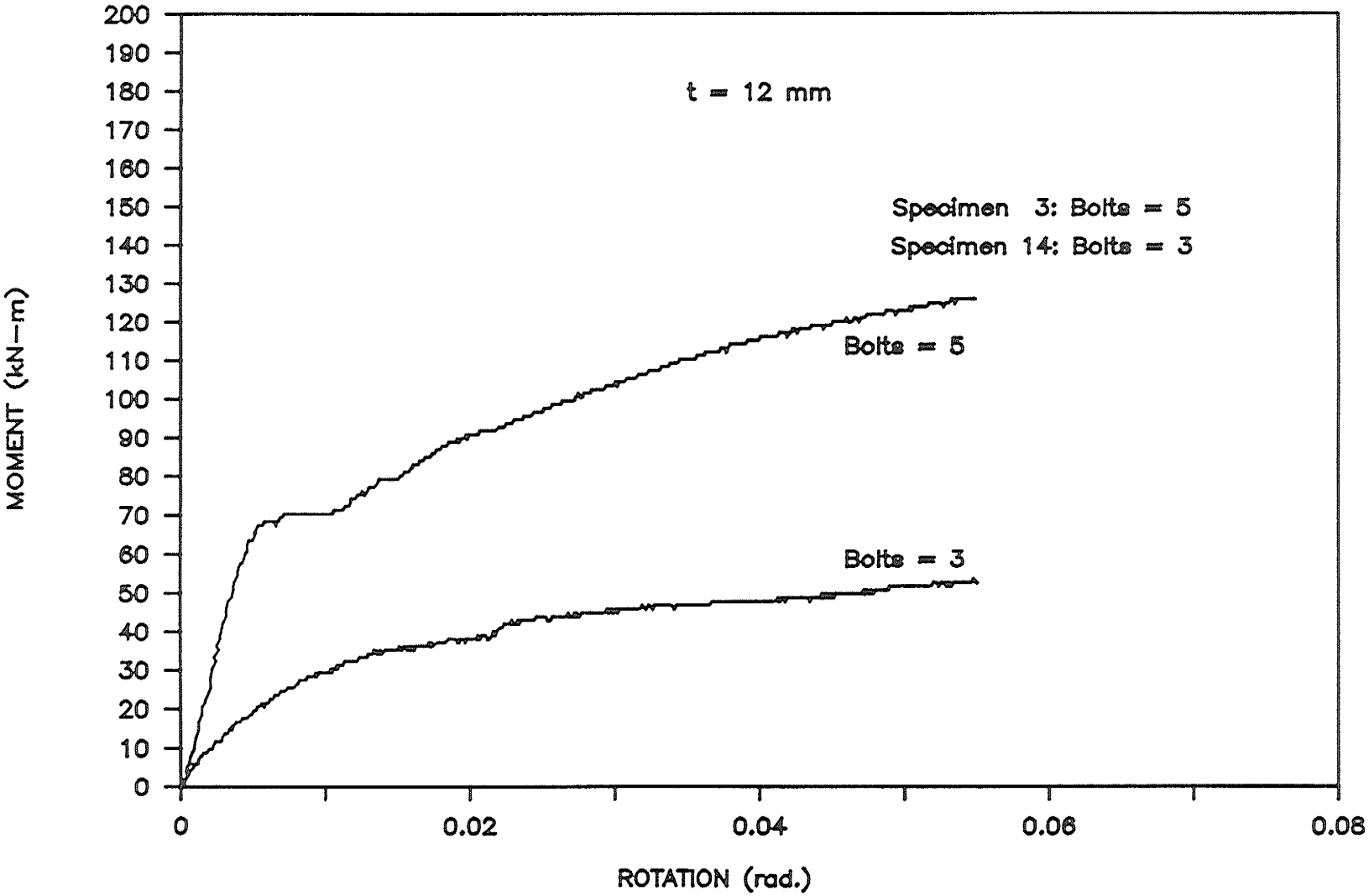

Figure 5.44: Effect of the Number of Bolts per Angle Leg on the M-Ø Curves of Specimens 3 and 14.

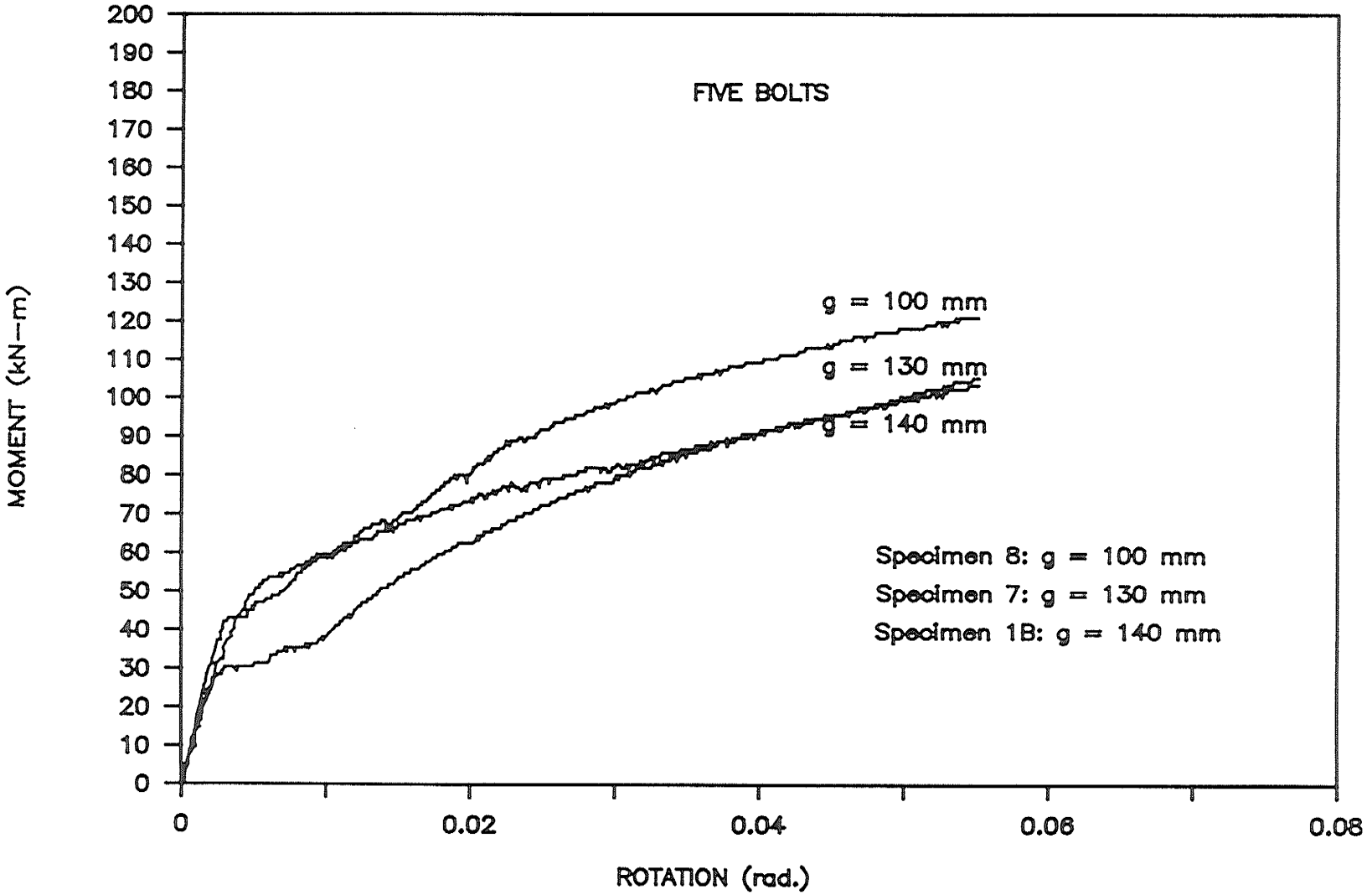

Figure 5.45: Effect of the Column Gauge on the M-Ø Curve of Specimens 1B, 7 and 8.

CHAPTER 6

APPLICATION OF MODELLING PROCEDURE

6.1 GENERAL

In this chapter, the Richard function fits to the experimentally-measured moment-rotation data for connections tested in this study, and for similar connection specimens tested by others, are presented. The approximation errors in the curve fitting are presented in order to permit comparisons of the accuracy of the various fits.

Results of the application of the standardization procedure, as described in section 3.3, to connections tested in this study, for three different combinations of significant connection parameters, are presented. Also presented are the results obtained when the standardization procedure was applied to connections tested in this study plus appropriate ones from other studies, for the optimum combination of parameters.

6.2 RICHARD FUNCTION FITS

The Richard function parameters, $\emptyset_o$, M_o, n and S_p, and the corresponding approximation errors obtained by fitting the Richard function to the test data from this study and to data from other studies, are shown in Table 6.1. It can be seen that the Richard function was fitted to only fourteen out of a total of twenty tests from this study. Specimens 6 and 6A were excluded because they had A307 bolts and their behaviour differed significantly from that of the other

specimens, which employed A325 bolts. Specimen 5 was subjected to multiple loading and unloading cycles and thus the moment-rotation data were not amenable to fitting by the Richard function. Specimen 1A was a duplicate of 1B, and thus it was not included. Finally, for Specimens 9 and 12, convergence of the least squares curve fitting procedure could not be achieved.

Other experimental moment-rotation data for double web angle connections to which the Richard function was fitted were those published by Bell (1958), Bose (1981), Lewitt et al. (1966), Rathbun (1936), Sommer (1969) and Thompson et al. (1970). The experimental data for all of these were obtained from summaries published by Goverdhan (1984) and by Kishi and Chen (1986). The connections were either bolted, bolted-welded or riveted. The test data reported in Table 6.1, represent those from studies in which at least one connection size parameter was varied.

The errors of approximation for the fitted curves ranged from 0.00 to 0.43 percent, suggesting that the Richard function is very suitable for modelling the moment-rotation behaviour of double web angle connections. Figures 6.1 and 6.2, show the moment-rotation curves plotted directly from the experimental data, as a set of lines connecting closely-spaced data points, and the corresponding Richard function fits, for Specimens 1B and 8, respectively. It can be observed in Table 6.1 that the errors associated with fitting the Richard function to the experimental data

were 0.002 and 0.431 percent for Specimens 1B and 8, respectively. These fits are the best and the worst of those for the specimens tested in this study. The experimental curves in Figures 6.1 and 6.2 were terminated at the moment and rotation values corresponding to those at which convergence was achieved in the least squares curve fitting process.

6.3 STANDARDIZATION OF RICHARD FUNCTION

6.3.1 GENERAL

The Richard function parameters and the connection size parameters were used in the procedure described in section 3.3, to produce a standardized moment-rotation function for double web angle connections. The standardization procedure establishes relationships between the Richard function parameters and the connection size parameters. For a given connection, the Richard function parameters are obtained from those relationships and substituted into Equation (3.8) to obtain the standardized, or predicted, moment-rotation curve.

The standardization process was applied to five different cases. Cases 1 through 3 involved the experimental data for the connection tested in this study, while cases 4 and 5 involved the combination of the latter and data from other sources.

In the design of the experimental study, different lengths of angle were used to accommodate the different

numbers of bolts in a vertical row. Consequently, it was assummed initially that the effects of the angle length, l, and the number of bolts per angle leg on the column flange, b, on the moment-rotation behaviour of the test specimens might not be independent. Nonetheless, in the standardization process the individual effects of l and b, as well as their combined effect, were investigated.

The standardized Richard function parameters are presented in the sections to follow. Comparisons between the experimental moment-rotation curves and those constructed from the standardized functions are presented in Tables 6.2 through 6.6. In the tables, the data headed "experimental" are determined from "raw" plots of the experimental data. Those labelled "predicted" are obtained from moment-rotation plots obtained by substituting the parameters for a given connection into the standardized function, thereby giving the M-Ø function for the specific connection. Data presented are the initial slopes of the M-Ø curves, the moment values corresponding to a rotation of 0.024 radians, the percentage errors in the predictions of those values and the approximation errors for the "predicted" curves relative to the experimental ones. Because of the way they are defined, the percentage errors in the predictions are extremely sensitive to differences between the experimental and predicted data. Consequently, the numerical values of the errors are sometimes extremely large. Nonetheless, they

provide a good indication of the relative accuracy of the fits for different specimens.

The percentage errors in the stiffness and moment values were computed as:

$$\text{Percentage Error} = \frac{\text{Predicted Value} - \text{Experimental Value}}{\text{Experimental Value}} \times 100 \qquad (6.2)$$

The average percentage error was computed as:

$$\text{Average Error} = \frac{\sum(\text{Absolute errors for each test})}{\text{Total number of tests}} \qquad (6.3)$$

6.3.2 CASE 1

The effects of five connection size parameters on the moment-rotation behaviour of the bolted double web angle connections tested in this study were considered. The parameters were the angle thickness, t, the column gauge, g, the angle length, l, the beam depth, d, and the number of bolts per angle leg on the column, b.

The expressions obtained for the Richard function parameters, in terms of the connection size parameters are:

$$\begin{aligned} \phi_o &= t^{0.595}\, g^{-2.817}\, l^{4.737}\, d^{-0.784}\, b^{-5.957} \\ M_o &= t^{1.136}\, g^{-1.515}\, l^{1.139}\, d^{0.258}\, b^{0.309} \\ n &= t^{0.522}\, g^{1.564}\, l^{-1.073}\, d^{-0.737}\, b^{1.704} \\ S_p &= t^{0.955}\, g^{2.044}\, l^{-4.445}\, d^{0.327}\, b^{7.555} \end{aligned} \qquad (6.4)$$

For a given connection, the Richard function parameters obtained from Equation (6.4) were substituted into Equation (3.8) to obtain the predicted moment-rotation curve. Figures 6.3 and 6.4, illustrate the experimental and the predicted moment-rotation curves for Specimens 1B and 8, respectively.

Table 6.2 summarizes data obtained from the experimental curves and the corresponding predicted values. Average errors of 26.4 and 7.6 and 68.5 percent were recorded for the initial slope, the moment at 0.024 radians, and the approximation error of the moment-rotation function, respectively.

6.3.3 CASE 2

In this case, the effects of four connection size parameters - the angle thickness, t, the column gauge, g, the angle length, l, and the beam depth, d - were considered.

The Richard function parameters are expressed in terms of the connection size parameters as follows:

$$
\begin{aligned}
\emptyset_o &= t^{1.149}\, g^{0.883}\, l^{-0.614}\, d^{-0.304} \\
M_o &= t^{1.108}\, g^{-1.707}\, l^{1.416}\, d^{0.233} \\
n &= t^{0.363}\, g^{0.506}\, l^{0.457}\, d^{-0.874} \\
S_p &= t^{0.253}\, g^{-2.648}\, l^{2.341}\, d^{-0.282}
\end{aligned}
\qquad (6.5)
$$

Figures 6.5 and 6.6, show the experimental and the predicted moment-rotation curves for Specimens 1B and 8, respectively.

The experimental and predicted values are presented in Table 6.3. The average errors for the initial slope, the moment at 0.024 radians and the approximation error of the moment-rotation function were 24.6, 15.1 and 966.4 percent, respectively.

6.3.4 CASE 3

The effects of four connection size parameters - the angle thickness, t, the column gauge, g, the beam depth, d, and the number of bolts per angle leg on the column, b - were considered.

The relationships between the Richard function parameters and the connection size parameters are:

$$\begin{aligned} \emptyset_o &= t^{1.064}\, g^{-0.111}\, d^{0.272}\, b^{-1.375} \\ M_o &= t^{1.248}\, g^{-0.864}\, d^{0.512}\, b^{1.411} \\ n &= t^{0.416}\, g^{0.951}\, d^{-0.976}\, b^{0.666} \\ S_p &= t^{0.516}\, g^{-0.495}\, d^{-0.663}\, b^{3.256} \end{aligned} \qquad (6.6)$$

The experimental and predicted moment-rotation curves for Specimens 1B and 8, are presented in Figures 6.7 and 6.8.

Table 6.4 gives a comparison of experimental and predicted values. The average errors for the initial slope, the moment at 0.024 radians, and the approximation error of

the moment-rotation function were 24.3, 8.3 and 126.6 percent, respectively.

6.3.5 CASE 4

The effects of five connection size parameters - the angle thickness, t, the column gauge, g, the angle length, l, the beam depth, d, and the number of bolts per angle leg on the column, b - were considered. The experimental data from this study, plus five sets of test data from other sources were employed in the analysis. The data from other sources, presented in Table 6.5, comprised all of that available on bolted-bolted connections.

The Richard function parameters were computed to be:

$$\begin{aligned} \phi_o &= t^{-0.267}\, g^{0.920}\, l^{-0.414}\, d^{0.084}\, b^{-0.347} \\ M_o &= t^{0.348}\, g^{-1.261}\, l^{1.653}\, d^{-0.017}\, b^{-0.241} \\ n &= t^{0.578}\, g^{0.390}\, l^{0.540}\, d^{-0.973}\, b^{0.150} \\ S_p &= t^{0.871}\, g^{-1.432}\, l^{4.686}\, d^{-3.587}\, b^{-0.547} \end{aligned} \qquad (6.7)$$

Figures 6.9 and 6.10, show the experimental and predicted moment-rotation curves for Specimens 1B and 8, respectively.

The results obtained from the test data and the corresponding predicted values are tabulated in Table 6.5. The average errors for the initial slope, the moment at 0.024 radians, and the approximation error of the moment-rotation curve were 25.0, 20.5 and 4,300.9 percent, respectively.

6.3.6 CASE 5

For this case, all of the available test data on double web angle connections, namely those on bolted-bolted, bolted-welded and riveted connections, were considered. The data from other sources, as shown in Table 6.6, were obtained from Rathbun (1936), Bell (1958), Lewitt et al. (1966), Sommer (1969), Thompson et al. (1970) and Bose (1981). The five connection size parameters, t, g, l, d and b, were considered in the analysis.

The Richard function parameters were computed to be:

$$\begin{aligned} \phi_o &= t^{-0.468}\, g^{-0.690}\, l^{0.969}\, d^{0.569}\, b^{-2.127} \\ M_o &= t^{0.351}\, g^{-1.770}\, l^{2.728}\, d^{-0.540}\, b^{-0.620} \\ n &= t^{0.310}\, g^{0.329}\, l^{0.211}\, d^{-0.414}\, b^{-0.275} \\ S_p &= t^{-0.136}\, g^{-0.399}\, l^{2.989}\, d^{-2.876}\, b^{1.269} \end{aligned} \qquad (6.8)$$

Figures 6.11 and 6.12, show the experimental and predicted moment-rotation curves for Specimens 1B and 8, respectively.

The results obtained from the test data and the corresponding predicted values are tabulated in Table 6.6. The average errors for the initial slope, the moment at 0.024 radians, and the approximation error of the moment-rotation curve were 36.8, 24.8 and 11,197.2 percent, respectively.

6.4 DISCUSSION OF RESULTS

Comparisons of the average errors for the initial slope, the moment at 0.024 radians and the approximation error, for cases 1 through 3, as presented in Tables 6.2 through 6.4, reveal that the standardized Richard function parameters based on case 1 provided the best fit to the experimental data for this study. The average approximation errors for cases 2 and 3 were 14.1 and 1.8 times, respectively, that for case 1.

It is concluded therefore that the five connection size parameters - the angle thickness, t, the gauge on the column, g, the length of the angle, l, the beam depth, d, and the number of bolts per angle leg, b - all had significant influence on the moment-rotation behaviour of double web angle connections. The average errors for the predicted initial slope and moment at 0.024 radians for the three cases compared very well with one another, implying that the errors based on the specific points on the moment-rotation curves may not be sufficient as the basis for comparing the different prediction models.

It can be seen from Tables 6.2, 6.5 and 6.6, which provide data for Cases 1, 4 and 5, that the average approximation error for case 4 is 62.7 times larger than that for case 1, while the error for case 5 is 163.5 times larger than that for case 1. This shows that the error of approximation increased as the number of the test data from other sources increased. The different conditions under

which the various tests were performed, was probably the primary reason for the large discrepancies observed for case 4. The even larger error of approximation for case 5 was probably due to the fact that the latter case included bolted-welded and all-riveted connections, in addition to bolted-bolted ones. An examination of Figures 6.3, 6.4 and 6.9 to 6.12, shows that the standardized functions for cases 1, 4 and 5 give good predictions of the moment-rotation curves.

The approximation error for case 5 is 2.6 times that for case 4. This observation further indicates that the greater the number of test data from different sources that are included in the modelling procedure, the larger the error of approximation.

Based on all of the above findings, it is suggested that the standardization procedure employed for this study is adequate for use with all available pertinent data for a given connection type.

Since the standardized Richard function parameters for case 5 [Equation (6.8)] utilized data for different types of double web angle connections, it is best suited for use in general-purpose structural analysis procedures. The accuracy of the function can be improved by utilizing, in the standardization procedure, additional test data that are obtained under testing conditions which are as similar as possible.

TABLE 6.1: RICHARD FUNCTION PARAMETERS AND APPROXIMATION ERRORS FOR DOUBLE WEB ANGLE CONNECTIONS.

Name of investigator	Test identity	Richard Function Parameters				Approximation error (%)
		Øo (radians)	Mo (kN-m)	n	Sp (kN-m/rad)	
Onuah*	Test-1B	3.63	58.82	1.60	0.827	0.002
"	Test-2	6.89	59.83	2.24	0.637	0.004
"	Test-3	4.50	63.43	6.75	1.271	0.061
"	Test-4	6.37	75.79	1.58	0.378	0.013
"	Test-7	1.31	32.97	0.88	1.582	0.129
"	Test-8	12.83	104.77	1.49	0.411	0.431
"	Test-10	7.69	17.42	2.50	0.186	0.003
"	Test-11	8.94	27.41	1.52	0.212	0.083
"	Test-13	6.07	16.89	1.49	0.148	0.015
"	Test-14	9.60	42.49	1.62	0.211	0.044
"	Test-15	2.79	35.06	2.19	0.768	0.108
"	Test-16	2.32	53.01	1.61	1.039	0.011
"	Test-18	1.71	60.00	1.64	1.642	0.013
"	Test-19	4.24	93.11	2.15	2.400	0.008
Bell	FK-4A	4.20	34.25	1.30	0.301	0.001
Bose	B-1	1.72	34.24	3.98	6.667	0.000
Lewitt et al.	FK-3	7.33	34.73	1.85	0.176	0.000
"	Wk-4	1.96	15.90	1.09	0.135	0.001
"	FK-4AB-M	1.86	26.50	1.23	0.264	0.000
"	FK-5	4.66	67.61	1.69	0.724	0.001
Rathbun	A-1	18.04	2.01	5.93	0.011	0.006
"	A-2	2.28	5.48	1.99	0.370	0.020
"	A-3	7.00	12.33	2.00	0.057	0.300
"	A-4	6.19	16.86	2.25	0.221	0.002
"	A-5	0.34	7.13	1.63	2.330	0.001
"	A-6	2.07	37.62	1.81	1.337	0.219
"	A-7	0.43	17.66	2.74	11.790	0.000
Sommer	Test21	13.91	34.61	2.84	0.315	0.000
"	Test22	12.29	80.06	1.97	0.290	0.000
"	Test23	8.99	68.91	2.27	0.658	0.000
"	Test24	8.52	98.42	2.28	1.020	0.000
Thompson et al.	B1-2	2.33	36.19	1.20	0.176	0.057
	D1-1	4.42	33.52	1.45	0.128	0.019
"	E1-1	2.92	49.79	1.68	0.114	0.101
"	A2-1	11.84	16.05	0.93	0.171	0.130
"	C2-1	1.34	13.20	1.96	0.764	0.001
"	D2-1	0.65	15.65	1.20	0.740	0.000

NOTE:

* Fourteen Tests were fitted with the Richard Function.

TABLE 6.2: Initial Slopes, Moments at 0.024 rad., and Approximation Errors For Experimental and Predicted M-Ø curves.

CASE 1: Prediction model considered the effects of t, g, l, d and b on connection behaviour, based on data from experimental testing program.

	EXPERIMENTAL		PREDICTED				
Specimen number.	Initial slope of M-Ø curve. (kN-m/rad)	Moment at 0.024 rad. (kN-m)	Initial slope of M-Ø curve, Mo/Øo. (kN-m/rad)	Moment at 0.024 rad. (kN-m)	Error in initial slope. (%) *	Error in moment at 0.024 rad. (%) *	Approximation error for M-Ø curve. (%)
1B	11,870	78.19	14,690	76.94	+23.7	- 1.6	0.1
2	7,710	70.37	13,010	60.31	+68.7	-14.3	68.8
3	14,280	95.78	16,210	93.87	+13.5	- 1.9	0.2
4	11,870	78.19	14,690	76.94	+23.7	- 1.6	23.1
7	12,730	70.38	13,340	79.28	+ 4.7	+12.6	123.3
8	16,240	89.92	9,480	83.70	-41.6	- 6.9	42.7
10	2,450	20.85	2,410	20.47	- 1.6	- 1.8	4.3
11	3,240	28.60	3,000	32.24	- 7.4	+12.7	9.9
13	2,780	19.55	3,550	22.15	+27.7	+13.3	117.5
14	5,760	43.01	4,410	35.24	-23.4	-18.0	464.5
15	10,650	52.78	8,290	49.93	-22.1	- 5.4	97.2
16	22,890	78.20	19,470	82.58	-14.9	+ 5.6	2.6
18	25,040	100.35	27,650	93.77	+10.4	- 6.5	3.9
19	18,520	152.48	34,430	145.17	+85.9	- 4.7	1.6
				Average Error =	26.4	7.6	68.5

NOTE:

* A positive number represents a predicted value which is larger than the experimental value.
A negative number represents a predicted value which is smaller than the experimental value.

TABLE 6.3: Initial Slopes, Moment at 0.024 rad., and Approximation Errors For Experimental and Predicted M-Ø curves.

CASE 2: Prediction model considered the effect of t, g, l and d on connection behaviour, based on data from experimental testing program.

	EXPERIMENTAL		PREDICTED				
Specimen number.	Initial slope of M-Ø curve, (kN-m/rad)	Moment at 0.024 rad. (kN-m)	Initial slope of M-Ø curve, Mo/Øo. (kN-m/rad)	Moment at 0.024 rad. (kN-m)	Error in initial slope. (%) *	Error in moment at 0.024 rad. (%) *	Approximation error for M-Ø curve. (%)
1B	11,870	78.19	12,310	71.64	+ 3.7	- 8.3	7.4
2	7,710	70.37	12,420	59.07	+61.0	-16.0	138.8
3	14,280	95.78	12,220	84.22	-14.4	-12.0	141.9
4	11,870	78.19	12,310	71.64	+ 3.7	- 8.3	3.2
7	12,730	70.38	14,920	82.77	+17.2	+17.6	236.6
8	16,240	89.92	9,980	71.63	-38.5	-20.3	9556.3
10	2,450	20.85	3,480	23.52	+ 1.2	+12.8	40.4
11	3,240	28.60	3,430	33.84	+ 5.8	+18.3	46.9
13	2,780	19.55	4,250	23.84	+52.8	+21.9	585.3
14	5,760	43.01	4,180	34.47	-27.4	-19.8	821.8
15	10,650	52.78	7,730	48.56	-27.4	- 8.0	258.6
16	22,890	78.20	14,240	72.59	-37.7	- 7.1	7.6
18	25,040	100.35	14,370	82.42	-42.6	-17.8	499.5
19	18,520	152.48	20,640	117.32	+11.4	-23.0	1185.1
				Average Error =	24.6	15.1	966.4

NOTE:

* A positve number represents a predicted value which is larger than the experimental value.
A negative number represents a predicted value which is smaller than the experimental value.

TABLE 6.4: Initial Slopes, Moments at 0.024 rad., and Approximation Errors Experimental and Predicted M-Ø curves.

CASE 3: Prediction model considered the effect of t, g, d and b on connection behaviour, based on data from experimental testing program.

	EXPERIMENTAL		PREDICTED				
Specimen number.	Initial slope of M-Ø curve, (kN-m/rad)	Moment at 0.024 rad. (kN-m)	Initial slope of M-Ø curve, Mo/Øo, (kN-m/rad)	Moment at 0.024 rad. (kN-m)	Error in initial slope. (%) *	Error in moment at 0.024 rad. (%)*	Approximation error for M-Ø curve. (%)
1B	11,870	78.19	14,300	76.96	+20.4	- 1.5	0.1
2	7,710	70.37	13,720	61.23	+77.9	-12.9	31.2
3	14,280	95.78	14,790	93.10	+ 3.5	- 2.8	1.0
4	11,870	78.19	14,300	76.96	+20.4	- 1.5	19.0
7	12,730	70.38	15,120	81.15	+18.7	+15.3	181.8
8	16,240	89.92	18,420	97.05	+13.4	+ 7.9	33.2
10	2,450	20.85	3,020	21.13	+23.2	+ 1.3	0.0
11	3,240	28.60	3,260	32.68	+ 0.6	+14.2	17.5
13	2,780	19.55	3,310	21.98	+19.0	+12.4	89.1
14	5,760	43.01	3,560	34.21	-38.1	-20.4	1197.4
15	10,650	52.78	7,680	49.69	-27.8	- 5.8	164.3
16	22,890	78.20	15,260	79.81	-33.3	+ 2.0	0.4
18	25,040	100.35	24,340	91.23	- 2.8	- 9.0	25.2
19	18,520	152.48	26,230	138.63	+41.6	- 9.0	12.5
				Average Error =	24.3	8.3	126.6

NOTE:

* A positve number represents a predicted value which is larger than the experimental value.
A negative number represents a predicted value which is smaller than the experimental value.

TABLE 6.5: Initial Slopes, Moments at 0.024 rad., and Approximation Errors For Experimental and Predicted M-Ø curves.

CASE 4: Prediction model considered the effect of t, g, l, d and b on connection behaviour, based on data from experimental test program and five other data from bolted connections.

		EXPERIMENTAL		PREDICTED				
Name of investigator	Specimen number	Initial slope of M-Ø curve, (kN-m/rad)	Moment at 0.024 rad. (kN-m)	Initial slope of M-Ø curve, Mo/Øo (kN-m/rad)	Moment at 0.024 rad. (kN-m)	Error in initial slope. (%)*	Error in moment at 0.024 rad. (%)*	Approximation error for M-Ø curve. (%)
Onuah	1B	11,870	78.19	12,450	76.13	+ 4.8	- 2.6	0.2
"	2	7,710	70.37	10,850	66.41	+40.7	- 5.6	1.4
"	3	14,280	95.78	13,930	82.90	- 2.4	-13.4	55.6
"	4	11,870	78.19	12,450	75.07	+ 4.8	- 3.9	26.3
"	7	12,730	70.38	14,630	82.77	+14.9	+17.6	189.0
"	8	16,240	89.92	25,940	116.98	+59.7	+30.0	2,058.6
"	10	2,450	20.85	3,580	29.98	+46.1	+43.7	3,272.3
"	11	3,240	28.60	4,600	37.65	+41.9	+31.6	369.2
"	13	2,780	19.55	3,450	21.91	+24.1	+12.0	46.6
"	14	5,760	43.01	4,430	27.57	-23.0	-35.9	49,170.8
"	15	10,650	52.78	7,570	45.30	-28.9	-14.1	1,371.2
"	16	22,890	78.20	12,110	58.55	-47.0	-25.1	3,217.2
"	18	25,040	100.35	15,830	76.15	-36.7	-24.2	4,113.7
"	19	18,520	152.48	20,320	93.76	+ 9.7	-38.5	17,106.7
Bose**	B-1	19,960	-	19,790	110.94	- 0.8	-	0.0
Lewitt#	FK-3	4,740	32.81	3,530	41.73	-25.5	+27.1	538.9
Thompson#	B1-2	15,540	37.97	7,850	38.31	+ 0.9	+ 0.9	0.4
"	D1-2	7,580	34.72	11,780	45.26	+55.4	+30.3	156.3
"	E1-1	17,040	50.85	15,730	57.62	- 7.6	+13.3	22.0
					Average Error =	25.0	20.5	4,300.9

NOTE:

* A positive number represents a predicted value which is larger than the experimental value.
A negative number represents a predicted value which is smaller than the experimental value.

** Reference: Kishi and Chen, 1986.

Reference: Goverdhan, 1984.

TABLE 6.6: Initial Slopes, Moments at 0.024 rad., and Approximation Errors For Experimental and Predicted M-Ø curve.

CASE 5: Prediction model considered the effect of t, g, l, d and b on connection behaviour, based on data from experimental testing program and available data on double web angle connections.

		EXPERIMENTAL		PREDICTED				
Name of investigator	Specimen number.	Initial slope of M-Ø curve, (kN-m/rad)	Moment at 0.024 rad. (kN-m)	Initial slope of M-Ø curve, Mo/Øo, (kN-m/rad)	Moment at 0.024 rad. (kN-m)	Error in initial slope. (%)*	Error in moment at 0.024 rad. (%)*	Approximation error for M-Ø curve.
Onuah	1B	11,870	78.19	14,430	77.94	+21.5	- 0.4	0.4
"	2	7,710	70.37	12,020	73.85	+55.9	+ 4.9	14.2
"	3	14,280	95.78	16,750	81.44	+17.3	-14.9	174.2
"	4	11,870	78.19	14,430	77.94	+21.5	- 0.3	35.8
"	7	12,730	70.38	15,630	86.08	+22.7	+22.3	343.9
"	8	16,240	89.92	20,750	123.57	+27.7	+37.4	1,998.1
"	10	2,450	20.85	3,320	27.39	+35.5	+31.3	1,151.0
"	11	3,240	28.60	4,630	30.54	+42.9	+ 6.7	4.1
"	13	2,780	19.55	2,200	18.21	-20.8	- 6.8	21.8
"	14	5,760	43.01	3,060	21.21	-46.8	-50.6	381,095.1
"	15	10,650	52.78	6,880	42.16	-35.4	-20.1	4,170.9
"	16	22,890	78.20	10,690	57.17	-53.3	-26.8	3,658.3
"	18	25,040	100.35	16,270	87.52	-35.0	-12.7	185.7
"	19	18,520	152.48	22,680	97.91	+22.4	-35.7	12,813.4
Bell**	FK-4A	8,150	39.32	6,010	35.57	-26.2	- 9.5	6.6
Bose**	B-1	19,960	-	22,780	-	+14.1	-	0.1
Lewitt #	FK-3	4,740	32.81	3,590	25.31	-24.2	-22.8	152.1
"	WK-4	8,120	18.81	6,010	35.61	-25.9	+94.4	2.7
"	FK-4AB-M	14,260	31.19	21,230	46.10	+48.8	+47.8	157.0
"	FK-5	14,520	81.36	14,490	69.61	- 0.2	-14.4	6.9
Rathbun**	A-1	110	2.17	170	2.18	+54.5	+ 0.4	10.5
"	A-2	2,400	11.77	1,660	16.08	-30.8	+36.6	4.4
"	A-3	1,760	13.55	4,710	18.61	+167.6	+37.3	172.0
"	A-4	2,720	21.97	3,970	29.68	+45.9	+35.0	613.6
"	A-5	20,840	-	8,070	-	-	-	454.1
"	A-6	18,180	-	13,430	-	-	-	2.3
"	A-7	41,060	-	27,310	-	-	-	5,936.4
Sommer #	Test21	2,490	39.32	3,570	31.01	+43.3	-21.1	266.2
"	Test22	6,510	76.61	9,140	63.28	+40.4	-17.4	10.6
"	Test23	7,670	81.36	9,760	52.35	+27.2	-35.6	395.2
"	Test24	11,560	117.52	17,710	84.28	+53.2	-28.2	104.9

TABLE 6.6 (continued)

		EXPERIMENTAL		PREDICTED				
Name of investigator	Specimen number.	Initial slope of M-Ø curve, (kN-m/rad)	Moment at 0.024 rad. (kN-m)	Initial slope of M-Ø curve, Mo/Øo, (kN-m/rad)	Moment at 0.024 rad. (kN-m)	Error in initial slope. (%)*	Error in moment at 0.024 rad. (%)*	Approximation error for M-Ø curve.
Thompson#	B1-2	15,540	37.97	8,980	31.49	-42.2	-17.0	31.5
"	D1-2	7,580	34.72	8,620	43.08	+13.7	+24.0	1.3
"	E1-1	17,040	50.85	12,660	50.78	-25.7	- 0.1	4.7
"	A2-1	4,030	17.63	6,110	27.54	+51.6	+56.2	106.2
"	C2-1	9,850	31.87	8,980	31.49	- 8.8	- 1.1	2.1
"	D2-1	23,970	33.90	12,500	50.51	-47.8	+49.0	187.3
					Average Error =	36.8	24.8	11,197.2

NOTE:

* A positive number represents a predicted value which is larger than the experimental value.
A negative number represents a predicted value which is smaller than the experimental value.

** Reference: Kishi and Chen, 1986.

Reference: Goverdhan, 1984.

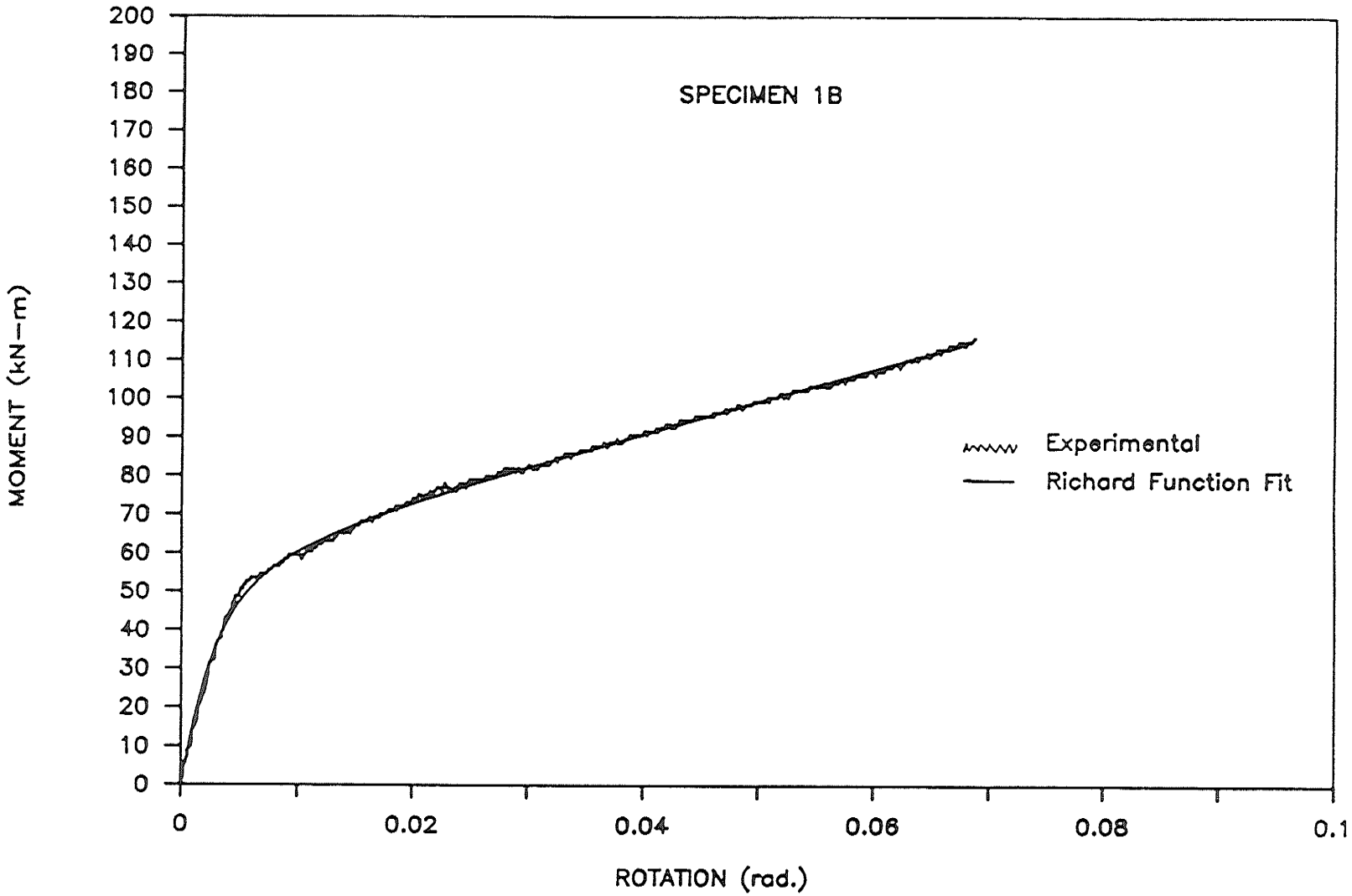

Figure 6.1: Moment-Rotation Curve for Specimen 1B Compared with the Richard Function Fit.

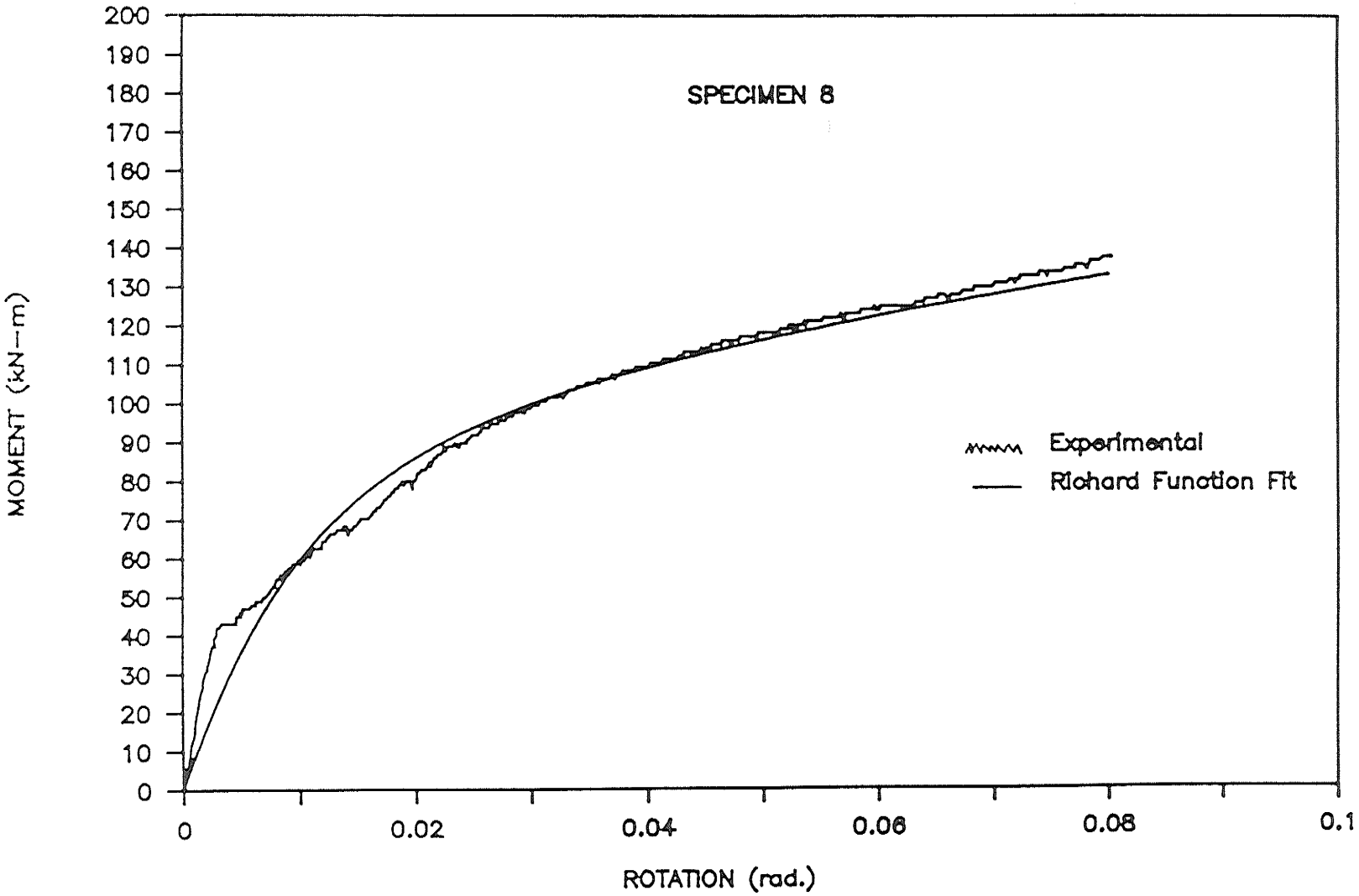

Figure 6.2: Moment-Rotation Curve for Specimen 8
Compared with the Richard Function Fit.

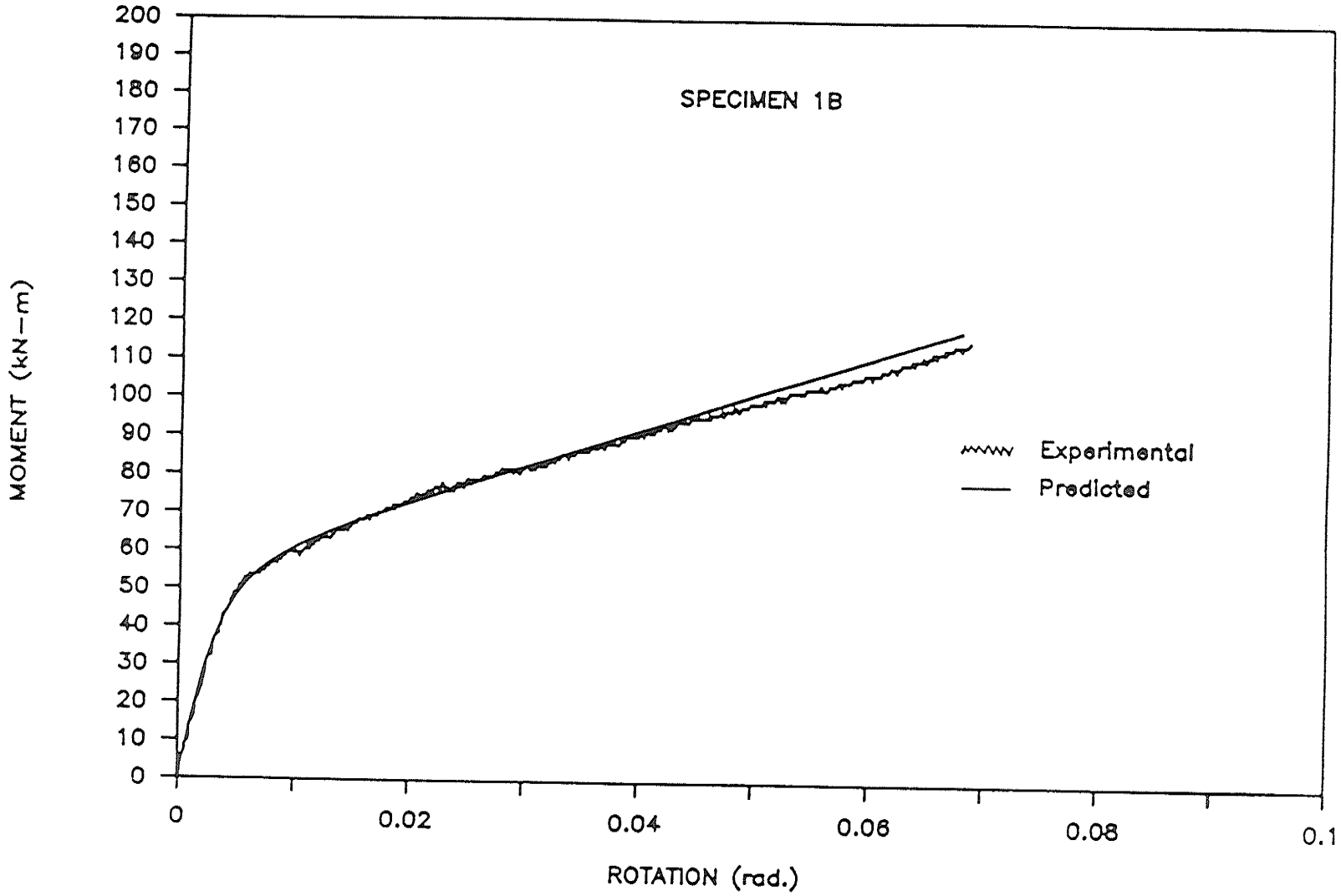

Figure 6.3: Case 1 - Experimental and Predicted Moment-Rotation Curves for Specimen 1B.

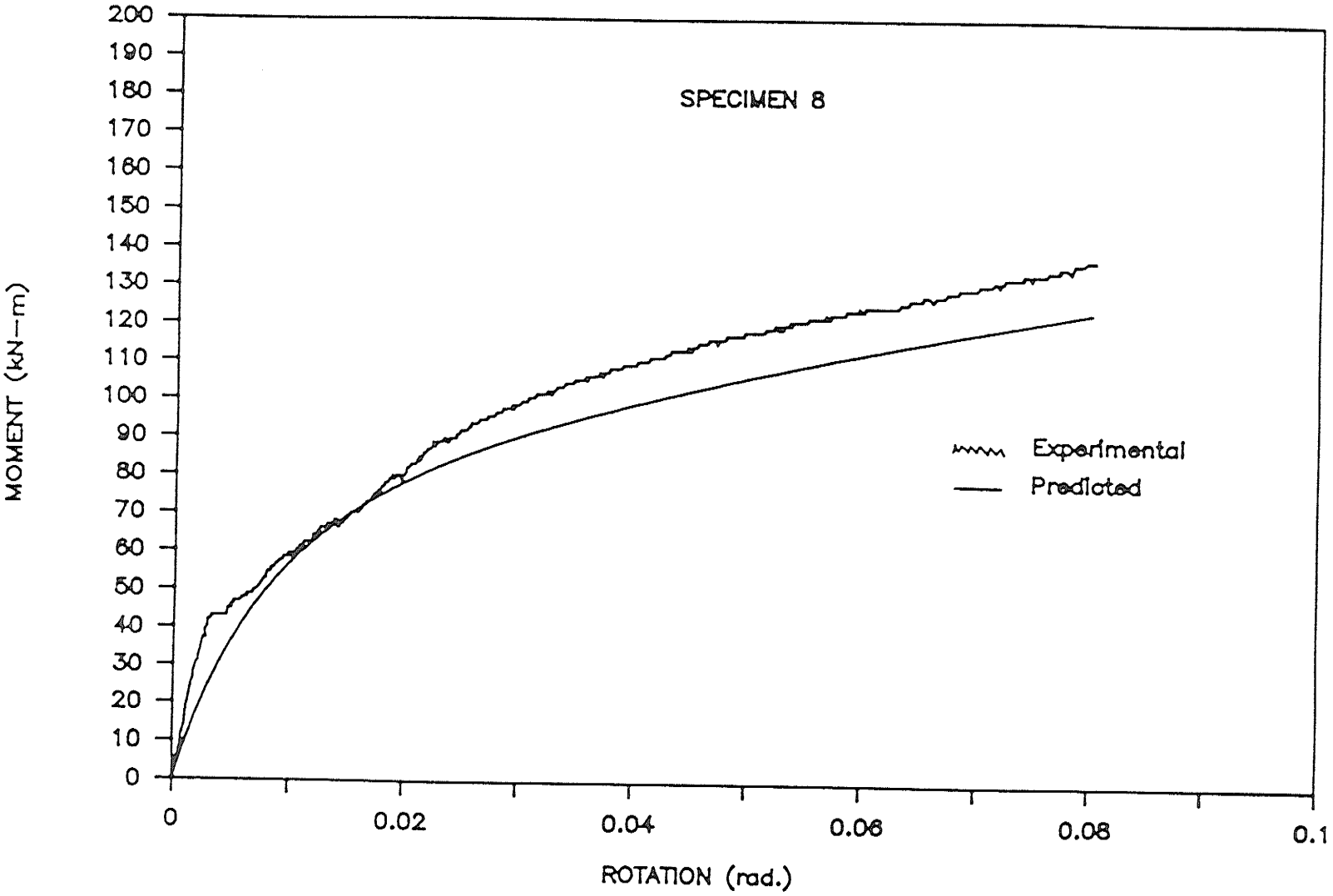

Figure 6.4: Case 1 - Experimental and Predicted Moment-Rotation Curves for Specimen 8.

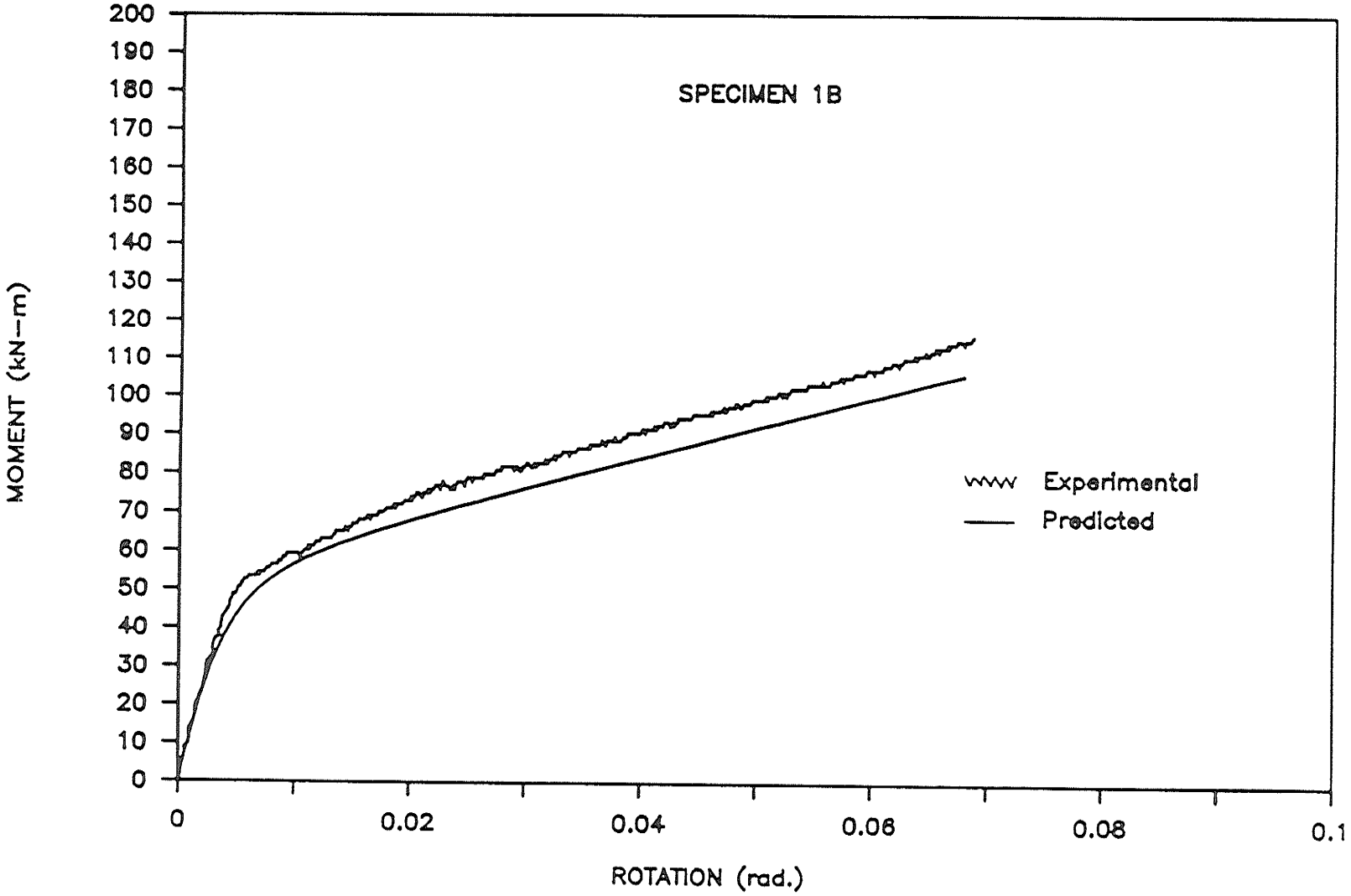

Figure 6.5: Case 2 - Experimental and Predicted Moment-Rotation Curves for Specimen 1B.

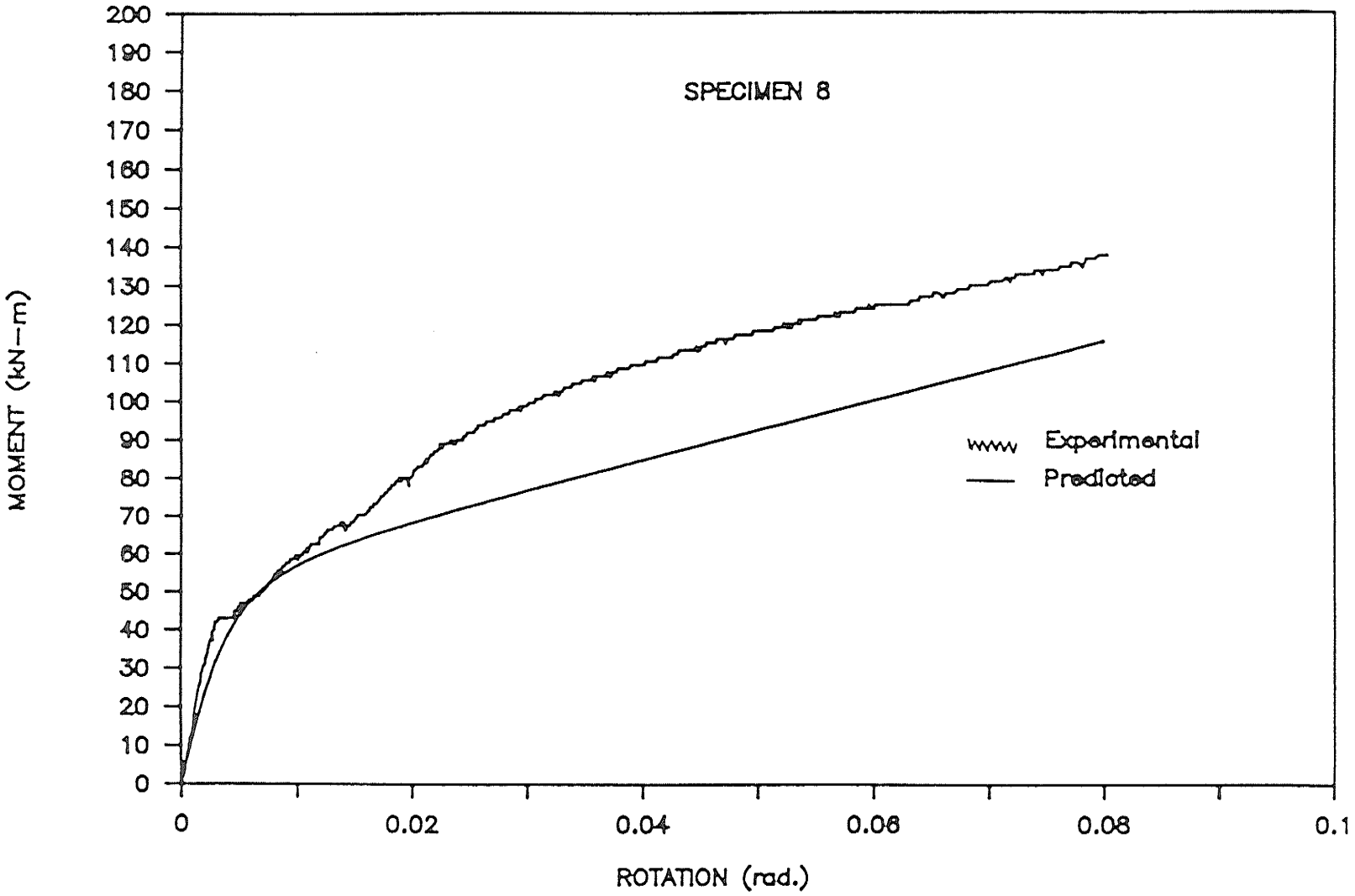

Figure 6.6: Case 2 - Experimental and Predicted Moment-Rotation Curves for Specimen 8.

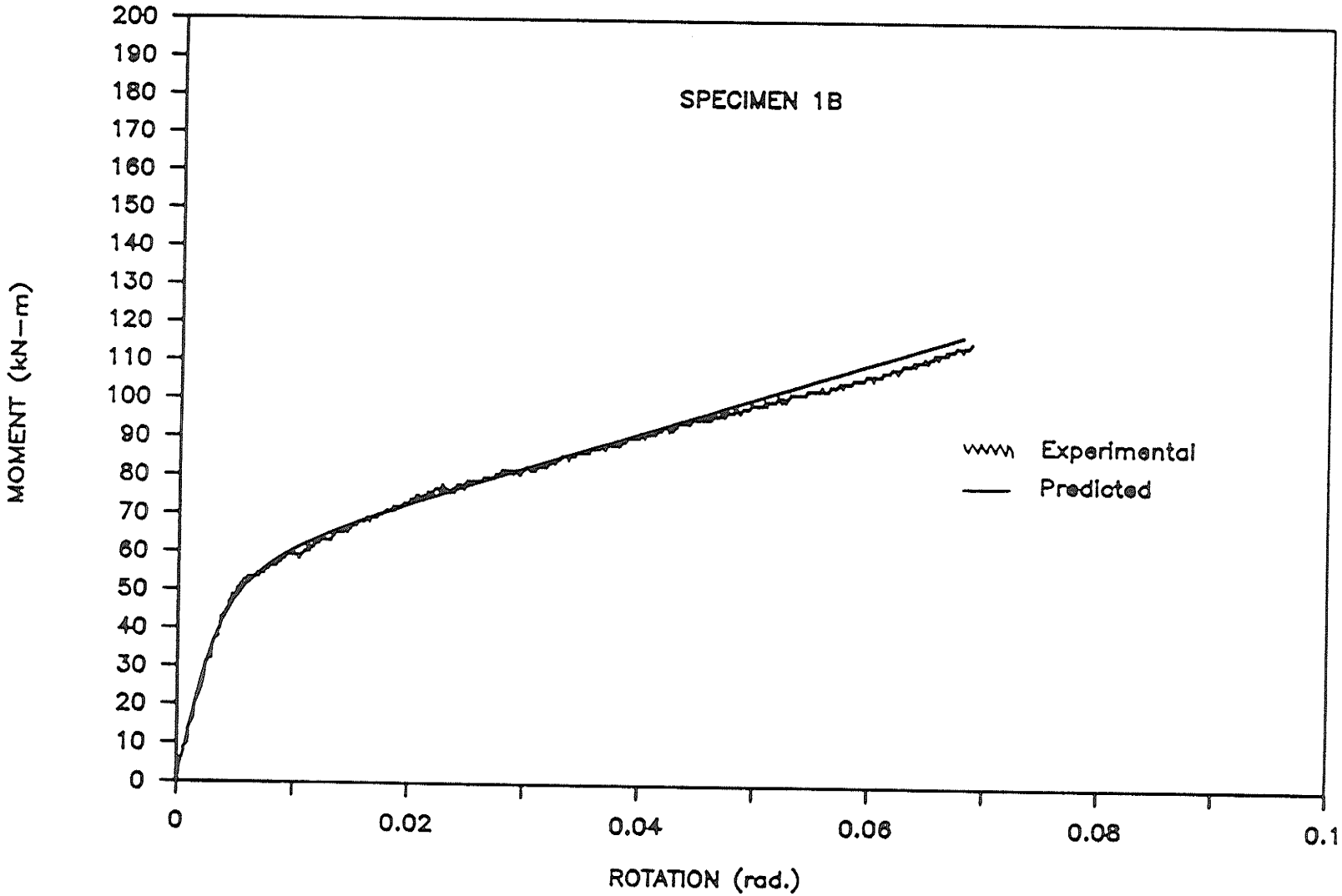

Figure 6.7: Case 3 - Experimental and Predicted Moment-Rotation Curves for Specimen 1B.

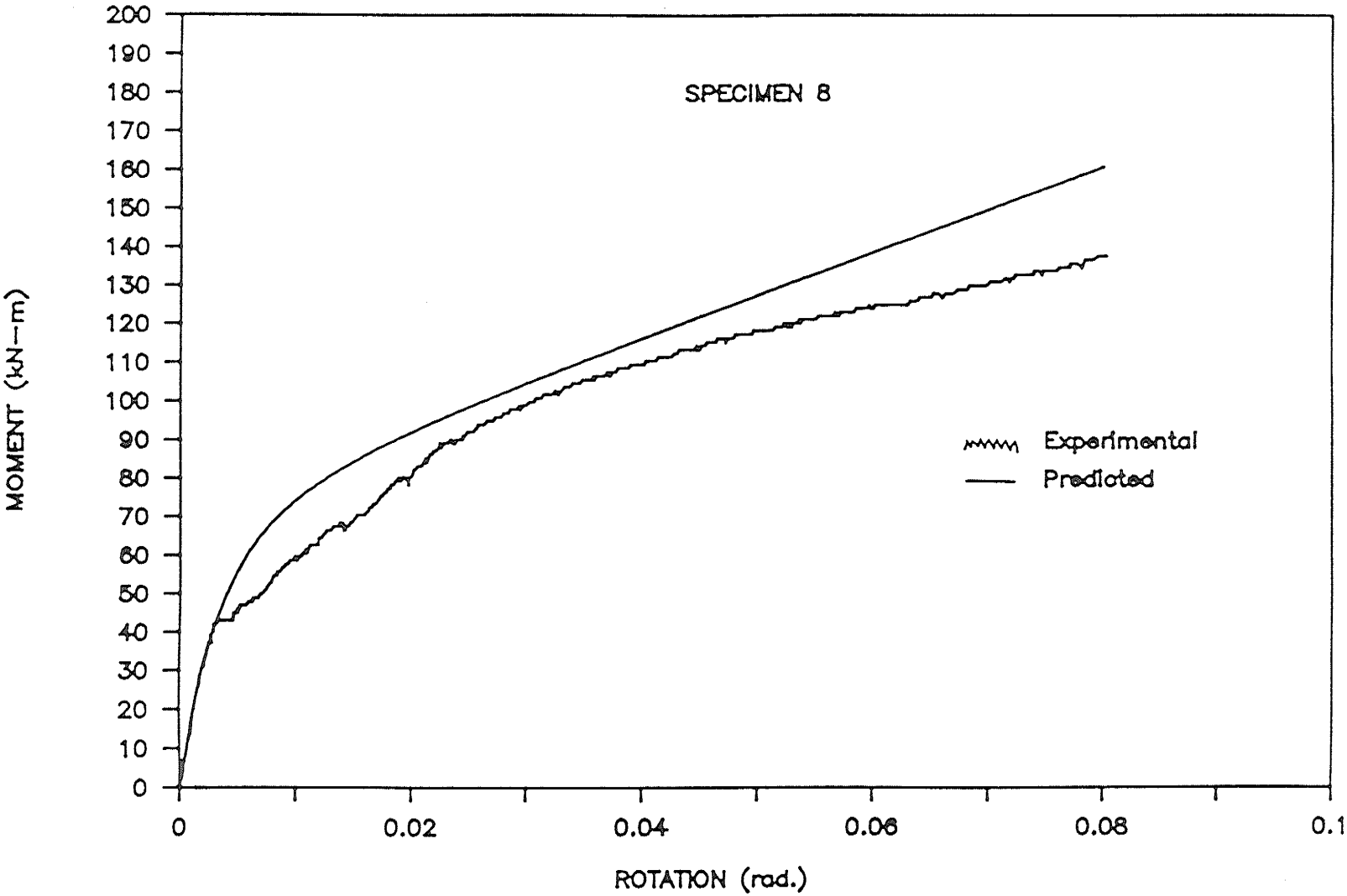

Figure 6.8: Case 3 - Experimental and Predicted Moment-Rotation Curves for Specimen 8.

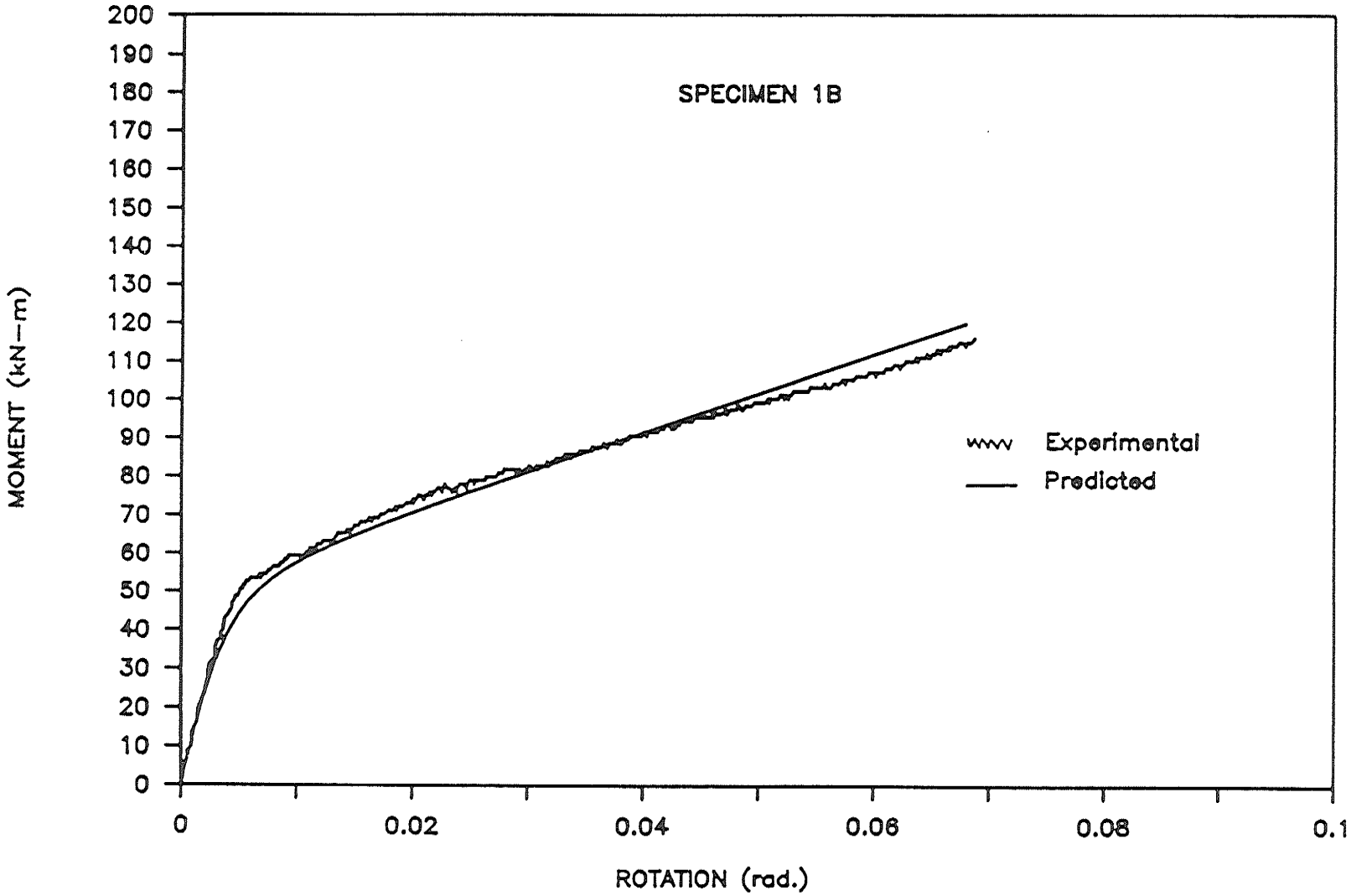

Figure 6.9: Case 4 - Experimental and Predicted Moment-Rotation Curves for Specimen 1B.

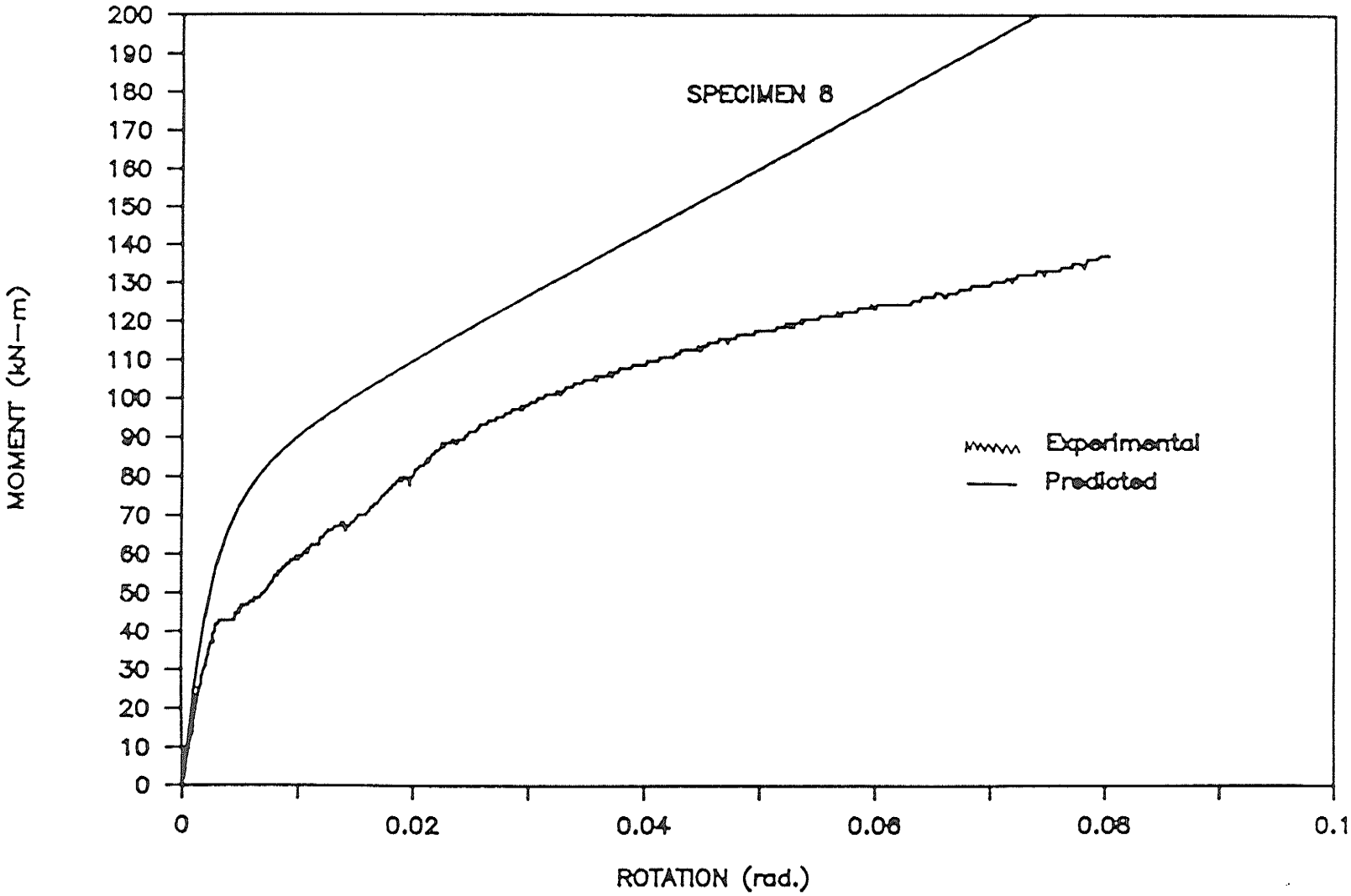

Figure 6.10: Case 4 - Experimental and Predicted Moment-Rotation Curves for Specimen 8.

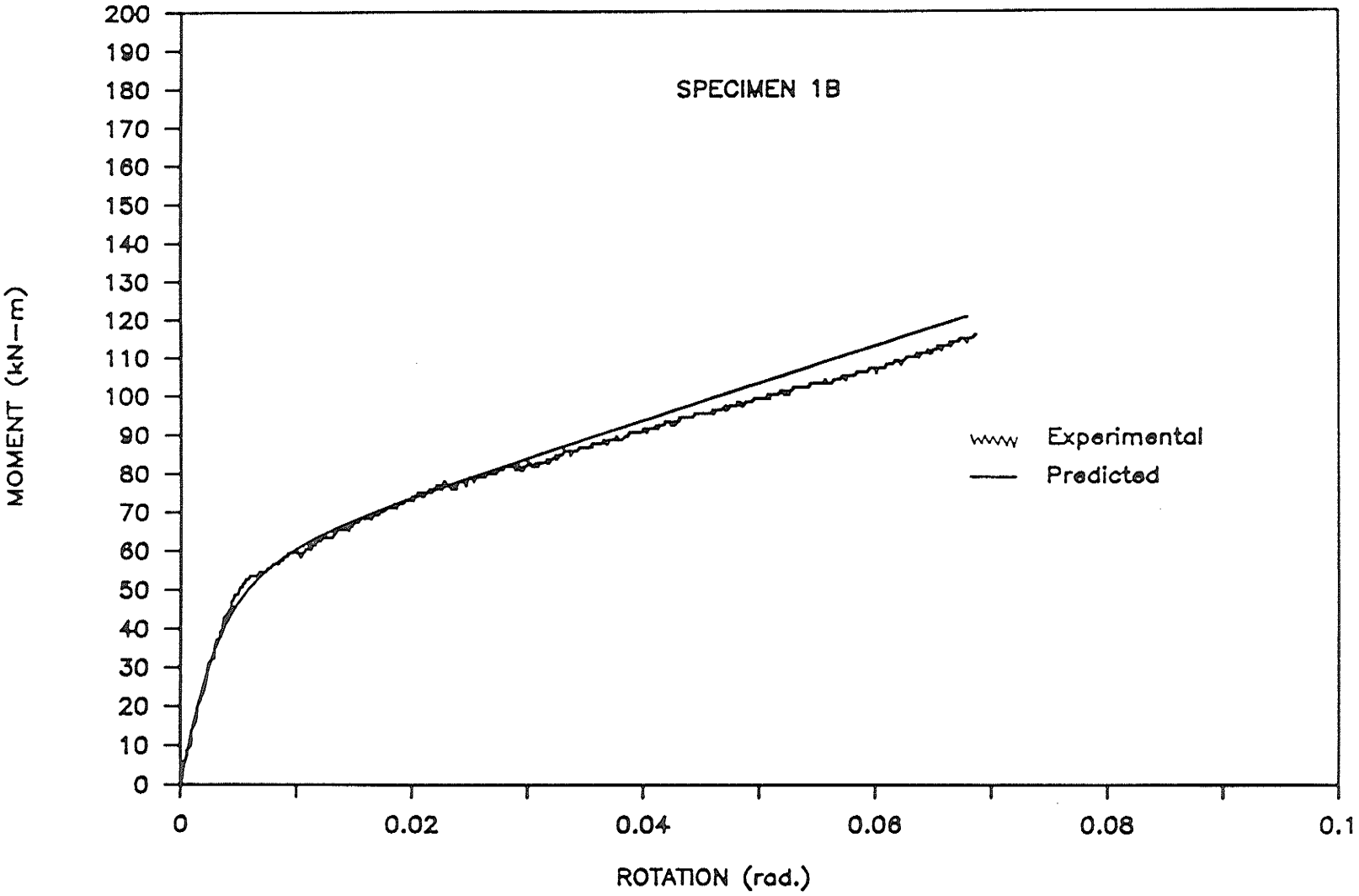

Figure 6.11: Case 5 - Experimental and Predicted Moment-Rotation Curves for Specimen 1B.

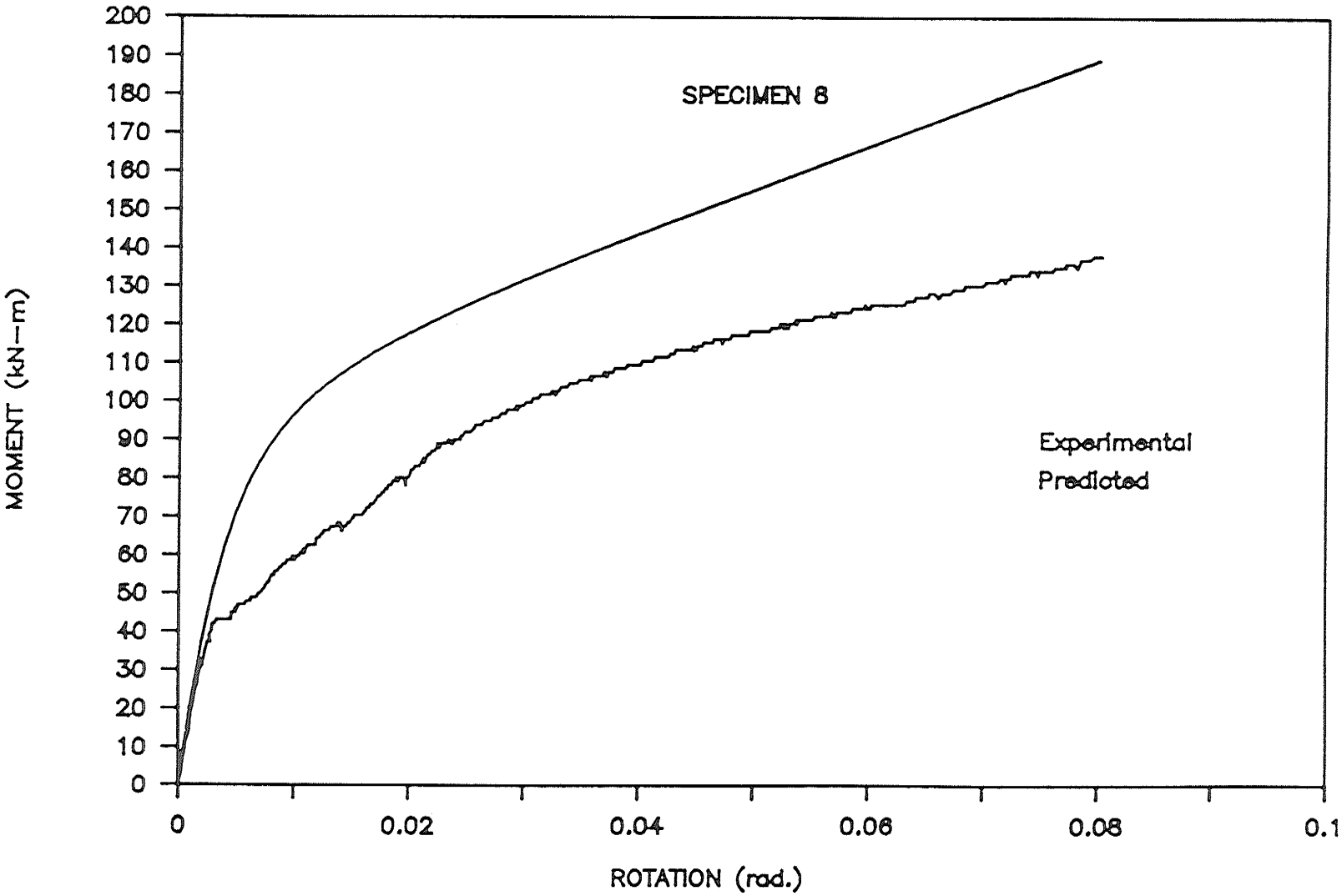

Figure 6.12: Case 5 - Experimental and Predicted Moment-Rotation Curves for Specimen 8.

CHAPTER 7

CONCLUSIONS AND RECOMMENDATIONS FOR FURTHER STUDY

7.1 CONCLUSIONS

Based upon tests of twenty specimens, each involving two bolted, double-web-angle connections symmetrically placed on the flanges of W-section stub columns, the following conclusions can be drawn:

1. The five connection geometric parameters which influenced most significantly the moment-rotation behaviour of double web angle connections were, the angle thickness, the gauge on the column, the angle length, the beam depth and the number of bolts per angle leg on the column flange.

2. The angle thickness and the number of bolts per angle leg on the column exhibited greater influence on the moment-rotation behaviour than the other three connection parameters.

3. The initial stiffness and the moment at 0.024 radians sustained by a particular double web angle connection, were increased by 107 and 120 percent, respectively, when the angle thickness was increased from 8 to 12 mm, and the connections had three bolts per angle leg in a vertical line.

4. For a connection with thick angles, when the number of bolts per angle leg on the column was increased from three to five, the initial stiffness and the maximum moment were increased by 177 and 290 percent, respectively.

5. When the gauge on the column was reduced from 140 to 100 mm, 37 and 13 percent increases for initial stiffness and maximum moment, respectively, were observed.

6. For a connection with 12 mm thick angles, when the beam depth was increased from 310 to 460 mm increases of 78 and 40 percent were observed in the initial stiffness and the maximum moment, respectively.

7. A connection with A325 fasteners and 10 mm thick angles had 41 percent larger stiffness than a similar connection with A307 fasteners. In addition, the former connection sustained a moment resistance which was 84 percent larger than that sustained by the latter.

A multiple regression analysis procedure has been developed for modelling the moment-rotation behaviour of double web angle connections, in a standardized form. The standardized function is expressed in terms of the pertinent connection geometric parameters. The function can be incorporated into a structural analysis computer program, and when the geometric parameters for a given connection are

substituted, the moment-rotation function for the connection is generated. The modelling procedure has been applied to the connections tested in this study, and then to them plus other similar connections tested by others. On the basis of the results, the following conclusions have been drawn:

1. For the connections tested in this study, the standardized function incorporating connection parameters t, g, d, b and l (angle thickness, gauge of column bolts, depth of beam, number of bolts per angle leg, and length of angle) yielded best accuracy.

2. For the connections tested in this study plus other similar connections tested by others, the average approximation errors for the predicted moment-rotation curves were 68, 4,300 and 11,197 percent for cases 1, 4 and 5, respectively. Case 1 was based on the M-Ø data for the connections of this study, while case 4 employed data for the connections of this study plus data for five similar connections tested by others. Finally, case 5 utilized data from this study plus all of the available pertinent data on bolted-bolted, bolted-welded and riveted double web angle connections.

7.2 RECOMMENDATIONS FOR FURTHER STUDY

1. While many tests of steel beam-to-column connections have been conducted, the present study is one of the few that have been conducted to isolate the effects of individual parameters on the moment-rotation behaviour of the connections. In this study, only double web angle connections were considered. Similar studies should be conducted on single web angle, header plate, top and seat angle and end plate connections.

2. Composite floor systems are becoming increasingly popular in steel frame construction. The few tests that have been done on steel beam-to-column connections in composite construction suggest that the latter behave differently than connections in bare steel frames. Therefore, it is recommended that a study similar to the present one be conducted on double web angle connections in composite construction. That study should, in turn, be extended to other common connection types.

3. Very little experimental information is available on the moment-rotation behaviour of connections between W-section beams and Hollow Structural Section columns. Thus it is recommended that a study similar to the present one be conducted on connections to Hollow Structural Section columns.

REFERENCES

1) Altman, W. G.Jr., Azizinamini, A., Bradburn, J. H. and Radziminski, J.B. 1982, "Moment-Rotation Characteristic of Semi-Rigid Steel Beam-To-Column Connections", A report of an investigation conducted by the Department of Civil Engineering, University of South Carolina.

2) American Institute of Steel Construction, 1983, " Proposed Load and Resistance Factor Design Specification For Structural Steel Buildings", American Institute of Steel Construction, Chigago, Illinois.

3) Ang, K. M. and Morris, G. A. 1984, "Analysis of Three-Dimensional Frames with Flexible Beam-Column Connections", Canadian Journal of Civil Engineering, Vol.11, pp. 245-254.

4) Attiogbe, E., Morris, G., and Onuah, C. 1989, "Standardization of Moment-Rotation Curves ", A Paper submitted to the Twelfth Canadian Congress of Applied Mechanics (CANCAM 1989), Carleton University, Ottawa, Ontario.

5) Attiogbe, E., Morris, G., and Pinkney, B. 1988, "Modelling of Moment-Rotation Behaviour of Steel Beam-To-Column Connections", Proceedings, Structural Stability Research Council Technical Session, Minneapolis, Minnesota.

6) Attiogbe, E., Morris, G., and Pinkney, B. 1989, "Modelling Functions for Moment-Rotation Curves", A Paper submitted to the Twelfth Canadian Congress of Applied Mechanics (CANCAM 1989), Carleton University, Ottawa, Ontario.

7) Batho, C., and Rowan, H. C, 1934, "Investigations on Beam and Stanchion Connections", 2nd Report of Steel Structures Research Committee, Her Majesty's Stationary Office, London, England.

8) Bergquist, D. J. 1977, "Tests on Columns Restrained by Beams with Simple Connections", Report No.1, American Iron and Steel Institute Project No.189, Department of Civil Engineering, University of Texas, Austin, Texas.

9) Canadian Standards Association, 1984, " Steel Structures for Buildings (Limit States Design)", CAN3-S16.1-M84, Canadian Standards Association, Rexdale, Ontario.

10) Frye, M. J., and Morris, G. A. 1975, "Analysis of Flexibly Connected Steel Frames", Canadian Journal of Civil Engineering, Vol.2.No.3. pp.280-291.

11) Goverdhan, A. V. 1984, "A Collection of Experimental Moment-Rotation Curves and Evaluation of Prediction

Equations for Semi-Rigid Connections", M.Sc. Thesis, Vanderbilt University, Nashville, Tenn., 512 pages.

12) Jones, W. S., Kirby, P. A. and Nethercot, D. A. 1980, "Effect of Semi-Rigid Connections on Steel Column Strength", Journal of Constructional Steel Research, London, Vol.1, pp.38-46.

13) Jones, W. S., Kirby, P. A. and Nethercot, D. A. 1981, "Modelling of Semi-Rigid Behaviour and its Influence on Steel Column Behaviour", Joints in the Structural Steel Work, John Wiley and sons, New York, pp. 5.73-5.87.

14) Jones, S. W., Kirby, P. A. and Nethercot, D. A. 1982, "Influence of Semi-Rigid Joints on Steel Column Behaviour", Journal of the Structural Division, American Society of Civil Engineers, Vol.108.No.ST2. pp. 361-372.

15) Kishi, N., Chen, W. F. 1986, "Data Base of Steel Beam-To-Column Connections, Vol.1", School of Engineering, Purdue University.

16) Lewitt, C. W., Chesson, E., and Munse, W. H. 1969, "Restraint Characteristics of Flexible Riveted and Bolted Beam-To-Column Connections", Bulletin No.500, Engineering Experimental Station, University of Illinois, 99 pages.

17) Lothers, J. E. 1951, "Elastic Restraint Equation for Semi-Rigid Connections", American Society of Civil Engineers Transactions, Vol.116, pp. 480-502.

18) Lui, E. M. and Chen, W. F. 1983, "Strengths of H-Columns with Small End Restraints", The Structural Engineer, Vol.61B, No.1, pp. 17-26.

19) Lui, E. M. 1985, "Effects of Connection Flexibility and Panel Zone Deformation on Behaviour of Plane Steel Frames", Ph.D. Dissertation, Department of Civil Engineering, Purdue University, West LaFayette, Indiana.

20) Morris, G. A. and Parker, J. A. 1987, "Beam-To-Column Connections in Steel Frames", Canadian Journal of Civil Engineering, Vol.14. No.1, pp. 68-76.

21) Munse, W. H., Bell, W. G. and Chesson, E. 1959, "Behaviour of Riveted and Bolted Beam-To-Column Connections", Proceedings of the American Society of Civil Engineers, Journal of the Structural Division, St 3, pp. 29-50.

22) Nethercot, D. A. 1985, "Steel Beam to Column Connections- A Review of Test Data", Construction Industry Research and Information, London, England, 79 pages.

23 Ostrander, J. R. 1970, "An Experimental Investigation of End Plate Connections", Master's Thesis at the University Saskatchewan, Canada.

24) Rathbun, J. C. 1936, "Elastic Properties of Riveted Connections", Transactions, ASCE, Vol. 101, pp. 524-563.

25) Ramberg, R. M. and Osgood, W. R. 1943, "Description of Stress-Strain Curves by Three Parameters", NACA Technical Report No. 902.

26) Richard, R. M. and Abbot, B. J. 1975, "Versatile Elastic-Plastic Stress-Strain Formula", Proceedings of the American Society of Civil Engineers, Journal of the Engineering Mechanics Division, Vol. 101, No. EM4, pp. 511-515.

27) Sommer, W. H. 1969, "Behaviour of Welded Header Plate Connections", Master's Thesis at the University of Toronto, Canada.

28) Thompson, L. E., Mckee, R. J. and Visintainer, D. A. 1970, "An Investigation of Rotation Characteristics of Web Shear Framed Connections Using A-36 and A-441 Steels", Department of Civil Engineering, University of Missouri-Rolla, Rolla, Missouri.

29) Wilson, W. M. and Moore, H. F. 1917, "Tests to Determine the Rigidity of Riveted Joints in Steel Structures", Bulletin 104, Engineering Experiment Station, University of Illinois.

APENDIX A
DERIVATION OF ROTATION EQUATION BASED ON THE PRINCIPLE OF SLOPE DEFLECTION.

APPENDIX A

THE DERIVATION OF EQUATION (5.1)

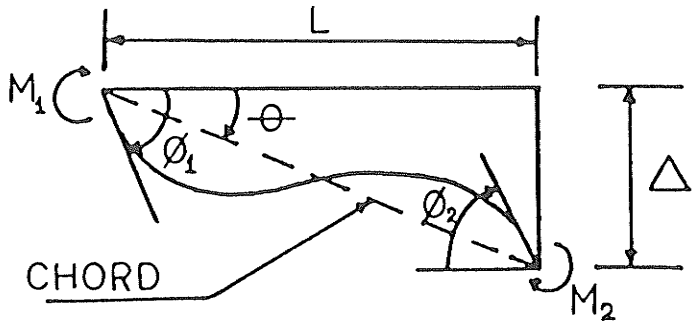

Figure A: Application of Slope Deflection Principle to a Beam Segment.

The moment M_1 at one of the supports can be expressed in terms of the flexural rigidity of the beam, the span length, the beam rotations and the chord rotation using the principle of slope deflection, as illustrated in Figure A. The moment M_2 at the connection can be expressed similarly using the same slope deflection principle.

At the support:

$$M_1 = \frac{2EI}{L} (- 2\emptyset_1 - \emptyset_2 + 3\theta) \qquad (A.1)$$

where

EI = flexural rigidity of the beam,

$\emptyset_1$ = beam rotation at the support,

$\emptyset_2$ = beam rotation at the connection,

θ = chord rotation,

Δ = vertical deflection at the connection, and

L = beam span length.

and

$$\theta = \frac{\Delta}{L} \tag{A.2}$$

Since the supports are pinned, $M_1 = 0$. Then, Equation (A.1) becomes:

$$\frac{2EI}{L} \left(- 2\phi_1 - \phi_2 + 3 \frac{\Delta}{L} \right) = 0 \tag{A.3}$$

Re-arranging Equation (A.3):

$$\frac{4EI}{L} \phi_1 + \frac{2EI}{L} \phi_2 = \frac{6EI}{L} \frac{\Delta}{L} \tag{A.4}$$

Hence,

$$2\phi_1 = \frac{3\Delta}{L} - \phi_2 \tag{A.5}$$

At the connection:

$$M_2 = \frac{2EI}{L} \left(- 2\phi_2 - \phi_1 + 3 \frac{\Delta}{L} \right) \tag{A.6}$$

Re-arranging Equation (A.6):

$$\frac{4EI}{L} \phi_2 = \frac{6EI}{L} \frac{\Delta}{L} - \frac{2EI}{L} \phi_1 - M_2 \tag{A.7}$$

Hence,

$$4\emptyset_2 = 6\frac{\Delta}{L} - 2\,\emptyset_1 - \frac{M_2 L}{EI} \qquad (A.8)$$

Substituting Equation (A.5) into Equation (A.8):

$$3\emptyset_2 = 3\frac{\Delta}{L} - \frac{M_2 L}{EI} \qquad (A.9)$$

Therefore,

$$\emptyset_2 = \frac{\Delta}{L} - \frac{M_2 L}{3EI} \qquad (A.10)$$

The moment, M_2, at the connection can be expressed in terms of the applied load, P, as follows:

$$M_2 = \frac{PL}{2} \qquad (A.11)$$

Substituting Equation (A.11) into Equation (A.10):

$$\emptyset_2 = \frac{\Delta}{L} - \frac{PL^2}{6EI} \qquad (A.12)$$

Equation (A.12) may be used to calculate the rotation at the connection.

APPENDIX B

MOMENT-ROTATION CURVES BASED ON HORIZONTAL AND VERTICAL DISPLACEMENTS OF TEST SPECIMENS

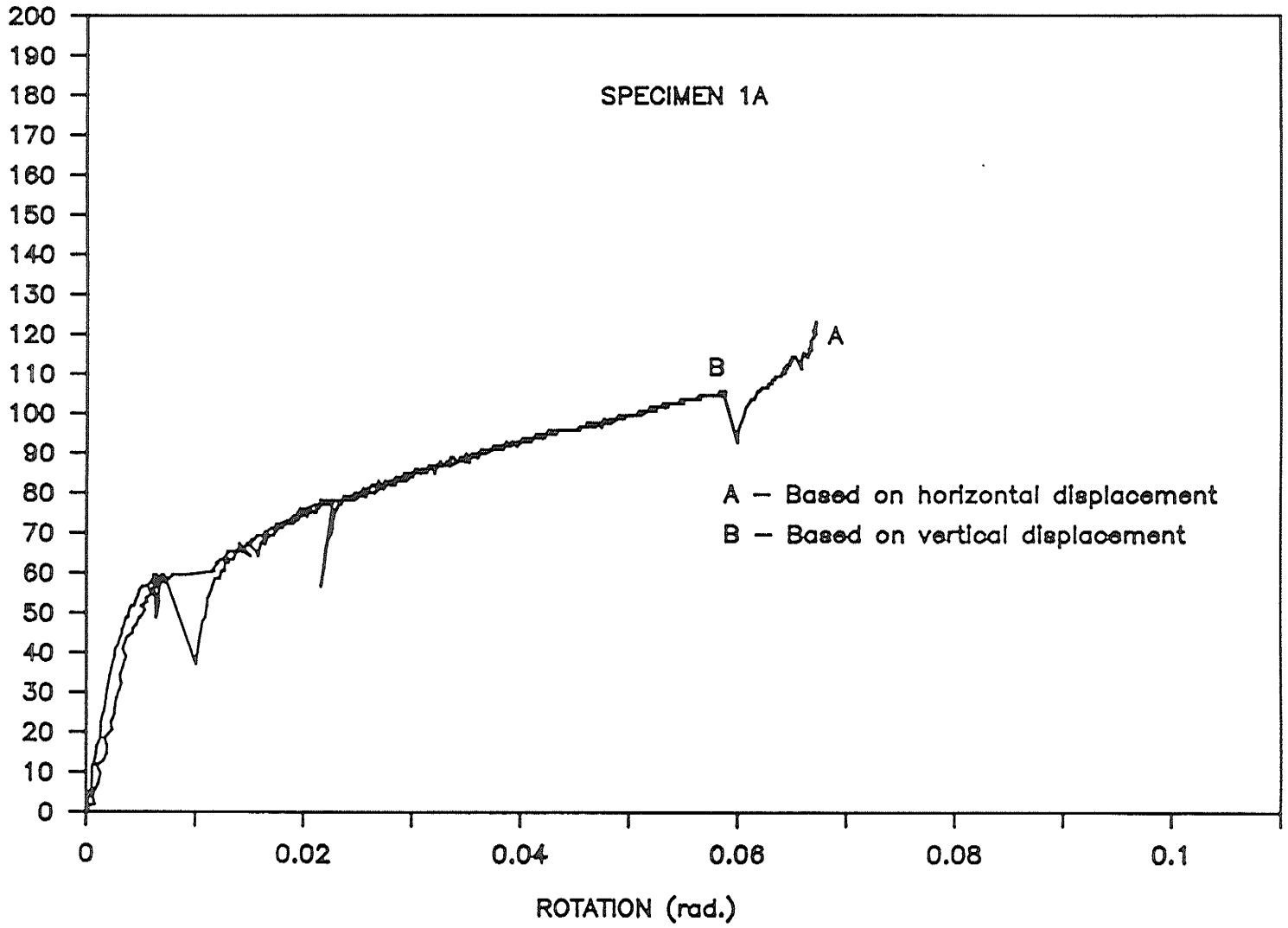

Figure B.1: Moment-Rotation Curves Based on Horizontal and Vertical Displacements of Specimen 1A.

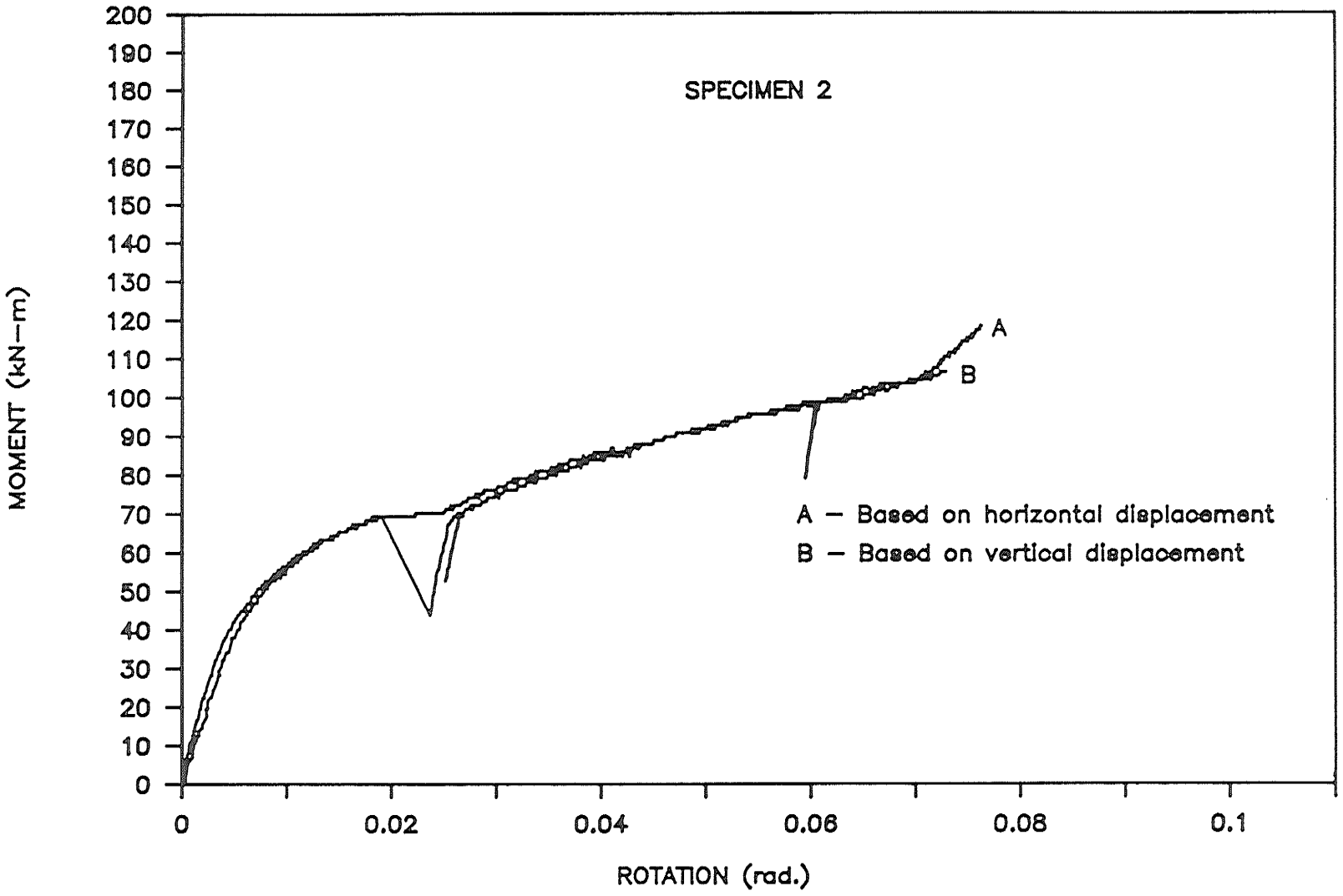

Figure B.2: Moment-Rotation Curves Based on Horizontal and Vertical Displacements of Specimen 2.

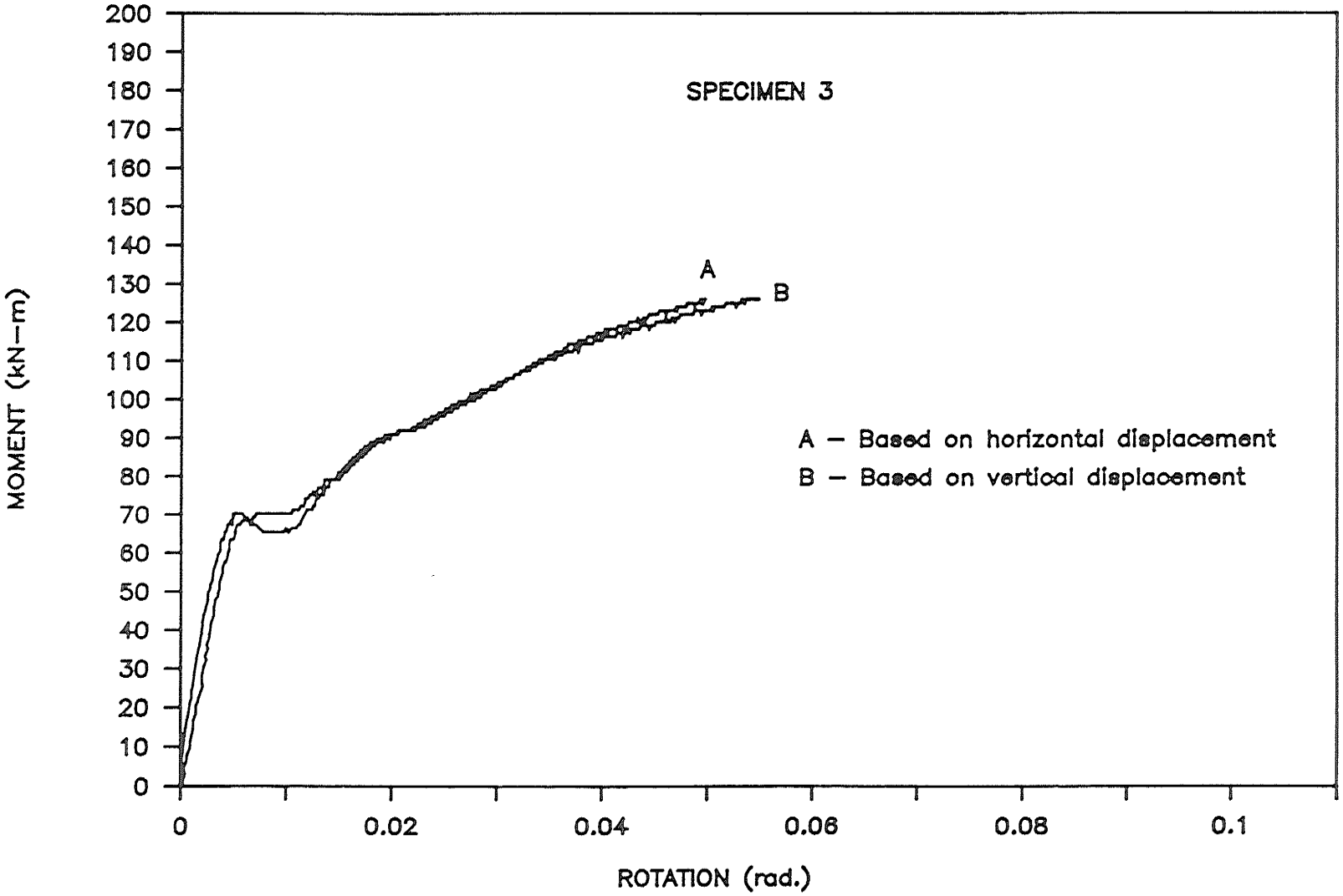

Figure B.3: Moment-Rotation Curves Based on Horizontal and Vertical Displacements of Specimen 3.

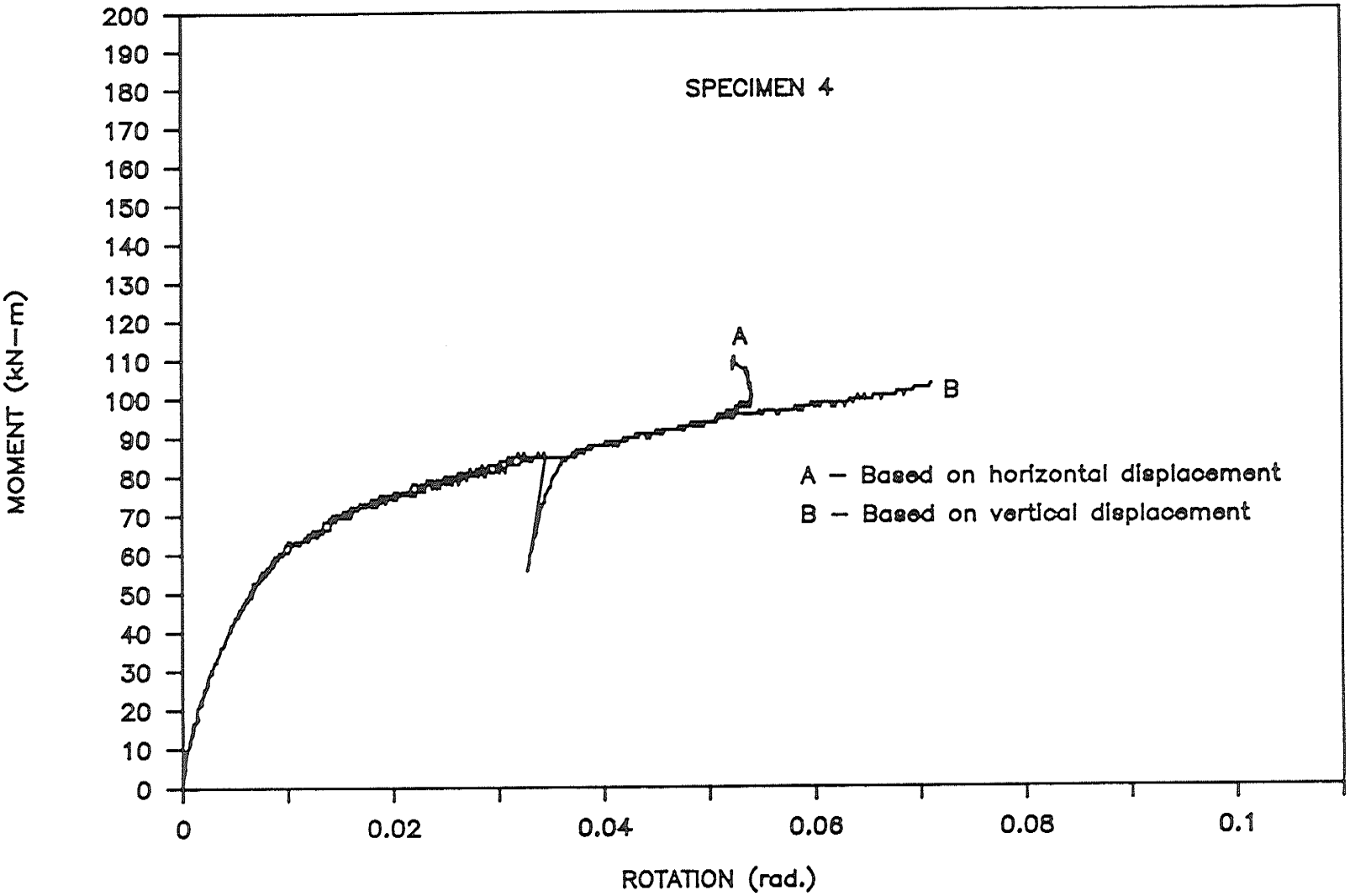

Figure B.4: Moment-Rotation Curves Based on Horizontal and Vertical Displacements of Specimen 4.

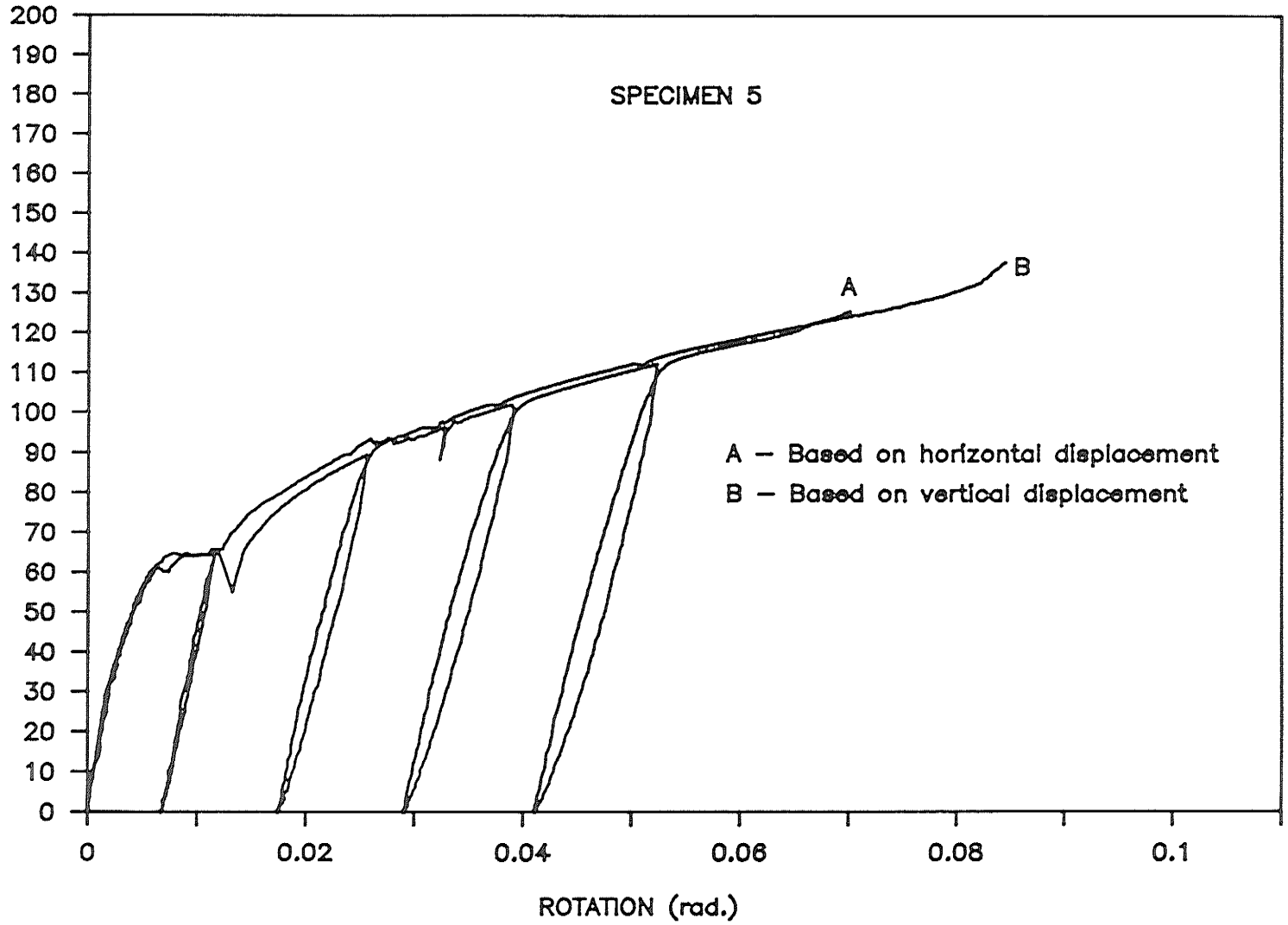

Figure B.5: Moment-rotation Curves Based on Horizontal and Vertical Displacements of Specimen 5.

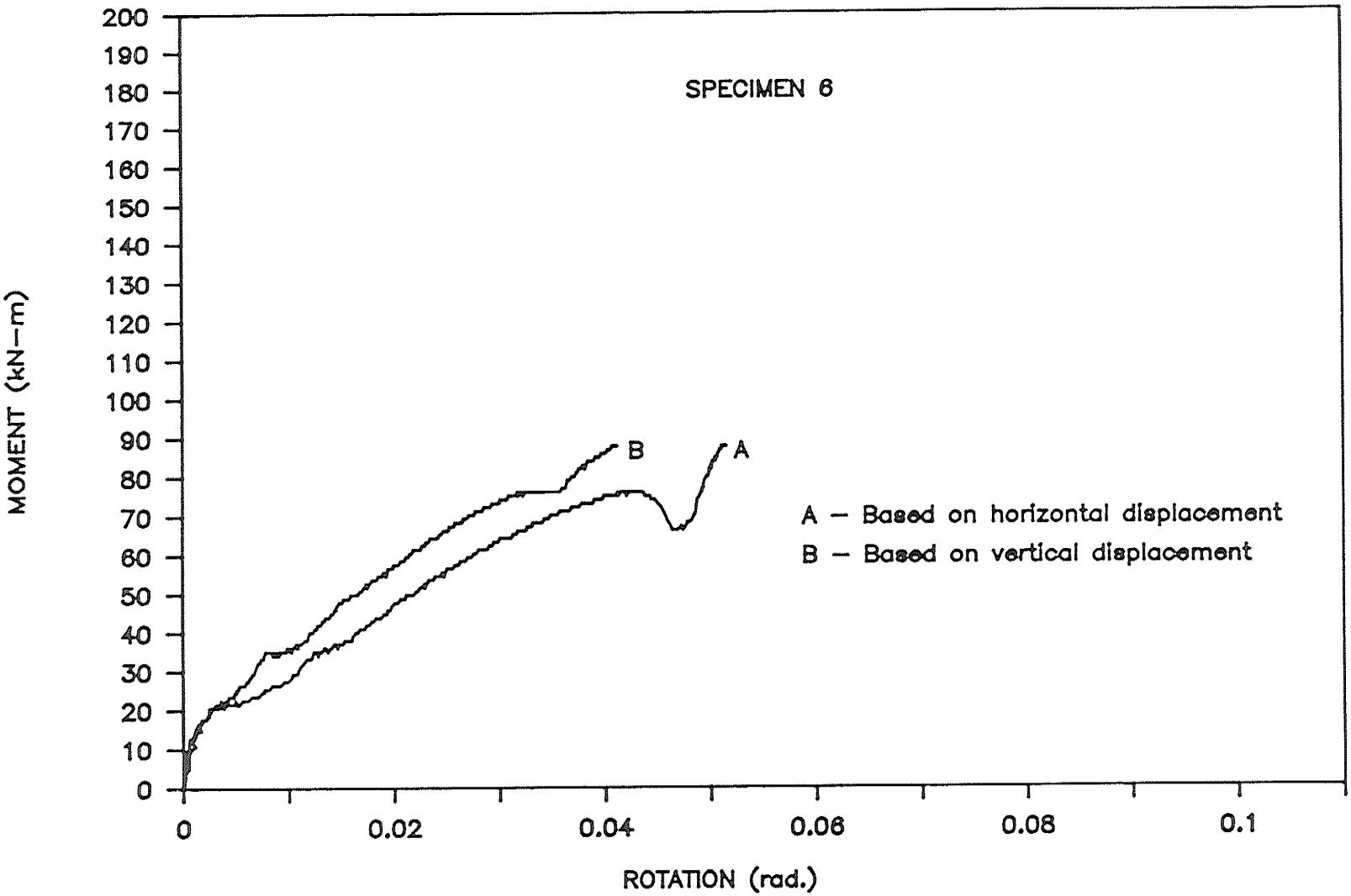

Figure B.6: Moment-Rotation Curves Based on Horizontal and Vertical Displacements of Specimen 6.

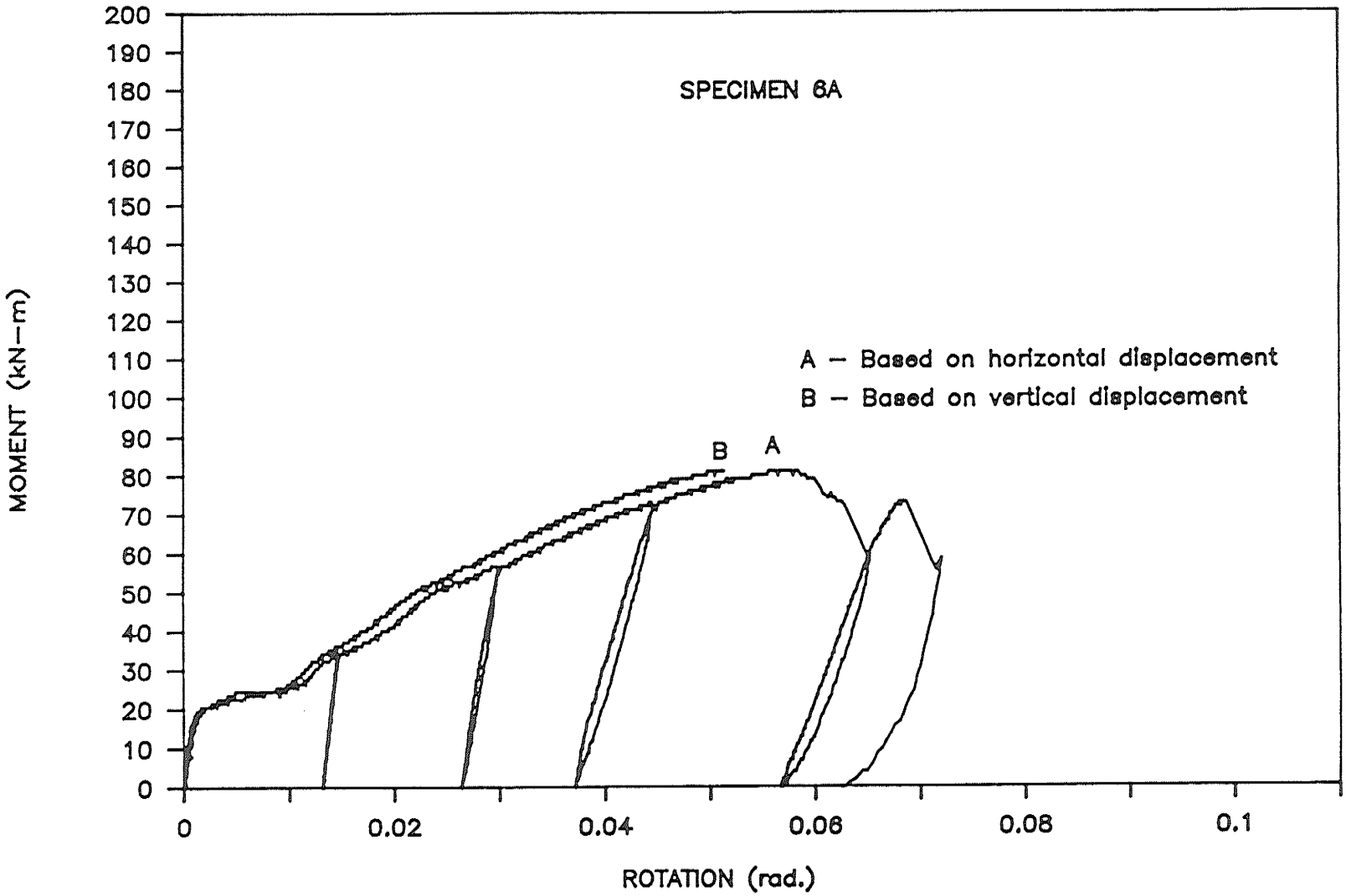

Figure B.7: Moment-Rotation Curves Based on Horizontal and Vertical Displacements of Specimen 6A.

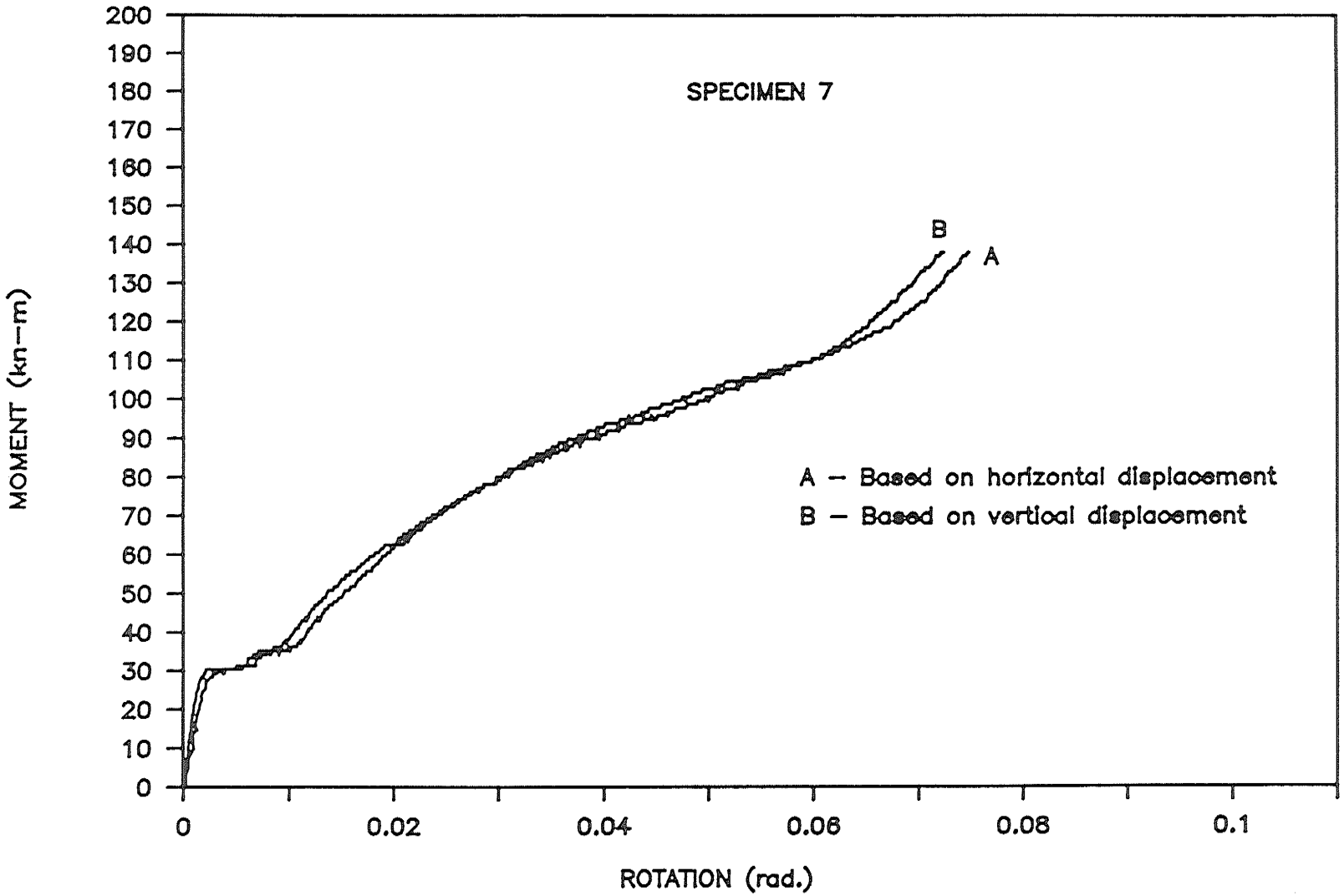

Figure B.8: Moment-Rotation Curves Based on Horizontal and Vertical Displacements of Specimen 7.

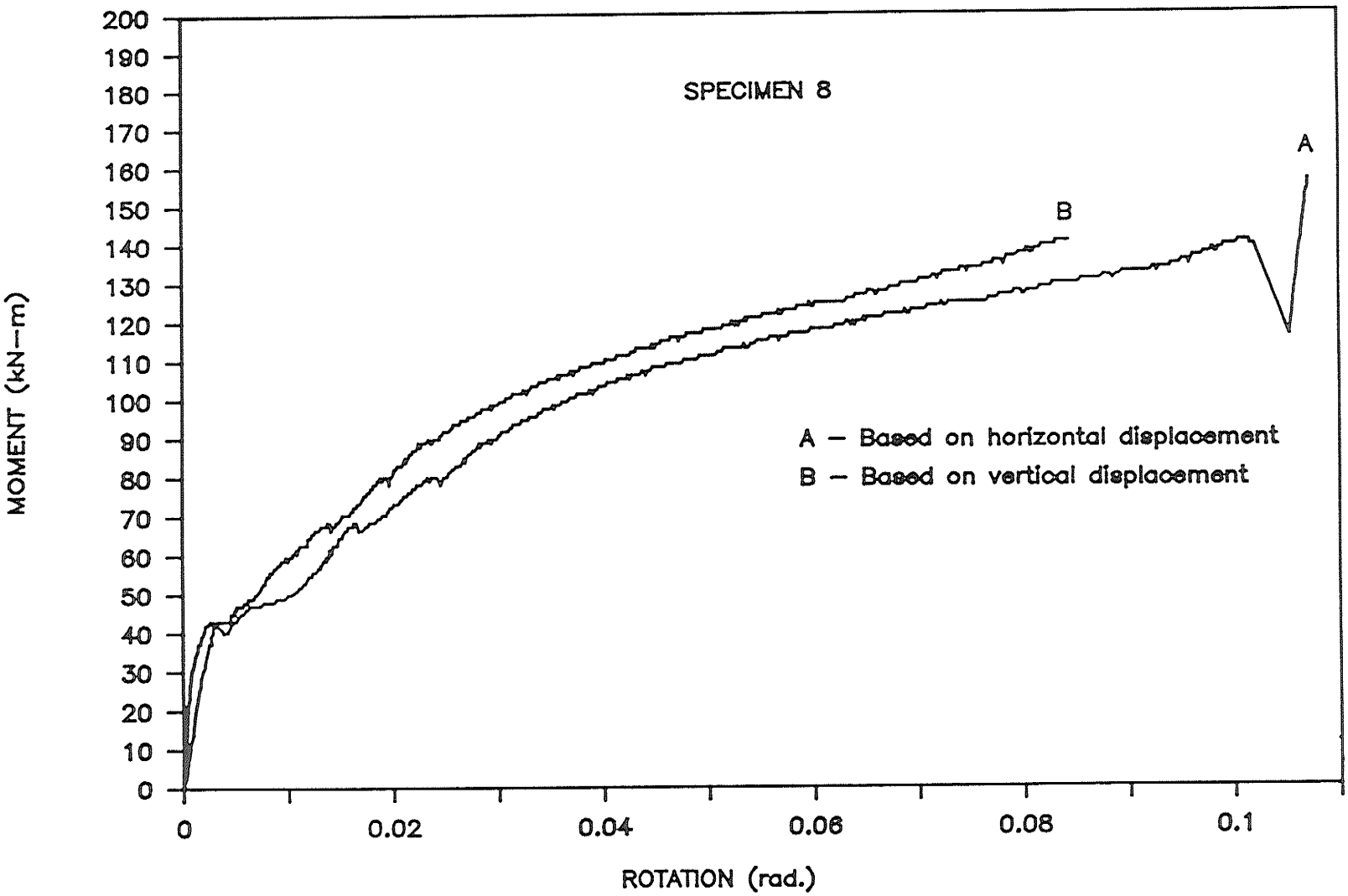

Figure B.9: Moment-Rotation Curves Based on Horizontal and Vertical Displacements of Specimen 8.

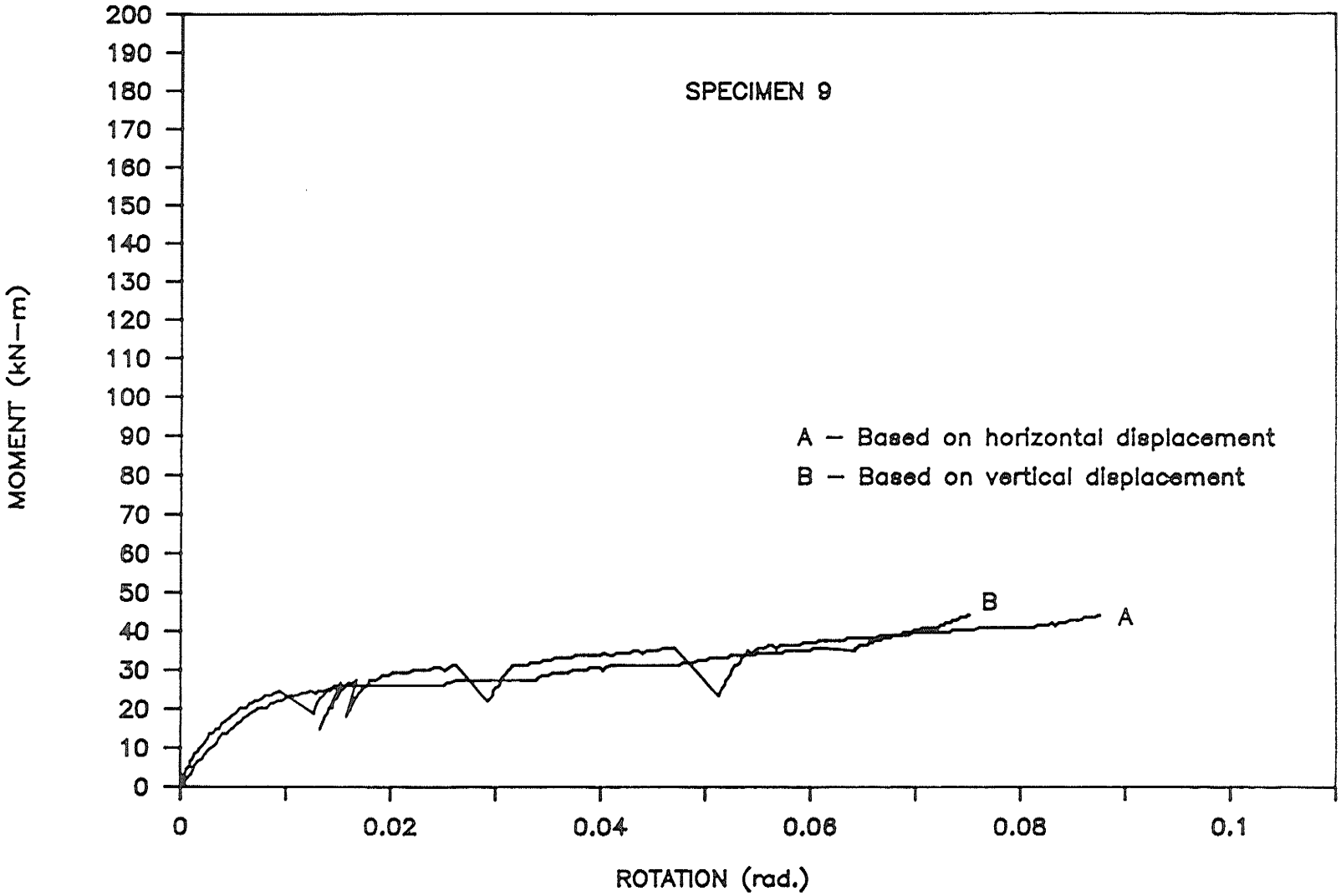

Figure B.10: Moment-Rotation Curves Based on Horizontal and Vertical Displacements of Specimen 9.

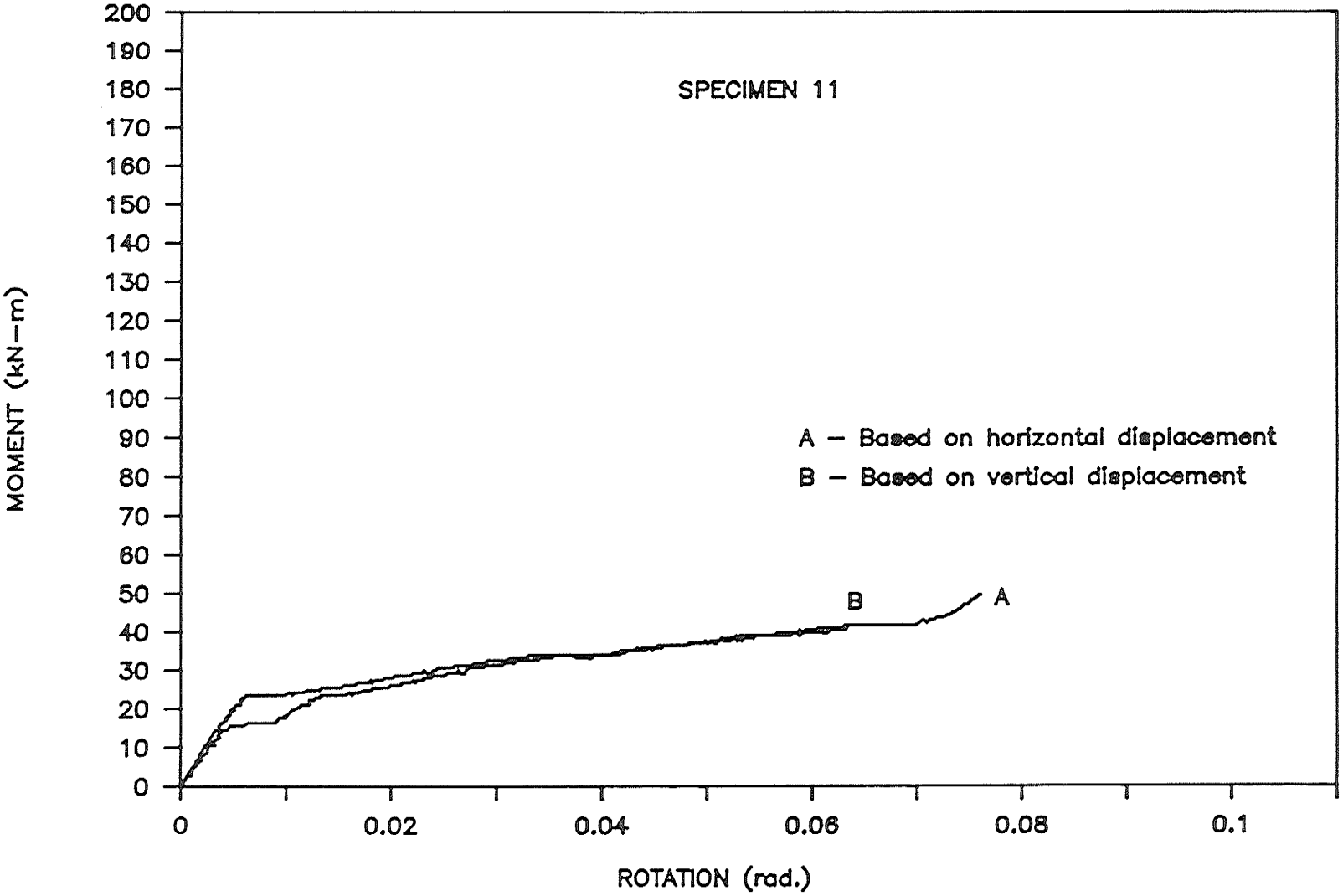

Figure B.11: Moment-Rotation Curves Based on Horizontal and Vertical Displacements of Specimen 11.

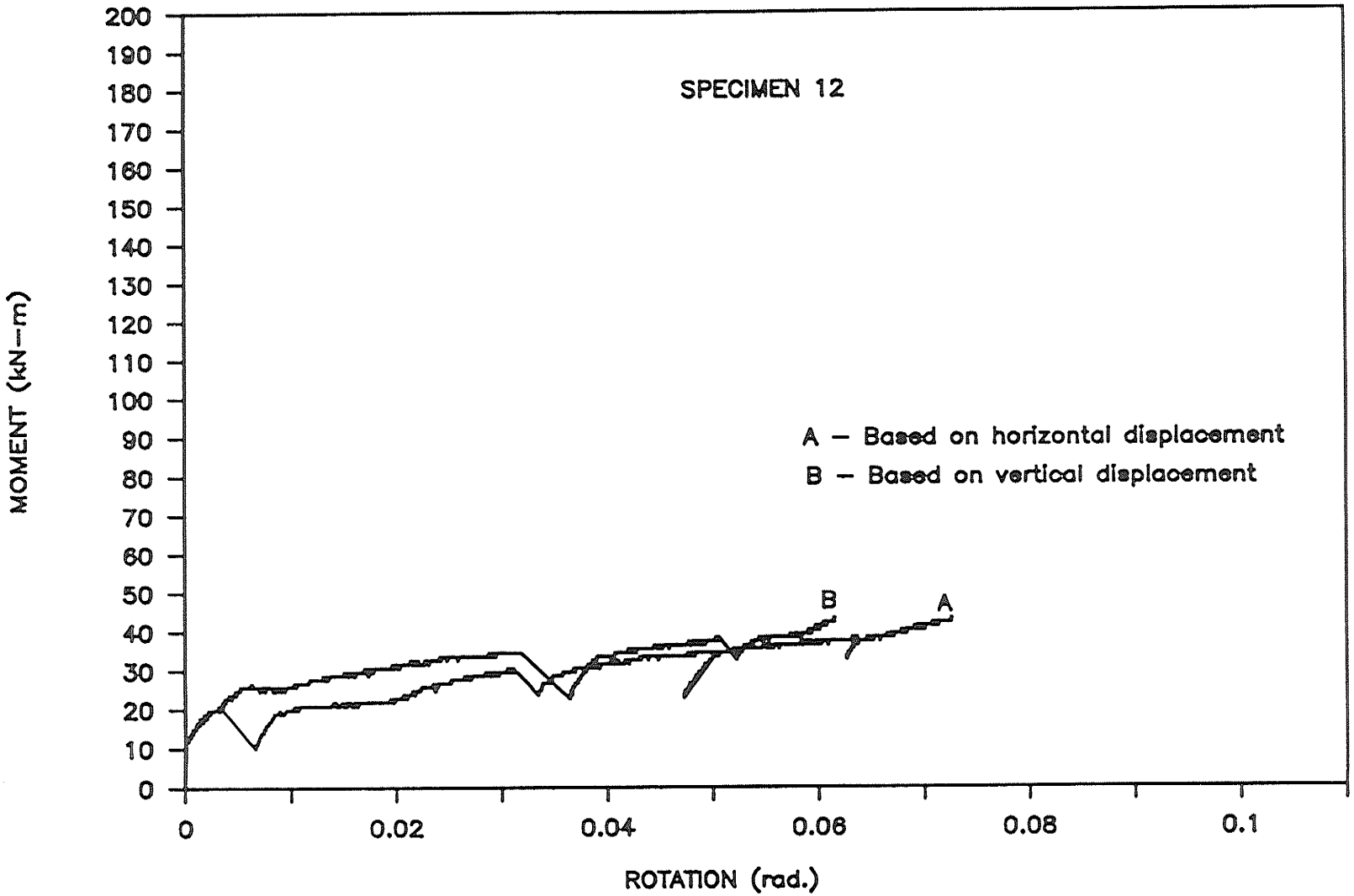

Figure B.12: Moment-Rotation Curves Based on Horizontal and Vertical Displacements of Specimen 12.

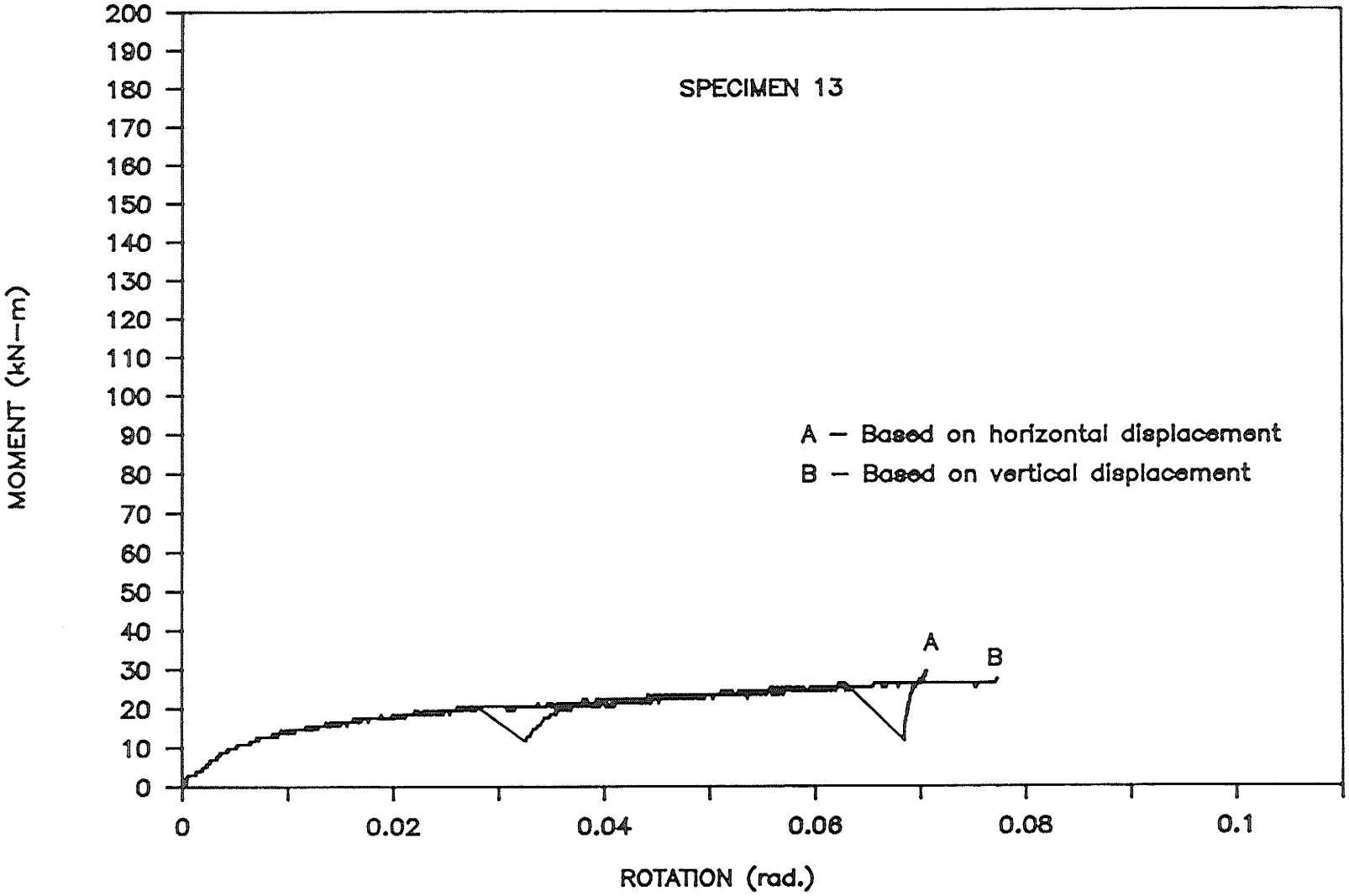

Figure B.13: Moment-Rotation Curves Based on Horizontal and Vertical Displacements of Specimen 13.

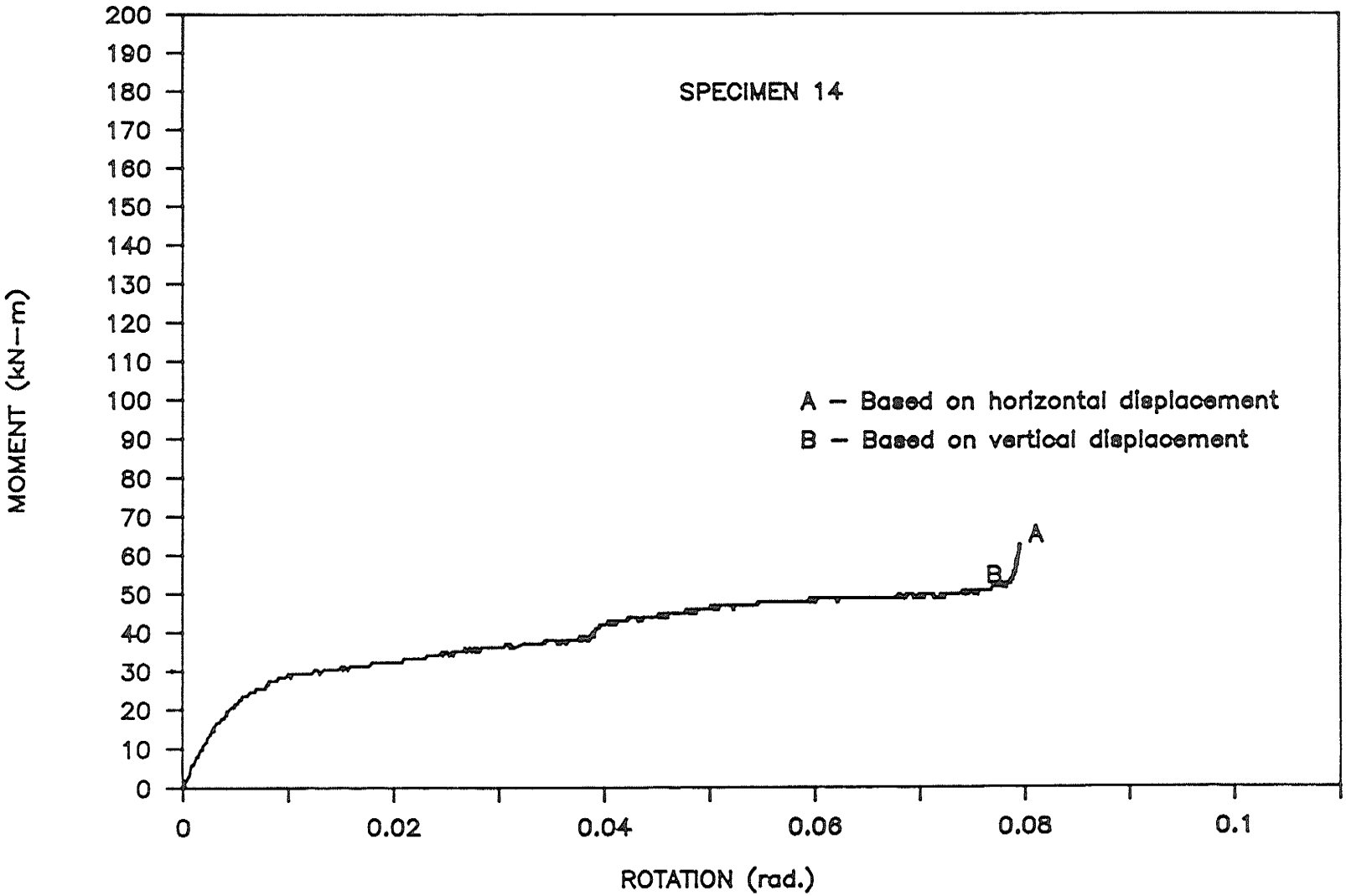

Figure B.14: Moment-Rotation Curves Based on Horizontal and Vertical Displacements of Specimen 14.

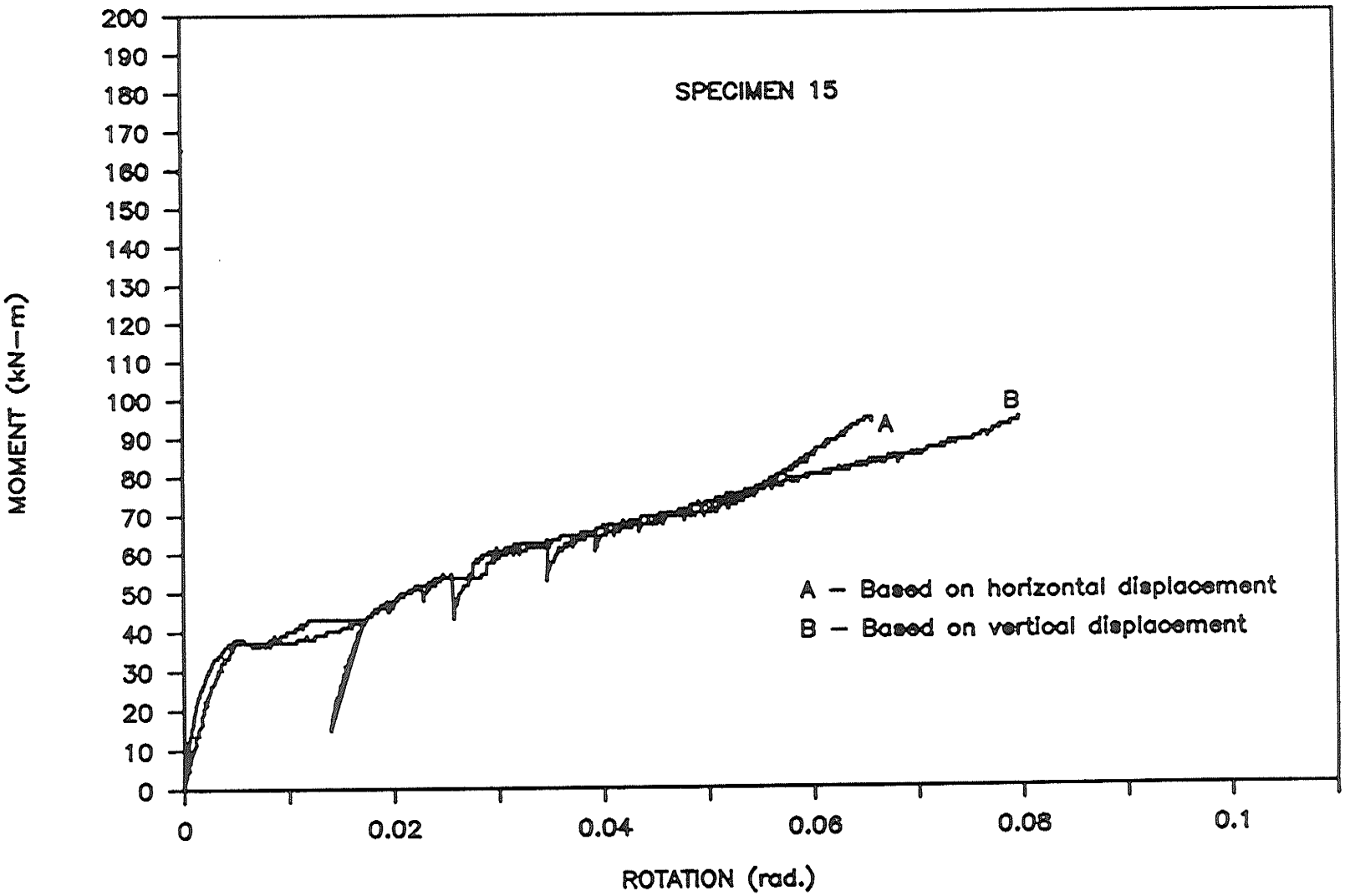

Figure B.15: Moment-Rotation Curves Based on Horizontal and Vertical Displacements of Specimen 15.

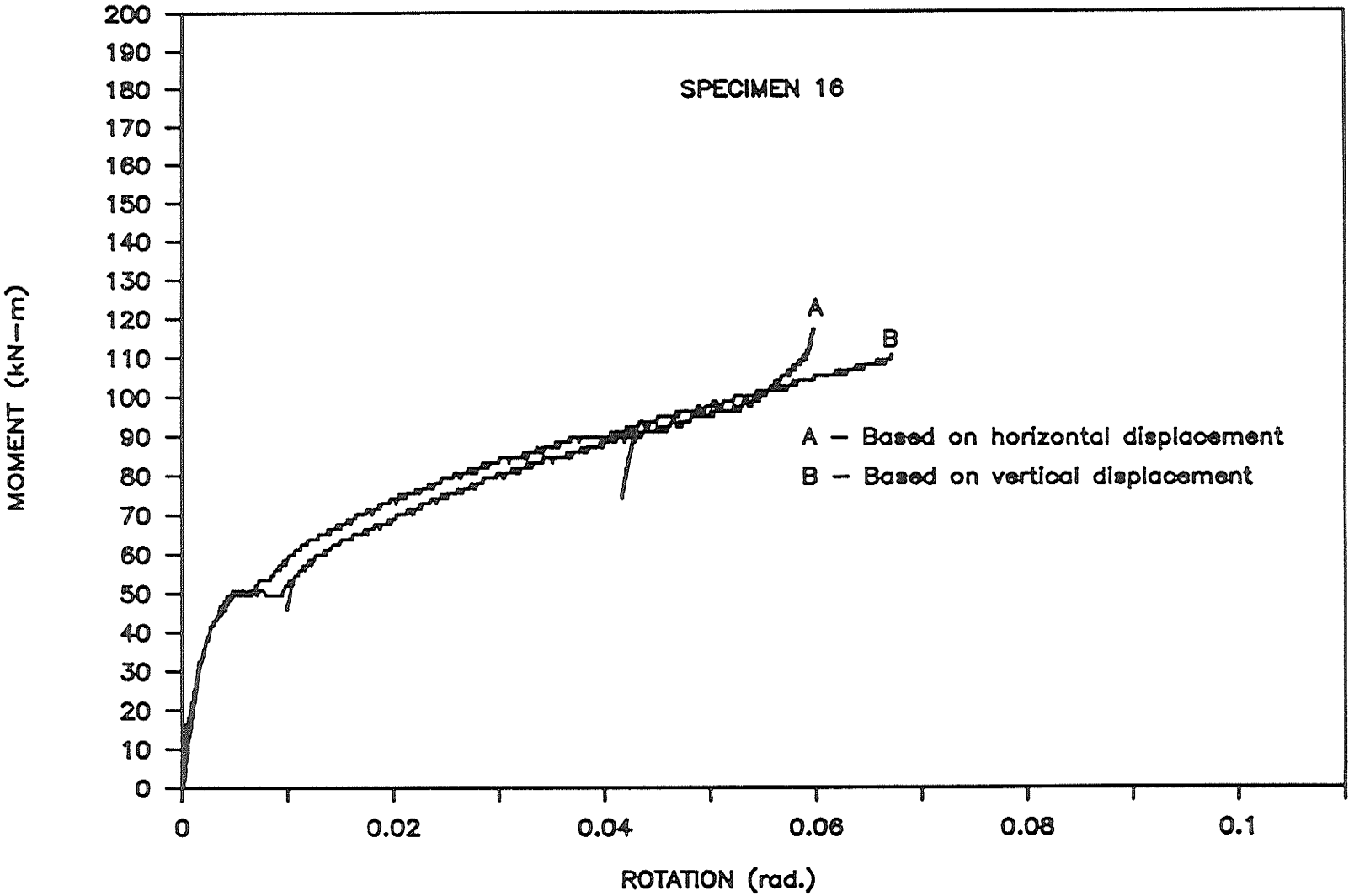

Figure B.16: Moment-Rotation Curves Based on Horizontal and Vertical Displacements of Specimen 16.

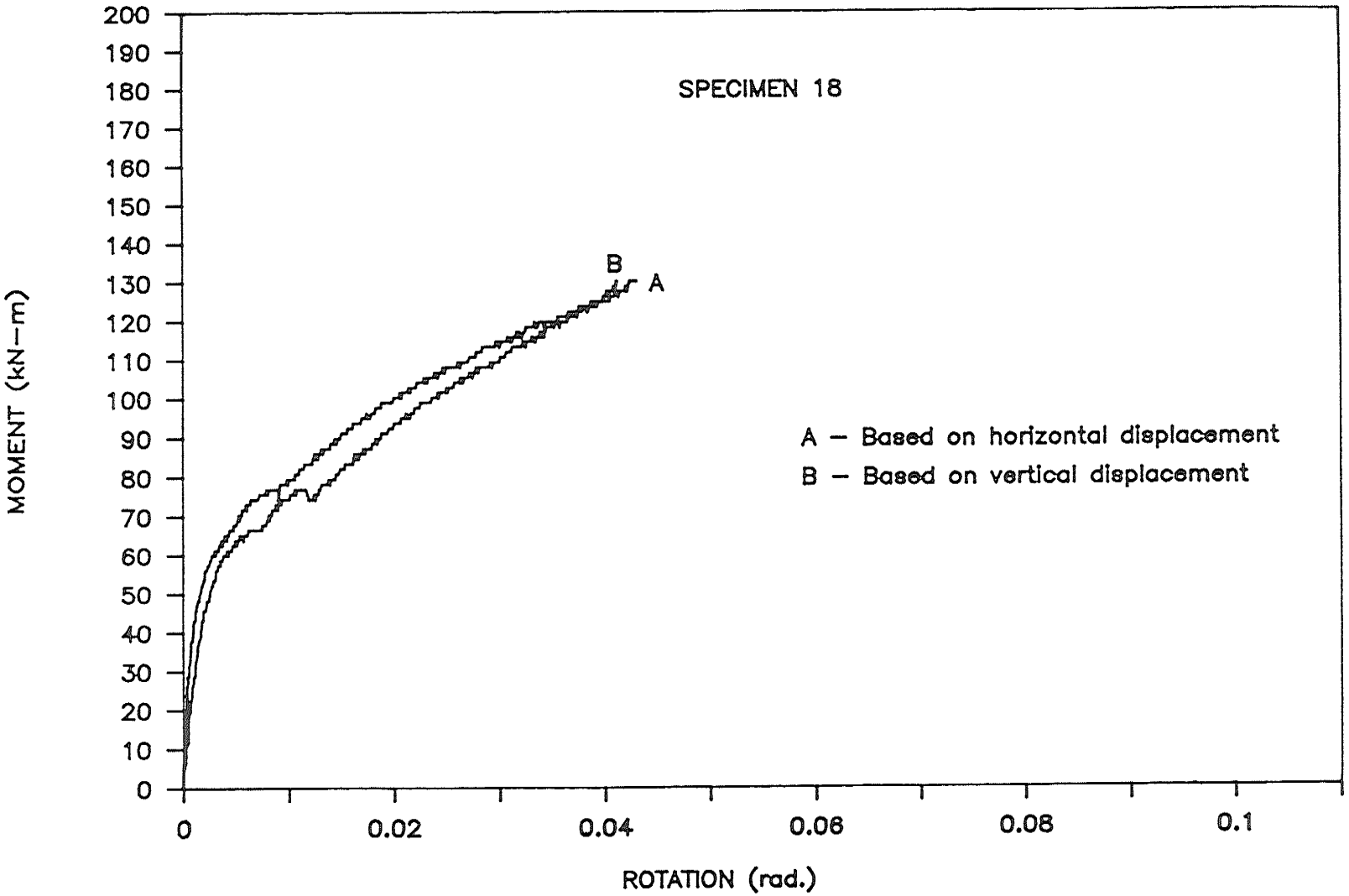

Figure B.17: Moment-Rotation Curves Based on Horizontal and Vertical Displacements of Specimen 18.

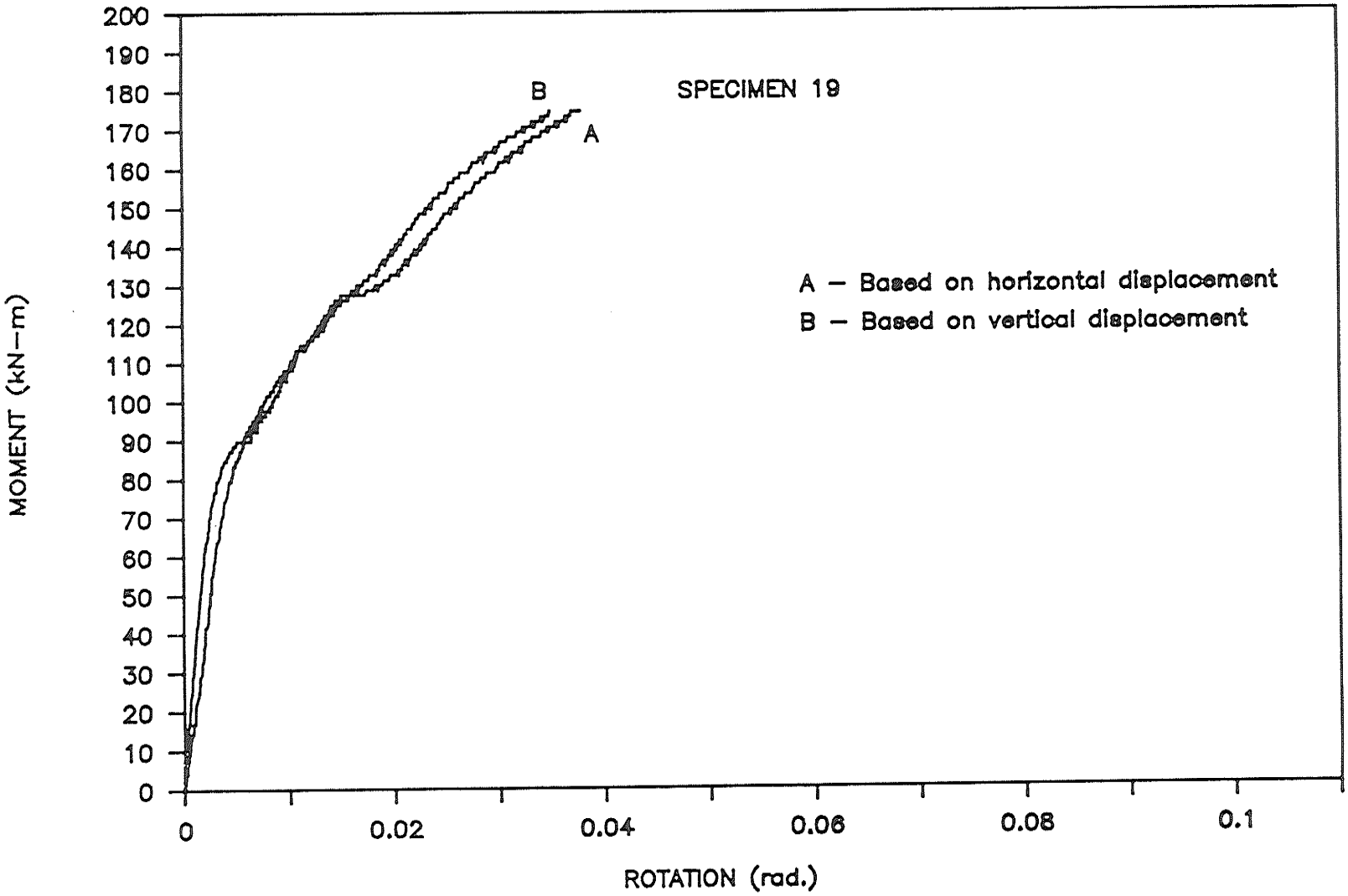

Figure B.18: Moment-Rotation Curves Based on Horizontal and Vertical Displacements of Specimen 19.